

1-1-2012

Pharmaceutical treatment options for aortic root pathology in Marfan syndrome

Darren McLoughlin

Royal College of Surgeons in Ireland

Citation

McLoughlin D. Pharmaceutical treatment options for aortic root pathology in Marfan syndrome. [MD Thesis]. Dublin: Royal College of Surgeons in Ireland; 2012.

This Thesis is brought to you for free and open access by the Theses and Dissertations at e-publications@RCSI. It has been accepted for inclusion in MD theses by an authorized administrator of e-publications@RCSI. For more information, please contact epubs@rcsi.ie.

— Use Licence —

Creative Commons Licence:



This work is licensed under a [Creative Commons Attribution-Noncommercial-Share Alike 3.0 License](https://creativecommons.org/licenses/by-nc-sa/3.0/).

**Pharmaceutical treatment options for
aortic root pathology in Marfan
syndrome.**

Darren McLoughlin
MB BCh BAO, MRCPI, MRCS

MD Thesis

2012

**Pharmaceutical treatment options for
aortic root pathology in Marfan
syndrome.**

Darren McLoughlin
MB BCh BAO, MRCPI, MRCS

A thesis presented for the award of MD to the Royal
College of Surgeons in Ireland, 123 St Stephen's Green,
Dublin 2, based on research conducted at the Department of
Surgery, RCSI Education and Research Centre, Beaumont
Hospital, Dublin 9.

2012

Supervisors: Professor JM Redmond
Dr Jonathan McGuinness

Contents

	Page
Declaration	7
Acknowledgements	8
Abbreviations	9
Summary	10
Chapter 1	
General Introduction	
1.1 Introduction	12
1.2 Background	13
1.3 Pathogenesis of aortic disease in Marfan syndrome	19
1.4 Beta-blockade therapy	21
1.5 Surgical treatment	23
1.6 New potential therapeutic intervention	25
1.7 Losartan	26
1.8 Statins inhibit MMP-9 production	27
1.9 Aims of thesis	32
1.10 References	33
Chapter 2	
Materials and Methods	
2.1 A study of aortic root pathology in a murine model of Marfan syndrome	36
2.1.1 Background	36
2.1.2 Genetically typing the C1039G murine model	36
2.1.3 Drug administration	39
2.1.4 Transthoracic echocardiographic measurements of aortic root diameter	40

2.1.5	Millar cardiac catheter measurements of aortic and ventricular pressures	41
2.1.6	Harvesting tissues & histological analysis	43
2.1.7	Electron Microscopy protocol	46
	Histological protocol	46
	Stereological parameters investigated from images obtained by TEM	47
2.2	Ethical approval and animal care	49
2.3	Statistical Analysis	50
2.4	References	51

Chapter 3

Natural history of Marfan syndrome

3.1	Introduction	52
3.2	Materials and methods	57
3.3	Results	59
	3.3.1 Aortic root diameter	59
	3.3.2 Cardiac catheterization results	62
	3.3.3 Histology results	67
	3.3.4 Electron-microscopy of Aortic wall	74
3.4	Discussion	100
3.5	References	104

Chapter 4

A comparison of pharmaceutical treatments for attenuation of aortic root pathology in Marfan syndrome

4.1	Introduction	106
	4.1.1 Potential mechanism of Losartan	107
	4.1.2 Potential mechanism of Doxycycline	108
	4.1.3 Potential mechanism of Pravastatin	108

4.2	Aims and objectives	109
4.3	Materials and methods	110
4.4	Results	114
4.4.1	Aortic root diameter results	115
4.4.2	Cardiac catheterization results	117
4.4.3	Histology results	118
4.4.4	Electron Microscopy / Ultra-structural analysis	123
4.4.5	Electron photomicrographs of aortic tissue from different treatment and control groups.	124
4.5	Discussion	135
4.6	References	141

Chapter 5

Pravastatin attenuates aortic root pathology, optimisation of dose and timing of therapy in Marfan syndrome.

5.1	Introduction	143
5.2	Materials and methods	145
5.3	Results	147
5.3.1	The effect of pravastatin on the normal aorta	147
5.3.2	Optimising the dose of pravastatin for aortic pathology in Marfan syndrome	150
5.3.3	Investigation of the optimum timing of initiation of pravastatin therapy for aortic pathology in Marfan syndrome	153
5.3.4	Effect of pravastatin on proteoglycan deposition within the aortic wall.	156
5.4	Discussion	158
5.5	References	162

Chapter 6

Discussion

6.1	Discussion	164
6.2	References	171
	References	173
	Appendix 1	
1.	Ethical approval	179

Declaration

I declare that this thesis, which I submit to RCSI for examination in consideration of the award of a higher degree, Doctor of Medicine (MD), is my own personal effort. Where any of the content presented is the result of input or data from a related collaborative research programme this is duly acknowledged in the text such that it is possible to ascertain how much of the work is my own. I have not already obtained a degree in RCSI or elsewhere on the basis of this work. Furthermore, I took reasonable care to ensure that the work is original, and, to the best of my knowledge, does not breach copyright law, and has not been taken from other sources except where such work has been cited and acknowledged within the text.

Signed _____

Student Number _____

Date _____

Acknowledgements

I am most grateful to both my supervisors Professor Mark Redmond and Dr Jonathan McGuinness for their help and encouragement over my two years of research. I am also indebted to Martin Dunphy and Derek Borwick in the Biomedical Laboratory for their help with the animals, and to everyone in the Department of Surgery lab for answering all my basic science questions. Dr John Byrne and Dr Jonathan McGuinness, who initially set up this model prior to my starting this research, were invaluable in the early stages in teaching me the basics of animal and laboratory work. This was a complex animal model and as such could not have been possible without the practical help of veterinary radiologists Eloisa Terzo and Hester McAllister, veterinary anaesthetist Vihelmiina Huuskonen, along with the help of electron microscopists Alex Black and Sinead Kearney. Dr. Gang Chen's expertise with cardiac catheterisation was also of great assistance.

Most importantly, I would like to thank my family and friends for their support and encouragement throughout these two years.

Abbreviations

ANOVA = Analysis of variance

AP-1 = Activator protein-1

CVP = Central venous pressure

CT = Computed Tomography

DNA = Deoxyribonucleic acid

dP/dt = rate of change in pressure

FPP = Farnesyl pyrophosphate

GGPP = Geranylgeranylpyrophosphate

H&E = Haematoxylin and eosin

HMG-CoA reductase = 3-hydroxy-3-methyl-glutaryl-CoA reductase

LVEDP = Left ventricular end diastolic pressure

LVESP = Left ventricular end systolic pressure

MABP = Mean arterial blood pressure

MMP = Matrix metalloproteinase

MR = Magnetic Resonance

mRNA = Messenger ribonucleic acid

NF-kB = nuclear factor kappa B

PCR = Polymerase chain reaction

RER = Rough Endoplasmic Reticulum

S_v = Surface density

SMC = Smooth muscle cells

TEM = Transmission Electron Microscopy

TIMP = Tissue inhibitor of matrix metalloproteinase

TGF-beta = Transforming Growth Factor beta

V_v = Volume fraction

Summary

Aortic pathology can have devastating consequences with significant morbidity and mortality. Marfan syndrome patients have a profound predisposition to develop aortic root pathology and can develop complications of aortic root pathology such as aneurysm of the aorta (especially the aortic root), aortic dissection and aortic valve regurgitation.

Recent advances in understanding the pathophysiology of the consequences of fibrillin-1 deficiency in Marfan syndrome and the development of murine models of this condition have opened up the possibility for translational research to be conducted in this area. Potential pharmacological treatments can now be extensively researched prior to clinical trials.

Pravastatin, a 3-hydroxy-3-methyl-glutaryl-CoA (HMG-CoA) reductase inhibitor has been shown to have a beneficial effect on atherosclerosis via “pleiotropic,” or non-cholesterol related, anti-inflammatory mechanisms. These mechanisms may have a beneficial effect in aortic root pathology in Marfan syndrome.

The first aim of this research was to establish a natural history of aortic root pathology in Marfan syndrome and to study multiple aspects of aortic root pathology to gain an insight into the pathophysiology of the disease. The second aim was to compare the efficacy and mechanism of potential pharmacological treatments to attenuate aortic root pathology in Marfan syndrome, Pravastatin, Losartan and Doxycycline. The third aim was to optimise the dose and timing of administration of Pravastatin for aortic root pathology in Marfan syndrome. These aims were studied in a murine model of Marfan syndrome.

The results obtained demonstrate that Pravastatin is equipotent to Losartan in attenuation of aortic root dilatation in a murine model of Marfan syndrome. Doxycycline's performance was inferior to both Pravastatin and Losartan in attenuation of aortic root pathology.

This research provides a basis for further study into the mechanisms of aortic pathology. It also provides evidence for a novel potential treatment for aortic root pathology in Marfan syndrome, namely, Pravastatin.

Chapter 1

General Introduction

1.1 Introduction:

Marfan syndrome is an autosomal dominant inherited disorder due to a defective form of the fibrillin-1 gene. Aortic pathology presents the major challenge and is responsible for the most significant morbidity and mortality, through the complications of aortic aneurysm, dissection, and aortic regurgitation. Through the development of the Marfan murine models, we now understand that aortic pathology in Marfan syndrome is not due to a congenital defect in elastogenesis but rather to secondary haemodynamic and inflammatory processes that develop as a consequence of lack of fibrillin-1 expression (Ramirez and Pereira 1999; Bunton, Biery *et al.* 2001). This suggests that pharmacological therapy to modify these processes may be useful in ameliorating aortic pathology, particularly if they are applied in a prophylactic form before clinically detectable aortic pathology develops.

Statins (HMG-CoA reductase inhibitors) are commonly used, relatively safe drugs, developed for the management of hypercholesterolaemia. They represent a drug that patients are generally started on for lifelong therapy. Used in the management of documented vascular disease they have also been shown to have anti-inflammatory actions through inhibition of certain MMP (matrix metalloproteinases) secretion from monocytes (Grip, Janciauskiene *et al.* 2002), macrophages (Bellosta, Via *et al.* 1998; Luan, Chase *et al.* 2003) and vascular smooth muscle cells (Luan, Chase *et al.* 2003); as well as anti-proliferative and anti-migratory effects on vascular smooth muscle cells (Porter, Naik *et al.* 2002). It is these properties of statins combined with their

prophylactic use before aortic inflammation and elastolysis develops that could be particularly beneficial in Marfan syndrome.

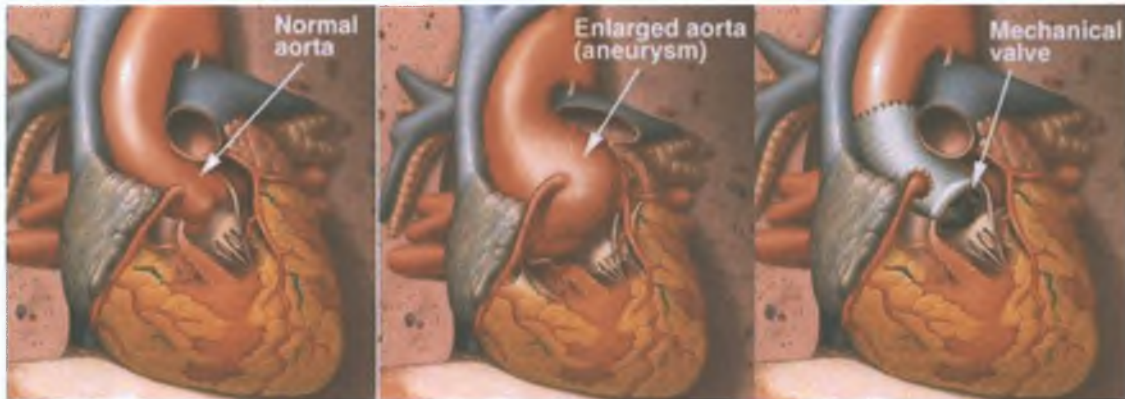


Figure 1.1{Ref.:www.marfanresearchfoundation.ie (with permission from author given by Dr.John Byrne)}: The diagram above and to the left, shows a normal heart with the arrow pointing to the beginning of the aorta as it leaves the heart called the "aortic root". The middle diagram shows the heart of a person with Marfan syndrome showing dilation of the aortic root which predisposes to a leaky aortic valve, excessive enlargement where the aorta can rupture called an aneurysm, or spontaneous tearing of the wall of the aorta called a dissection. The diagram on the right shows the heart of a patient with Marfan syndrome who has had surgery to replace the aortic root and valve with an artificial tube and mechanical valve to prevent development of an aneurysm or dissection, or to repair a leaking stretched aortic valve.

1.2 Background:

Marfan syndrome is uncommon, but cardiovascular pathology occurs in more than 90% of those affected and manifests in young people often necessitating complex cardiac and

aortic surgery. In many cases, surgery arises as an emergency due to aortic dissection or symptomatic aneurysm, but with increasing awareness among both physicians and the population in general, there is now a move towards earlier surgical intervention when aortic root size is increasing on serial echocardiography, computed tomography or magnetic resonance angiography studies. Of note, echocardiographic studies measure the internal diameter, whereas most patients undergo definitive imaging by CT and/or MR, which measures the external diameter (expected to be 0.2 to 0.4 cm larger than internal diameter), and external diameter is the measurement used in most cases to determine the threshold for surgical repair. Aortic root replacement then removes the potential risk of Type A dissection, ascending aortic aneurysm formation and aortic regurgitation. There are a number of classification systems to stage dissection of the aorta. The Stanford classification of aortic dissection distinguishes between *type A* and *type B*. (DeBakey, Beall *et al.* 1966) *Type A* means the dissection involves the ascending aorta, whereas *type B* dissection does not involve the ascending aorta. The De Bakey classification subdivides the dissection process, with *type I* dissection involving the entire aorta, *type II* dissection involving only the ascending aorta, and *type III* dissection sparing the ascending aorta and the arch. (DeBakey, Henly *et al.* 1965) Various attempts to further subdivide both classifications have not yet been established in the medical community. (Lansman, McCullough *et al.* 1999) There is also an established benefit with the use of beta blockers to retard aortic dilation in those with documented aortic enlargement. However, there is currently no treatment to delay or attenuate the development of aortic pathology.

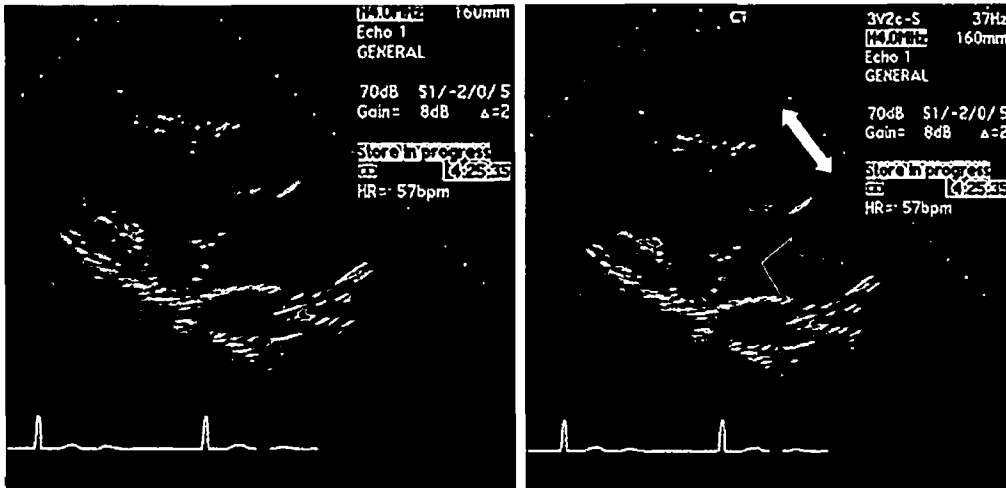


Figure 1.2: Transthoracic echocardiogram of a patient with Marfan syndrome with mitral valve (green arrow) prolapse and 4-cm ascending aortic aneurysm (white arrow).

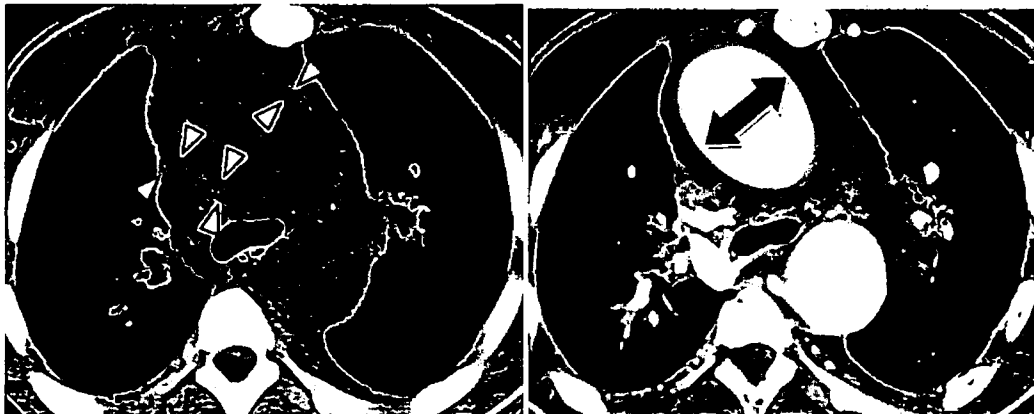


Figure 1.3: Axial CT images of an aortic root aneurysm, non-contrast (left) and contrast (right). White arrows display the aortic wall and black arrow displays the dilated aortic root diameter.

In a study of life expectancy of patients with Marfan syndrome published in 1995, cardiovascular complications which were the cause of death in patients were as follows: congestive heart failure, aortic dissection, aneurysm rupture, sudden death, perioperative

and others(including cerebral haemorrhage, myocardial infarction, arrhythmia and infective endocarditis).(Silverman, Burton *et al.* 1995) The mean age of death in this study was 41+/-18 years compared to 32+/-16 years in 1972.(Murdoch, Walker *et al.* 1972) Life expectancy continues to improve with improved diagnosis, prospective management, lifestyle adaptations, beta-blockade and most importantly aortic aneurysm repair.(Pyeritz 2009) Despite these measures, causes of late death in patients after aortic aneurysm repair include: rupture/dissection of an aneurysm, congestive heart failure, perioperative death during subsequent aneurysm surgery, stroke, arrhythmia, prosthetic valve endocarditis, and valve failure.(Finkbohner, Johnston *et al.* 1995)

Much of our new understanding of aortic pathology in Marfan syndrome comes from the development of the Marfan mouse (Pereira, Andrikopoulos *et al.* 1997). The discovery that the problematic gene in Marfan syndrome was fibrillin 1, a component of microfibrils, allowed for the development of two forms of the Marfan mouse(Arteaga-Solis, Gayraud *et al.* 2000). The mg^{Δ} mouse has internally deleted fibrillin-1 proteins at a level that is 10 times less than that expressed normally and is a structurally smaller protein. The homozygous mg^{Δ} mouse dies within 2 weeks of birth from aortic complications which limits the ability to follow the natural history of the disease (Arteaga-Solis, Gayraud *et al.* 2000). However, the homozygous mg^R mouse possesses 4 times less fibrillin-1 protein than normal and the protein is of the same size as the wild type fibrillin-1 protein. This produces a mouse that dies of aortic complications between 12 and 24 weeks of age, allowing for more detailed study of the natural history of aortic pathology (Arteaga-Solis, Gayraud *et al.* 2000). Examination of pathological vascular

specimens from patients who died with Marfan syndrome or who underwent aortic surgery shows that the changes that occur in the elastic vessels of these patients are the same that one sees with the mgR mouse, again reinforcing the suitability of this model for interventional studies (Bunton, Biery *et al.* 2001). The problem with the mgR mouse is that they are homozygous recessive which does not mirror the true clinical scenario in which patients with Marfan syndrome inherit it in an autosomal dominant manner.

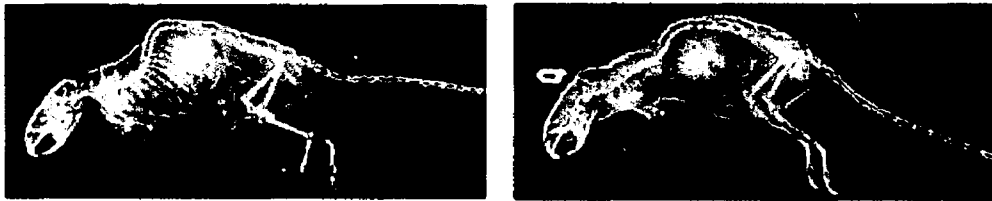


Figure 1.4: X-ray images of the C1039G “Marfan-mouse” on left (with prominent thoracic kyphosis) and wild-type mouse on right.(Judge, Biery *et al.* 2004)

Recently a team at Johns Hopkins University successfully developed a heterozygous Marfan mouse that has a missense mutation in the fibrillin-1 gene sufficient to cause the phenotypic problems with Marfan syndrome when only one copy of the mutated fibrillin-1 gene is inherited. This allows for an autosomal dominant pattern of inheritance similar to the clinical situation. These mice have the mutation C1039G in which a cysteine residue in the fibrillin-1 protein is replaced with glycine, and mirrors a mutation seen in patients with Marfan syndrome. The heterozygous C1039G Marfan mouse has a reduced amount of microfibrils as a result of the mutation which produces skeletal deformities and deterioration in aortic wall architecture, similar to the changes seen in human Marfan syndrome. These Marfan mice however, do not die of aortic dilation related

complications but do develop aortic wall thickening and classic Marfan-type histological changes within the aortic wall (Judge, Biery *et al.* 2004).

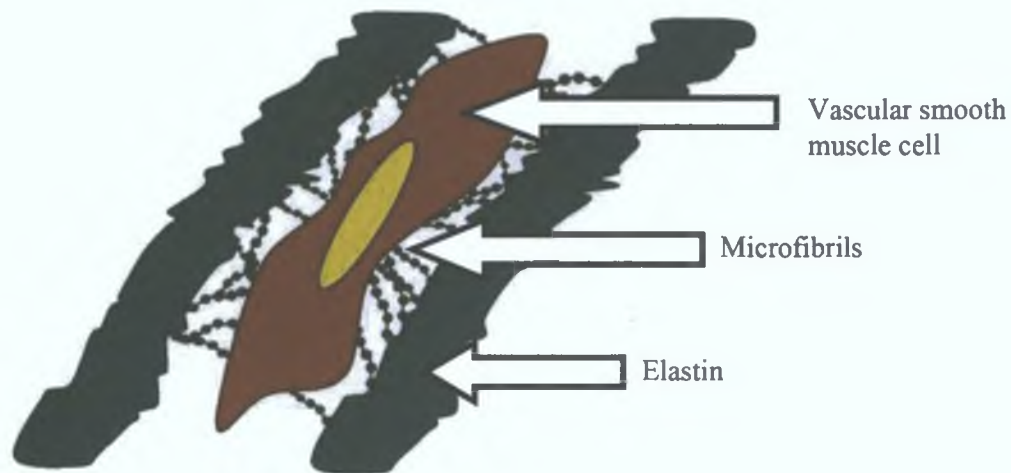


Figure 1.5: Diagram of arrangement of vascular smooth muscle cell, elastin and microfibril assembly (polymerised fibrillin-1)

In order to understand the aortic pathology in Marfan syndrome, knowledge of normal aortic structure and function is essential. Common to all vessels is an intima composed of an endothelial monolayer, and an adventitia composed of fibrous collagen bundles. It is the intervening medial layer that varies depending on vessel size and function. The aortic medial layer is composed primarily of elastic fibres, with some smooth muscle cells, unlike smaller vessels which would have a more muscular medial layer (Ramirez and Pereira 1999). The function of this is that the elastic medial layer provides a very compliant vessel that can resist dynamic systolic and diastolic pulsations, transmitting a pulse wave along the arterial tree (Ramirez and Pereira 1999). The elastic aortic medial layer is composed of elastin fibres interwoven in a matrix of microfibrils (Arteaga-Solis, Gayraud *et al.* 2000). The fibrillin-1 protein that is defective or diminished in Marfan

syndrome is a protein component of microfibrils. Microfibrils through fibrillin-1 provide anchoring connections to surrounding smooth muscle cells, the endothelial monolayer, and connective tissue of the adventitia (Ramirez and Pereira 1999; Arteaga-Solis, Gayraud *et al.* 2000). Microfibrils have been described as, "flexible links that make the aortic wall a working unit"(Arteaga-Solis, Gayraud *et al.* 2000).

1.3 Pathogenesis of aortic disease in Marfan syndrome.

Initially it was thought that fibrillin-1 deficiency leads to impaired elastic fibre formation in the embryo producing a congenitally weak aortic wall.(Ramirez and Pereira 1999) We now realize that this is not the case and that fibrillin-1 appears to play a role in the normal homeostasis of the aortic wall.(Ramirez and Pereira 1999; Bunton, Biery *et al.* 2001) The pathological consequences of a fibrillin-1 deficiency are not purely due to the mechanical stress being imposed on an intrinsically weak, poorly connected medial aortic layer. Vascular smooth muscle cells which have lost their fibrillin-1 connectivity appear to acquire abnormal synthetic and inflammatory properties (Bunton, Biery *et al.* 2001). This is often an early detectable change in the aortic wall, where the smooth muscle cells secrete more matrix components and MMP-9, one of the main metalloproteinases mediating elastic fibre destruction (Bunton, Biery *et al.* 2001). This leads to the initial phase of elastic fibre fragmentation (Bunton, Biery *et al.* 2001). Macrophages then seem to localize to these sites of elastic fibre damage and liberate more metalloproteinases in a second more intense inflammatory phase.(Pereira, Lee *et al.* 1999; Bunton, Biery *et al.* 2001) When this is coupled with intense haemodynamic strain, and the loss of tensile strength from lack of fibrillin connections with the collagenous adventitial layer, aortic

dilation ensues.(Pereira, Lee *et al.* 1999; Ramirez and Pereira 1999; Arteaga-Solis, Gayraud *et al.* 2000) In advanced stages there is an intense infiltration of macrophages at the adventitial surface of the elastic medial layer, which extend into a now severely diminished aortic medial layer, predisposing to pathological aneurysmal dilation and dissection (Pereira, Lee *et al.* 1999).

It is this inflammation mediated matrix destruction both early with vascular smooth muscle cell induced matrix destruction through MMP-9, and later with macrophage induced elastolysis, that may be able to intervene against clinically(Arteaga-Solis, Gayraud *et al.* 2000; Bunton, Biery *et al.* 2001). The ability to provide an anti-inflammatory strategy prophylactically in this scenario to minimize secondary events may maximize any potential therapeutic benefit.

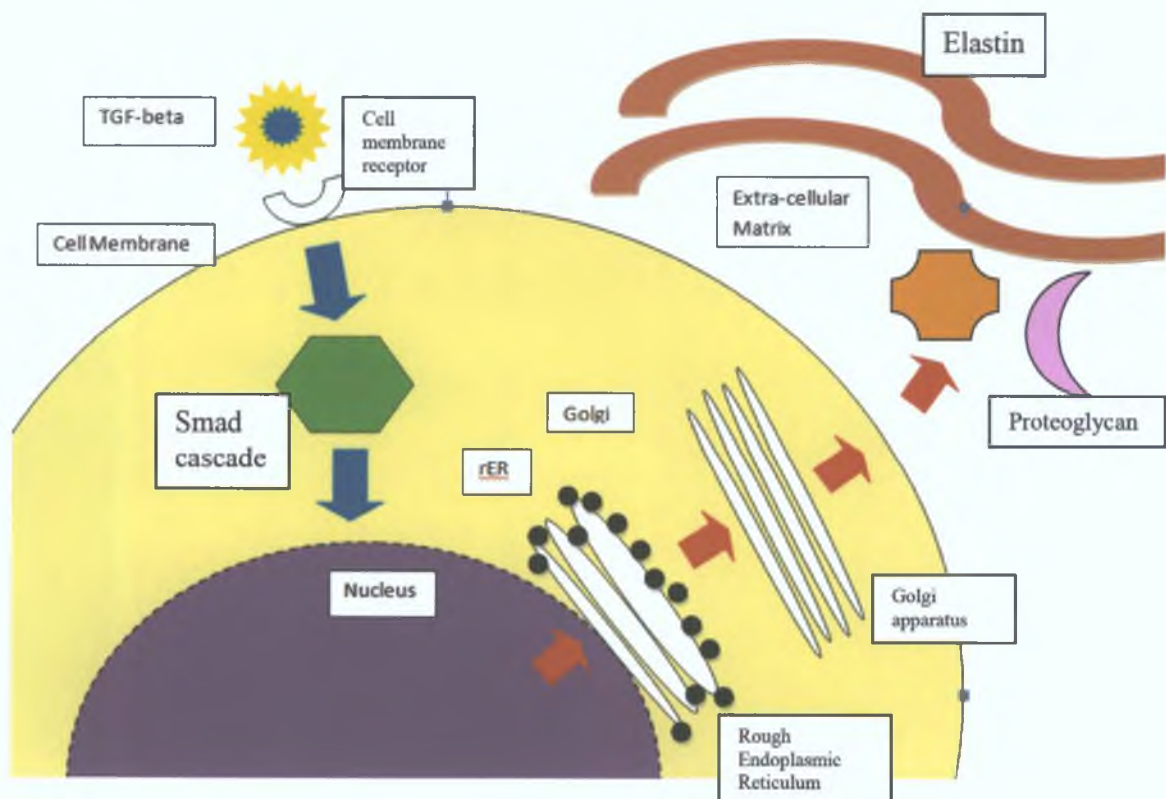


Figure 1.6: Diagrammatic representation of the vascular smooth muscle cell (yellow) and pathophysiology involved in Marfan syndrome. Fibrillin-1, is an important component of the elastin (brown) microfibril. It is secreted as a proteoglycan into the extracellular matrix and polymerises to form microfibrils. These microfibrils help to stabilise a complex that includes latent transforming growth factor-beta and transforming growth factor-beta. With less fibrillin-1, there is less latent transforming growth factor-beta to bind with transforming growth factor-beta, and thus it becomes active transforming growth factor-beta (blue & yellow star). It then activates the Smad cascade (green) by interacting at the cell membrane receptor (white). The Smad cascade induces transcription at the level of the nucleus (purple). Excess messengerRNA for matrix metalloproteinases (orange) and proteoglycan (pink), such as Versican are transcribed. These are then processed by the rough Endoplasmic Reticulum and secreted by the Golgi complexes.

1.4 Beta-blockade therapy

Propranolol is a non-selective beta-blocker which is mainly used in the treatment of hypertension. Its use has been advocated as a preventative therapeutic strategy to decrease the rate of aortic root dilatation and progression to aortic root dissection in patients with Marfan syndrome. Beta-blockade is used conceptually because of the negative inotropic and chronotropic effects on the heart. The proposed mechanisms of benefit of beta-blockers in Marfan syndrome include reduction in the rate of pressure increase in aorta (dP/dt) and reduction in heart rate, which reduces the number of systolic

impulses in a given period.(Prokop, Palmer *et al.* 1970) However, several studies have shown that beta-blocker treatment may not produce the desired haemodynamic effects in patients with marked dilation of the aortic root.(Yin, Brin *et al.* 1989; Baumgartner, Baumgartner *et al.* 2006) Atenolol, a selective β_1 inhibitor which more effectively reduces contractility and slows the heart rate, would in theory be more suitable for this purpose, with a lower side-effect profile. Some studies have shown slower aortic root growth, fewer cardiovascular end points (defined as aortic regurgitation, dissection, surgery, heart failure or death), and improved survival.(Shores, Berger *et al.* 1994) The response to beta-blocker therapy has been found to be heterogeneous.(Rios, Silber *et al.* 1999) Responders tended to be younger, with a smaller more compliant pre-treatment aorta. Non-responders tended to have more elastic fibre degeneration and more advanced disease of the aorta. A recent meta-analysis concluded that there is no evidence that beta-blockade therapy has a clinical benefit in patients with Marfan syndrome.(Gersony, McClaughlin *et al.* 2007)

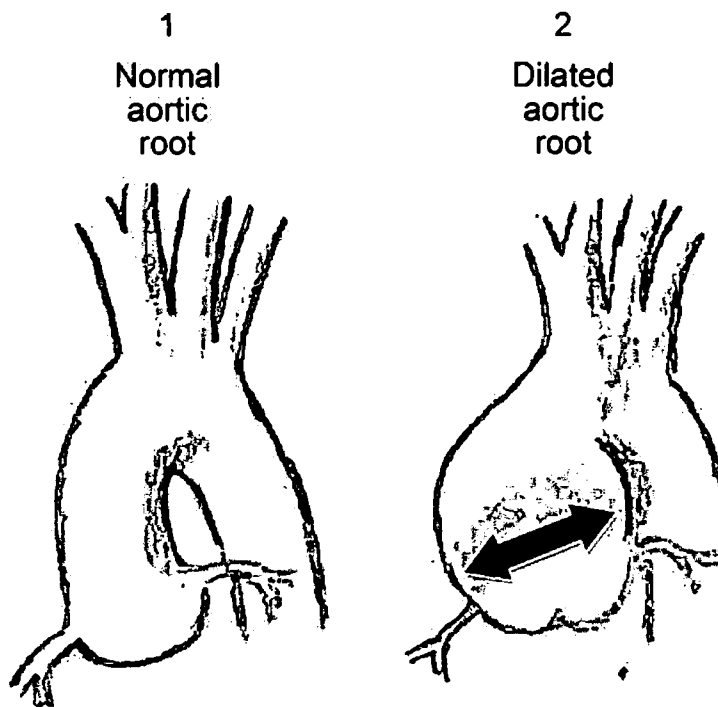


Figure 1.7: Diagram of normal and dilated aortic root with origin of coronary arteries and proximal branches of the aorta. Arrow showing direction of transmural pressure at which the change in pressure (dP/dt) affects the aortic wall. Original diagram from British Medical Bulletin(De Mozzi, Longo *et al.* 2008)

1.5 Surgical treatment

If medical treatment fails, and aortic root dilatation reaches 5cm or more, prophylactic surgery should be considered.(Groenink, Lohuis *et al.* 1999) One can also refer to a Z-score, which compares the maximum dimension at the level of the sinuses of Valsalva and compares to the predicted dimension for that person's body surface area.(Colan, McElhinney *et al.* 2006) Other factors such as sex, (one study suggests a threshold 0.5cm lower in females(Meijboom, Timmermans *et al.* 2005)), family history of dissection and aortic root growth rate of more than 0.5cm per year.(Hiratzka, Bakris *et al.* 2010) The

options for surgical repair include the Bentall composite graft repair, in which both the aortic root and the aortic valve are replaced, or a valve conserving technique such as re-implantation of the native aortic valve in a Dacron tube (described by David *et al.* 2003) or remodelling of the aortic root (de Oliveira, David *et al.* 2003; Nataf and Lansac 2006) The Bentall procedure has a low mortality in experienced hands with a favourable long-term survival, though long term anti-coagulation is required for mechanical valves. Aortic valve re-implantation techniques have also shown durability of the aortic valve. (Kallenbach, Karck *et al.* 2005)

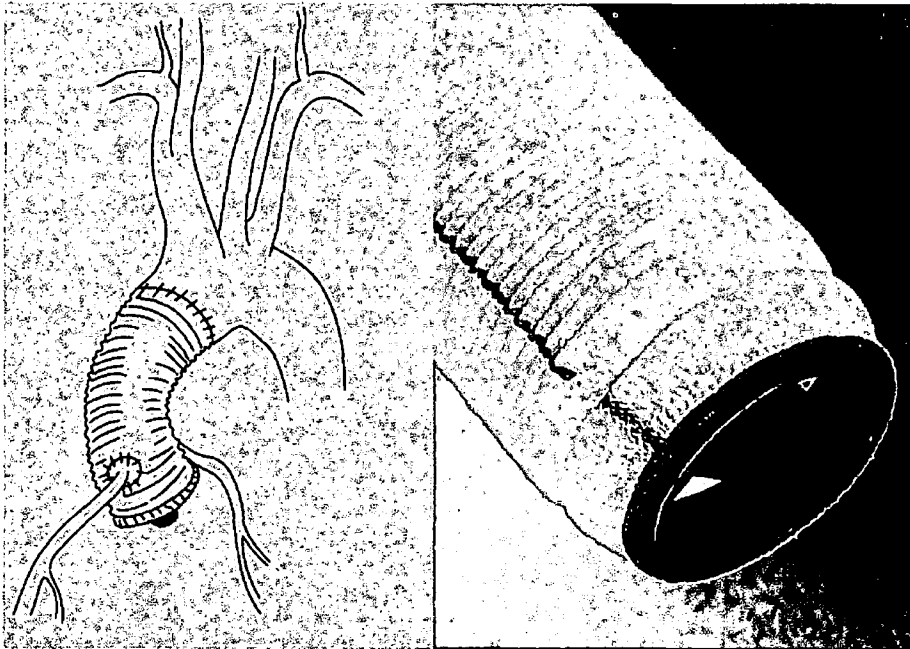


Figure 1.8: Drawing of implanted conduit with coronary arteries anastomosed to composite graft. Photograph of composite conduit with mechanical valve and Dacron tubing.(Lansac 2007)

1.6 New potential therapeutic intervention

The concept of therapeutic intervention for the aortic pathology of Marfan syndrome stems from the fact that the inflammatory fibro-proliferative response of macrophages could be attenuated with anti-inflammatory agents (Arteaga-Solis, Gayraud *et al.* 2000). Macrophages localize to the sites of elastic fibre fragmentation, and play a clear role in elastolysis (Arteaga-Solis, Gayraud *et al.* 2000). However, this occurs at a much later stage when significant elastic fibre destruction has already occurred. An even better strategy would be to intervene to prevent this occurring, i.e. at the stage in which vascular smooth cells are producing excessive matrix elements and secreting MMP-9 locally causing the initial phase of elastolysis (Bunton, Biery *et al.* 2001). This earlier process eventually leads to breach of the internal and external elastic laminae which then allows infiltration of inflammatory cells such as macrophages into the medial layer to cause the later intense elastolysis (Bunton, Biery *et al.* 2001). The importance of early MMP-9 production by the vascular smooth muscle cells is evidenced by the fact that immunoreactivity for MMP-9 is seen in early lesions before overt elastolysis or infiltration of inflammatory cells into the media (Bunton, Biery *et al.* 2001). Additionally, local expression of MMP-9 in the aortic media correlates with the extent of loss of elastin content, and elastic fibre architecture (Bunton, Biery *et al.* 2001). It has even been suggested that these enzymes from smooth muscle cells, such as MMP-9 may be sufficient to promote aneurysmal formation in patients with Marfan syndrome as the elastin that exists may be more prone to MMP-9 destruction due to a lack of fibrillin-1 (Marque, Kieffer *et al.* 2001). This early enhanced MMP-9 expression is not limited to

aortic pathology, but has also been described in the lungs of the Marfan mouse (Neptune, Frischmeyer *et al.* 2003).

As a result current interest exists in the antibiotic drug Doxycycline, which is a non-specific inhibitor of matrix metalloproteinases (Boyle, McDermott *et al.* 1998; Lalu, Gao *et al.* 2003; Peterson 2004). Doxycycline has mainly been investigated in relation to abdominal aortic aneurysm disease. In a rodent model of elastase induced aneurysms, pre-treatment with Doxycycline effectively suppresses the development of aneurysms and is associated with reduced aortic MMP-9 levels combined with reduced elastin destruction (Boyle, McDermott *et al.* 1998). In patients with established atheromatous abdominal aortic aneurysms, treatment with oral Doxycycline for 7 days prior to aneurysm repair significantly reduces aortic MMP-9 mRNA levels (Curci, Mao *et al.* 2000). Studies are currently underway using the Marfan mouse looking at the potential therapeutic benefit of Doxycycline treatment.

1.7 Losartan

Losartan belongs to the angiotensin II receptor antagonist class of drugs. Recent studies in a mouse model of Marfan syndrome with aortic disease similar to that seen in humans compared treatment with Losartan to propranolol. Losartan treatment prevented elastic fibre fragmentation, blunted TGF-beta signalling in the aortic media and normalized aortic root growth in comparison to propranolol and control groups. (Habashi, Judge *et al.* 2006) Elevated levels of Transforming Growth Factor Beta (TGF- β) activate the TGF- β receptor at the level of the cell membrane, which signals the receptor complex to phosphorylate Smad-2, which activates the Smad cascade within the cell, in turn

activating release of excessive amounts of matrix metalloproteinases. Losartan has been found to down-regulate the expression of TGF- β receptors Type I and II in a model of diabetic nephropathy in rats.(Guo and Qiu 2003) Losartan has an effect of reducing the level of TGF- β signalling and so the levels of phosphorylated Smad2 are reduced.(Habashi, Judge *et al.* 2006) This in turn, has reduced the destructive effect of excessive TGF- β levels on the cell matrix.

There is also a clinical trial using Losartan in Marfan syndrome patients under the age of 25 years which is in progress.(Lacro, Dietz *et al.* 2007; Brooke, Habashi *et al.* 2008)

1.8 Statins inhibit MMP-9 production

Statins were initially developed to manage hypercholesterolaemia by reducing endogenous hepatic cholesterol production through inhibition of the enzyme HMG-CoA reductase. In clinical practice, it was noted that patients on statins had less acute cardiovascular events before any angiographic improvements in their coronary disease were detectable with imaging studies(Crisby, Nordin-Fredriksson *et al.* 2001). This suggested that the statins were also working to stabilize the atherosclerotic plaques. This plaque stabilization was not just due to a reduction in lipid content of the plaque, but also due to reduced inflammation within the plaque (Crisby, Nordin-Fredriksson *et al.* 2001). When carotid plaques removed at endarterectomy from patients on statins are compared to those not on statins, they are shown to contain fewer macrophages, fewer T cells, less MMP-2 activity, reduced vascular smooth muscle cell apoptosis, enhanced TIMP-

1(tissue inhibitor of metalloproteinases-1) activity, and increased collagen levels(Crisby, Nordin-Fredriksson *et al.* 2001). Similarly, patients with acute coronary syndromes have elevated serum MMP-2 and MMP-9 levels which decrease significantly with 30 days of treatment with statins (Tziakas, Chalikias *et al.* 2004). Statins have been shown to attenuate MMP production from a number of cell types including human vascular smooth muscle cells isolated from peripheral veins(Luan, Chase *et al.* 2003), aortic vascular smooth muscle cells (of particular interest in Marfan syndrome)(Luan, Chase *et al.* 2003), macrophages (also of interest in those with Marfan syndrome)(Bellosta, Via *et al.* 1998), monocytes, and even in the aneurysmal wall removed from patients with abdominal aortic aneurysms subsequently cultured in-vitro(Nagashima, Aoka *et al.* 2002). In the case of human vascular smooth muscle cells treated with statin doses used clinically as "high dose" statin, there is significant inhibition of inducible MMP secretion, i.e.: MMP-1 secretion reduced by 52%, MMP-3 secretion reduced by 71%, and MMP-9 secretion reduced by 73% ($P<0.01$)(Luan, Chase *et al.* 2003). One of the key potential benefits for Marfan syndrome is that statins appear to inhibit MMP secretion from vascular smooth muscle cells no matter what the stimulus is for that MMP secretion (Bellosta, Via *et al.* 1998; Luan, Chase *et al.* 2003). This is because this process is not lipoprotein dependent, but instead involves post-transcriptional inhibition (Crisby, Nordin-Fredriksson *et al.* 2001; Luan, Chase *et al.* 2003). Fortunately, this post-transcriptional inhibitory mechanism of statins is selective for MMP's and not merely an overall inhibitory effect on protein synthesis (Luan, Chase *et al.* 2003). Additionally, a reduction in serum MMP-9 activity occurs not only in individuals with hypercholesterolaemia but also in healthy people on statins which suggests that those with Marfan syndrome may also be able to

benefit from a reduction in MMP-9 levels with statin use(Tziakas, Chalikias *et al.* 2004). Statins also do not affect production of TIMP-1 or TIMP-2 (endogenous inhibitors of MMP activity), which further shifts the MMP / TIMP balance towards inactive enzymes (Luan, Chase *et al.* 2003).

Statins have also been shown to attenuate intimal hyperplasia through reducing vascular smooth muscle cell proliferation and migration (Porter, Naik *et al.* 2002). Statins have been shown to inhibit the proliferation, migration and invasion of vascular smooth muscle cells from saphenous veins. This appeared to be due to inhibition of prenylation.(Porter and Turner 2002)They also are anti-inflammatory through inhibition of NFκβ and AP-1, important transcription factors in inflammation (Dichtl, Dulak *et al.* 2003). Both of these effects could be of benefit in the aortic pathology with Marfan syndrome.

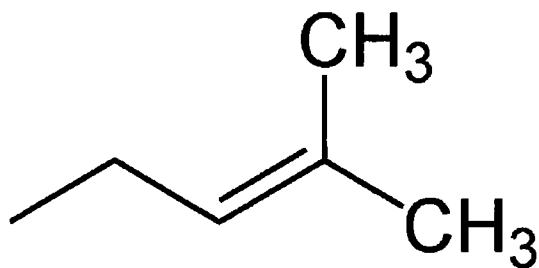


Figure 1.9: Prenyl Group

The intracellular mechanism of action of statins is illustrated below:

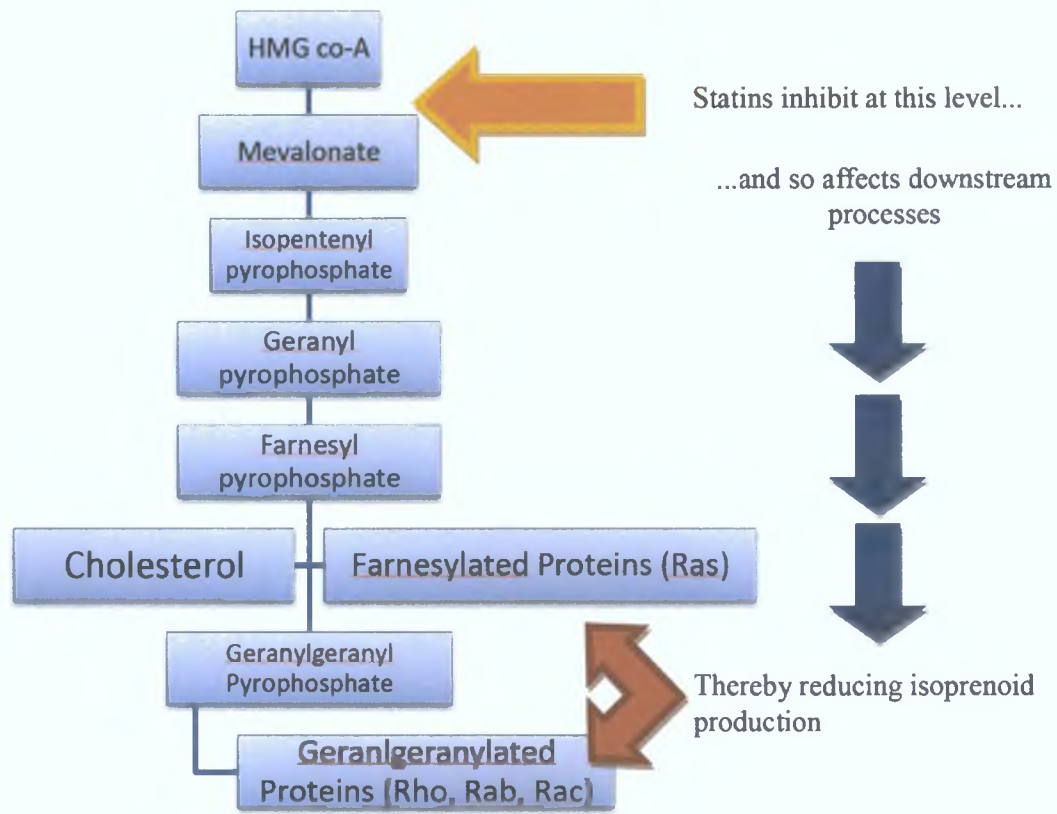


Figure 1.10: The HMG Co-A pathway with diagrammatic representation of the effect of statin therapy on this pathway.

Isoprenoids have important roles in mammalian cells in prenylation of proteins, a process which is required for their membrane localization and function (Zhang and Casey 1996). Statins are potent inhibitors of 3-hydroxy-3-methylglutaryl coenzyme A (HMG-CoA) and thereby affect the mevalonate pathway, which is important for the biosynthesis of isoprenoids such as geranylgeranyl pyrophosphate (GGPP) and farnesyl pyrophosphate (FPP), as well as cholesterol. (Goldstein and Brown 1990) GGPP and FPP are important lipid attachments for the posttranslational modification of several proteins that include the small GTP-binding proteins Ras, Rac, and Rho. Attachment of these lipids, so-called isoprenylation, is essential for activation and intracellular transport of proteins crucial for

various cellular functions, such as maintenance of cell shape, motility, factor secretion, differentiation, and proliferation. A decrease in HMG-CoA results in a decrease in the components of the pathway which finally results in less intracellular transport and less cisternae/Golgi.

It seems that statins have an effect on lipid raft-mediated intracellular transport and cell-surface expression of a variety of molecules or on the activation of certain proteins by isoprenylation, thereby affecting many cellular functions. Experimentally inhibiting such prenylation of a protein called Rab leads to a block in protein secretion from the cell (Bellosa, Via *et al.* 1998). This could have benefits in limiting excessive secretion of matrix elements from vascular smooth muscle cells in those with Marfan syndrome. In fact, it has been previously noted that the selected vascular smooth muscle cell and connective tissue abnormalities seen in Marfan syndrome are also common in the maturation of atheromatous lesions (Bunton, Biery *et al.* 2001). It is this exact pathology that statins appear to intervene in producing their "plaque stabilizing" effect. Clearly these parallels suggest a benefit for statin use in Marfan syndrome.

1.9 Aims of thesis

The natural history of Marfan syndrome will be investigated. Investigation will include *in-vivo* physiological measurement of the aortic root diameter, with a view to documenting progression of pathological dilatation and to compare these measurements to observed measurements of normal growth in a wild-type murine model. A histological analysis will be conducted to compare observed changes in the size of the aneurysm *in-vivo* and the pathological histology changes observed. The ultra-structure of the cells within the aortic wall tissue will be examined and analysed, with enumeration of the cell organelles or estimation of the volume of the cell organelles. The application of statins in a prophylactic setting for lifelong use will be investigated in terms of potential to attenuate the development and course of aortic pathology associated with Marfan syndrome. Statin therapy will be compared to angiotensin II receptor antagonism and Doxycycline therapy, using both physiological and histological parameters.

1.10 References

- Arteaga-Solis, E., B. Gayraud, *et al.* (2000). "Elastic and collagenous networks in vascular diseases." Cell Struct Funct **25**(2): 69-72.
- Baumgartner, D., C. Baumgartner, *et al.* (2006). "Different patterns of aortic wall elasticity in patients with Marfan syndrome: a noninvasive follow-up study." J Thorac Cardiovasc Surg **132**(4): 811-819.
- Bellosta, S., D. Via, *et al.* (1998). "HMG-CoA reductase inhibitors reduce MMP-9 secretion by macrophages." Arterioscler Thromb Vasc Biol **18**(11): 1671-1678.
- Boyle, J. R., E. McDermott, *et al.* (1998). "Doxycycline inhibits elastin degradation and reduces metalloproteinase activity in a model of aneurysmal disease." J Vasc Surg **27**(2): 354-361.
- Brooke, B. S., J. P. Habashi, *et al.* (2008). "Angiotensin II blockade and aortic-root dilation in Marfan's syndrome." N Engl J Med **358**(26): 2787-2795.
- Bunton, T. E., N. J. Biery, *et al.* (2001). "Phenotypic alteration of vascular smooth muscle cells precedes elastolysis in a mouse model of Marfan syndrome." Circ Res **88**(1): 37-43.
- Colan, S. D., D. B. McElhinney, *et al.* (2006). "Validation and re-evaluation of a discriminant model predicting anatomic suitability for biventricular repair in neonates with aortic stenosis." J Am Coll Cardiol **47**(9): 1858-1865.
- Crisby, M., G. Nordin-Fredriksson, *et al.* (2001). "Pravastatin treatment increases collagen content and decreases lipid content, inflammation, metalloproteinases, and cell death in human carotid plaques: implications for plaque stabilization." Circulation **103**(7): 926-933.
- Curci, J. A., D. Mao, *et al.* (2000). "Preoperative treatment with Doxycycline reduces aortic wall expression and activation of matrix metalloproteinases in patients with abdominal aortic aneurysms." J Vasc Surg **31**(2): 325-342.
- De Mozzi, P., U. G. Longo, *et al.* (2008). "Bicuspid aortic valve: a literature review and its impact on sport activity." Br Med Bull **85**: 63-85.
- de Oliveira, N. C., T. E. David, *et al.* (2003). "Results of surgery for aortic root aneurysm in patients with Marfan syndrome." J Thorac Cardiovasc Surg **125**(4): 789-796.
- DeBakey, M. E., A. C. Beall, Jr., *et al.* (1966). "Dissecting aneurysms of the aorta." Surg Clin North Am **46**(4): 1045-1055.
- DeBakey, M. E., W. S. Henly, *et al.* (1965). "Surgical Management of Dissecting Aneurysms of the Aorta." J Thorac Cardiovasc Surg **49**: 130-149.
- Dichtl, W., J. Dulak, *et al.* (2003). "HMG-CoA reductase inhibitors regulate inflammatory transcription factors in human endothelial and vascular smooth muscle cells." Arterioscler Thromb Vasc Biol **23**(1): 58-63.
- Finkbohner, R., D. Johnston, *et al.* (1995). "Marfan syndrome. Long-term survival and complications after aortic aneurysm repair." Circulation **91**(3): 728-733.
- Gersony, D. R., M. A. McCloughlin, *et al.* (2007). "The effect of beta-blocker therapy on clinical outcome in patients with Marfan's syndrome: a meta-analysis." Int J Cardiol **114**(3): 303-308.
- Goldstein, J. L. and M. S. Brown (1990). "Regulation of the mevalonate pathway." Nature **343**(6257): 425-430.

- Grip, O., S. Janciauskiene, *et al.* (2002). "Atorvastatin activates PPAR-gamma and attenuates the inflammatory response in human monocytes." Inflamm Res **51**(2): 58-62.
- Groenink, M., T. A. Lohuis, *et al.* (1999). "Survival and complication free survival in Marfan's syndrome: implications of current guidelines." Heart **82**(4): 499-504.
- Guo, Z. X. and M. C. Qiu (2003). "[Losartan downregulates the expression of transforming growth factor beta type I and type II receptors in kidney of diabetic rat]." Zhonghua Nei Ke Za Zhi **42**(6): 403-408.
- Habashi, J. P., D. P. Judge, *et al.* (2006). "Losartan, an AT1 antagonist, prevents aortic aneurysm in a mouse model of Marfan syndrome." Science **312**(5770): 117-121.
- Hiratzka, L. F., G. L. Bakris, *et al.* (2010). "2010 ACCF/AHA/AATS/ACR/ASA/SCA/SCAI/SIR/STS/SVM guidelines for the diagnosis and management of patients with Thoracic Aortic Disease: a report of the American College of Cardiology Foundation/American Heart Association Task Force on Practice Guidelines, American Association for Thoracic Surgery, American College of Radiology, American Stroke Association, Society of Cardiovascular Anesthesiologists, Society for Cardiovascular Angiography and Interventions, Society of Interventional Radiology, Society of Thoracic Surgeons, and Society for Vascular Medicine." Circulation **121**(13): e266-369.
- Judge, D. P., N. J. Biery, *et al.* (2004). "Evidence for a critical contribution of haploinsufficiency in the complex pathogenesis of Marfan syndrome." J Clin Invest **114**(2): 172-181.
- Kallenbach, K., M. Karck, *et al.* (2005). "Decade of aortic valve sparing reimplantation: are we pushing the limits too far?" Circulation **112**(9 Suppl): I253-259.
- Lacro, R. V., H. C. Dietz, *et al.* (2007). "Rationale and design of a randomized clinical trial of beta-blocker therapy (atenolol) versus angiotensin II receptor blocker therapy (Losartan) in individuals with Marfan syndrome." Am Heart J **154**(4): 624-631.
- Lalu, M. M., C. Q. Gao, *et al.* (2003). "Matrix metalloproteinase inhibitors attenuate endotoxemia induced cardiac dysfunction: a potential role for MMP-9." Mol Cell Biochem **251**(1-2): 61-66.
- Lansac, d. C., Jondeau (2007). "Distinctive features of thoracic aorta surgery in Marfan Syndrome " MT Cardiology **3**(3): 212-225.
- Lansman, S. L., J. N. McCullough, *et al.* (1999). "Subtypes of acute aortic dissection." Ann Thorac Surg **67**(6): 1975-1978; discussion 1979-1980.
- Luan, Z., A. J. Chase, *et al.* (2003). "Statins inhibit secretion of metalloproteinases-1, -2, -3, and -9 from vascular smooth muscle cells and macrophages." Arterioscler Thromb Vasc Biol **23**(5): 769-775.
- Marque, V., P. Kieffer, *et al.* (2001). "Aortic wall mechanics and composition in a transgenic mouse model of Marfan syndrome." Arterioscler Thromb Vasc Biol **21**(7): 1184-1189.
- Meijboom, L. J., J. Timmermans, *et al.* (2005). "Aortic root growth in men and women with the Marfan's syndrome." Am J Cardiol **96**(10): 1441-1444.
- Murdoch, J. L., B. A. Walker, *et al.* (1972). "Life expectancy and causes of death in the Marfan syndrome." N Engl J Med **286**(15): 804-808.

- Nagashima, H., Y. Aoka, *et al.* (2002). "A 3-hydroxy-3-methylglutaryl coenzyme A reductase inhibitor, cerivastatin, suppresses production of matrix metalloproteinase-9 in human abdominal aortic aneurysm wall." J Vasc Surg **36**(1): 158-163.
- Nataf, P. and E. Lansac (2006). "Dilation of the thoracic aorta: medical and surgical management." Heart **92**(9): 1345-1352.
- Neptune, E. R., P. A. Frischmeyer, *et al.* (2003). "Dysregulation of TGF-beta activation contributes to pathogenesis in Marfan syndrome." Nat Genet **33**(3): 407-411.
- Pereira, L., K. Andrikopoulos, *et al.* (1997). "Targetting of the gene encoding fibrillin-1 recapitulates the vascular aspect of Marfan syndrome." Nat Genet **17**(2): 218-222.
- Pereira, L., S. Y. Lee, *et al.* (1999). "Pathogenetic sequence for aneurysm revealed in mice underexpressing fibrillin-1." Proc Natl Acad Sci U S A **96**(7): 3819-3823.
- Peterson, J. T. (2004). "Matrix metalloproteinase inhibitor development and the remodeling of drug discovery." Heart Fail Rev **9**(1): 63-79.
- Porter, K. E., J. Naik, *et al.* (2002). "Simvastatin inhibits human saphenous vein neointima formation via inhibition of smooth muscle cell proliferation and migration." J Vasc Surg **36**(1): 150-157.
- Porter, K. E. and N. A. Turner (2002). "Statins for the prevention of vein graft stenosis: a role for inhibition of matrix metalloproteinase-9." Biochem Soc Trans **30**(2): 120-126.
- Prokop, E. K., R. F. Palmer, *et al.* (1970). "Hydrodynamic forces in dissecting aneurysms. In-vitro studies in a Tygon model and in dog aortas." Circ Res **27**(1): 121-127.
- Pyeritz, R. E. (2009). "Marfan syndrome: 30 years of research equals 30 years of additional life expectancy." Heart **95**(3): 173-175.
- Ramirez, F. and L. Pereira (1999). "Mutations of extracellular matrix components in vascular disease." Ann Thorac Surg **67**(6): 1857-1858; discussion 1868-1870.
- Rios, A. S., E. N. Silber, *et al.* (1999). "Effect of long-term beta-blockade on aortic root compliance in patients with Marfan syndrome." Am Heart J **137**(6): 1057-1061.
- Shores, J., K. R. Berger, *et al.* (1994). "Progression of aortic dilatation and the benefit of long-term beta-adrenergic blockade in Marfan's syndrome." N Engl J Med **330**(19): 1335-1341.
- Silverman, D. I., K. J. Burton, *et al.* (1995). "Life expectancy in the Marfan syndrome." Am J Cardiol **75**(2): 157-160.
- Tziakas, D. N., G. K. Chalikias, *et al.* (2004). "Serum profiles of matrix metalloproteinases and their tissue inhibitor in patients with acute coronary syndromes. The effects of short-term atorvastatin administration." Int J Cardiol **94**(2-3): 269-277.
- Yin, F. C., K. P. Brin, *et al.* (1989). "Arterial hemodynamic indexes in Marfan's syndrome." Circulation **79**(4): 854-862.
- Zhang, F. L. and P. J. Casey (1996). "Protein prenylation: molecular mechanisms and functional consequences." Annu Rev Biochem **65**: 241-269.

Chapter 2

Materials & Methods

2.1 A study of aortic root pathology in a murine model of Marfan syndrome.

2.1.1 Background

Mice heterozygous for a missense mutation in the fibrillin-1 gene which leads to a cysteine substitution in a calcium binding epidermal growth factor like domain of the fibrillin-1 protein (C1039G) express the phenotypic features of human Marfan syndrome. In particular they develop skeletal abnormalities, and progressive aortic pathology and dilatation. These mice transmit the mutation in an autosomal dominant fashion.

2.1.2 Genetically typing the C1039G murine model

A number of C1039G Marfan mice were cross bred with C57Bl6 females. C1039G mice were gifted from Department of Genetics and Cardiology, Johns Hopkins University. Marfan syndrome is inherited as an autosomal dominant disorder with high penetrance, but has great clinical variety in humans.(Dietz, Cutting *et al.* 1991) A high proportion of patients with Marfan syndrome manifest aortic pathology with an aortic root aneurysm. Once C1039G mice were identified for our study and entered into control groups, measurements of aortic root parameters were made at defined time-points to assess phenotypic expression of aortic root pathology as outlined in sections 2.1.4, 2.1.5, 2.1.6 & 2.1.7. Following weaning, male mice were identified and a small tail tissue sample was obtained from the offspring under Isoflurane anaesthesia (1-2% Forane, Abbott, Ireland). A small identifying tag was placed on the right ear to identify them for the duration of the study. DNA was isolated using a DNA extraction kit (DNA purification

kit, A1125, Promega, USA). The protocol used at Johns Hopkins University was used here to identify the mice. PCR was performed to amplify a 600bp fragment of the fibrillin-1 gene containing the missense mutation. The primers used for PCR were intron 24s (TTGTCCATGTGCTTTAAGTAGC) and intron 25s (ACAGAGGTCAGGAGATATGC) (Genosys, Sigma, UK). Successful PCR of the 600bp fibrillin-1 gene fragment was confirmed by gel electrophoresis.

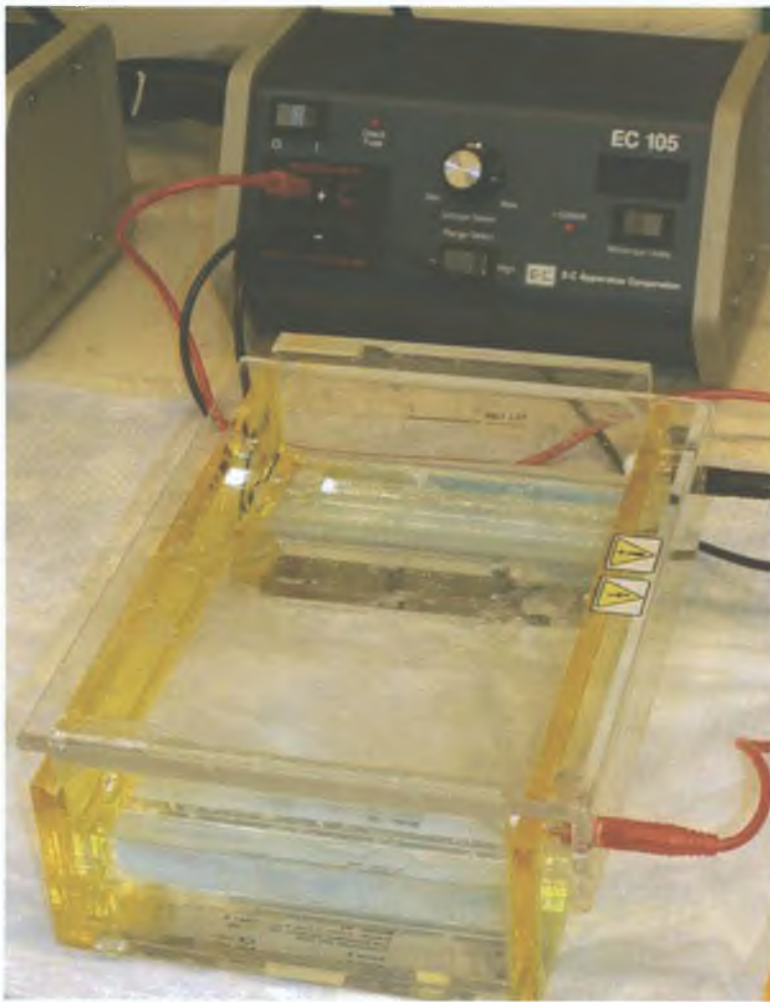


Figure 2.1 Electrophoresis bath, suitable for gel electrophoresis, with connection to power supply.

An 11% agarose gel was used as media for gel electrophoresis run at 9V/cm current for 40 minutes. The gel is impregnated with Ethidium Bromide and so DNA fluoresces under ultraviolet light. The positive bands show up bright in relation to a base pair ladder which is also loaded onto the gel. C1039G Marfan mice were identified by the presence of a Kpn1 restriction site introduced by the mutation into the fibrillin-1 gene. This was achieved using the restriction enzyme Asp 718 (Roche, UK) which split the PCR product containing the missense mutation into a 350bp and 250bp fragment(Judge, Biery *et al.* 2004) (Figure 2.2).

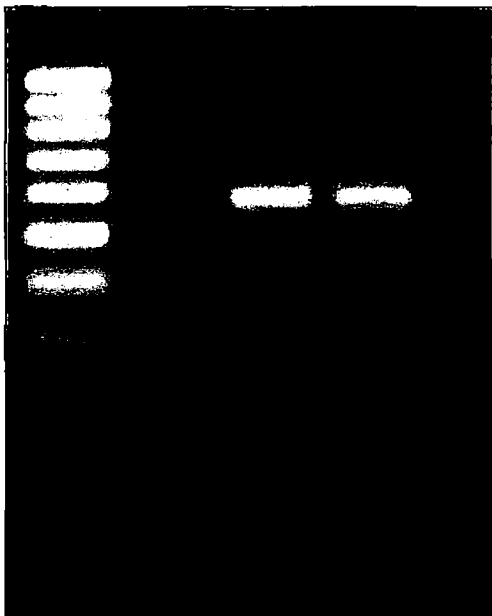


Figure 2.2: Gel electrophoresis, impregnated with Ethidium Bromide, illuminated with ultraviolet light, showing a base-pair ladder on the left and two “lanes” the first showing a 600bp fragment (homozygous for fibrillin-1) and the second showing a 350 & 250bp fragment (heterozygous for fibrillin-1).

The substrate was then subject to agarose gel electrophoresis. The gel was then analysed and imaged under ultraviolet light. Male mice were assigned as either wild type or

heterozygous Marfan mouse and the heterozygous Marfan mice were assigned to different groups according to each experimental protocol. Wild type mice that were entered into this study were bred from C57black6 with both male and female being wild type, free of genetic mutation. In the initial development of the C1039G model, homozygous Marfan mice developed a severe form of the disease and died perinatally.(Judge, Biery *et al.* 2004) Heterozygous Marfan mice showed kyphosis of the thoracic spine, so penetrance of the C1039G mutation could be confirmed phenotypically. In the untreated Marfan groups, the diameter of the aortic root showed the presence of aneurysmal dilatation which showed that those which were positive on testing genetically also had more than one phenotypic change.

Untreated C1039G Marfan mice were compared to normal C57black 6 mice as controls. The natural history of the disease compared to normal growth was examined. The aortic root diameter, cardiac function and aortic pathology at different time-points of development was observed.

2.1.3 Drug administration

For the comparison study of different pharmaceutical therapies, Pravastatin (Bristol Myers Squibb, USA), Losartan potassium (Sigma, Europe), or Doxycycline (Sigma, Europe) was administered from a 6 weeks of age, in the drinking water using a gravimetric dosing system. Equal volumes of water per mouse (or water with relevant drug added as per protocol concentration) was added to the gravimetric dosing system on a weekly basis. The volume remaining in the gravimetric dosing system prior to refilling was measured to assess the volume consumed by each litter of mice from the previous

week to ensure adequate dosing. Note was also made of the hydration status of each mouse to ensure adequate and equal intake of fluid. The concentrations of each drug used for each treatment regimen, along with that of the control groups, is specified in sections 3.2, 4.3 and 5.2 of chapters 3, 4 and 5, respectively for each of the three different experimental protocols.

2.1.4 Transthoracic echocardiographic measurements of aortic root diameter

Mice underwent 2 Echo measurements of their aortic root diameter at 3 and 8 months of age. Measurements were made, in association with the Department of Veterinary Medicine in University College Dublin, by members of the veterinary radiology team (University College Dublin). Transthoracic ECHO (Acuson Sequoia, Siemens) was used with a 12 MHz probe which the veterinary radiology team has successfully used previously to image the hearts of COX-2 knockout mice.(Neilan, Doherty *et al.* 2006) These mice were of the same size as Marfan mice and clear aortic root images were obtainable. Echocardiography is considered a reliable and validated method to measure aortic root dimensions of murine models in-vivo.(Liu and Rigel 2009)

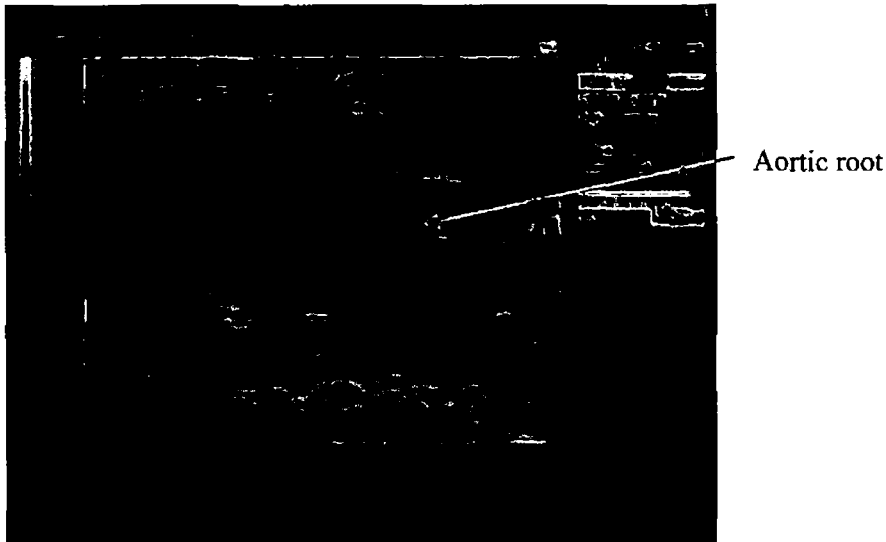


Figure 2.3: Parasternal long axis view of aortic root.

Measurements of aortic root diameter were made in the parasternal long axis view at sinus level, from leading edge to leading edge (Figure 2.3). An average of three measurements for each mouse was taken at each sitting, by two experienced sonographers blinded to the genotype and treatment group. Images were stored as TIFF / JPEG files. With the assistance of a specialist small animal veterinary anaesthetist, for the purpose of conducting echocardiography, each mouse was anaesthetized with Isoflurane in an anaesthetising box and maintained under anaesthesia using Isoflurane via a face-cone with 100% O₂. After the ECHO, the mice were recovered under a heat lamp in their cage and observed until fully mobile again.

2.1.5 Millar cardiac catheter measurements of aortic and ventricular pressures

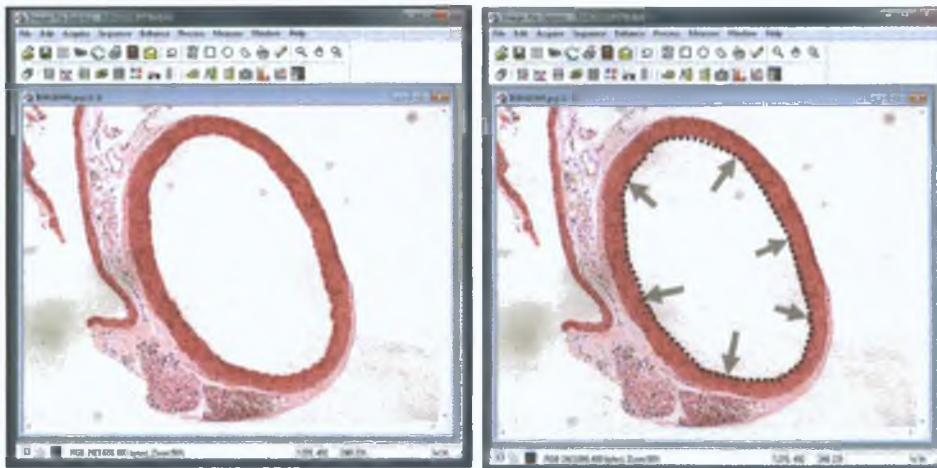
Within 2 weeks of the final 8 month echocardiogram being completed, the mice were anaesthetized for cardiac catheter measurements. Following anaesthesia with intraperitoneal xylazine 10mg/kg (Xylapan, Vetoquinol, France) and ketamine 100mg/kg

(Kctalar, Pfizer, Ireland), a midline vertical neck incision was made and the right carotid artery was exposed. Proximal and distal control of one carotid was obtained with 6/0 suture material. Using an operating microscope, a 1.2 French Millar cardiac catheter was introduced into the carotid artery with minimal blood loss. Once an aortic pressure trace was obtained the animal had a period of stabilization. A recording was then taken of the aortic pressure wave and a reading of systolic and diastolic blood pressure taken. The aortic pressure trace was shown to a cardiologist blinded to the treatment groups and asked to comment as to whether they thought it exhibited features consistent with aortic regurgitation. The dp/dt_{max} of the aortic downstroke was analysed, a positive value confirms that an upstroke was present. This upstroke reflected the presence of an aortic dirotic notch and a negative value showed that the dirotic notch was absent. The catheter was then advanced into the left ventricle and again followed by a period of stabilization. A 30 second recording of left ventricular pressure changes was taken. Powerquest software was used to analyse the pressure tracings. These recordings were used to calculate dp/dt_{max} , dp/dt_{min} , left ventricular end diastolic and end systolic pressure. Three readings from the 30 second transducer trace recording were then averaged. The left ventricle contractility index (dp/dt_{max} divided by LVEDP; p=pressure, t=time, LVEDP left ventricular end diastolic pressure) was used as a measure of cardiac function and hence haemodynamic stress on the aorta. Dr. Gang Chen contributed to this section of the experiments by facilitating measurement of both aortic pressure tracing and left ventricular pressure tracings. He conducted the micro-vascular technique of isolation of the right carotid artery, subsequent insertion of the Miller cardiac catheter into the aorta and advancement of the catheter into the left ventricle.

2.1.6 Harvesting tissues & histological analysis

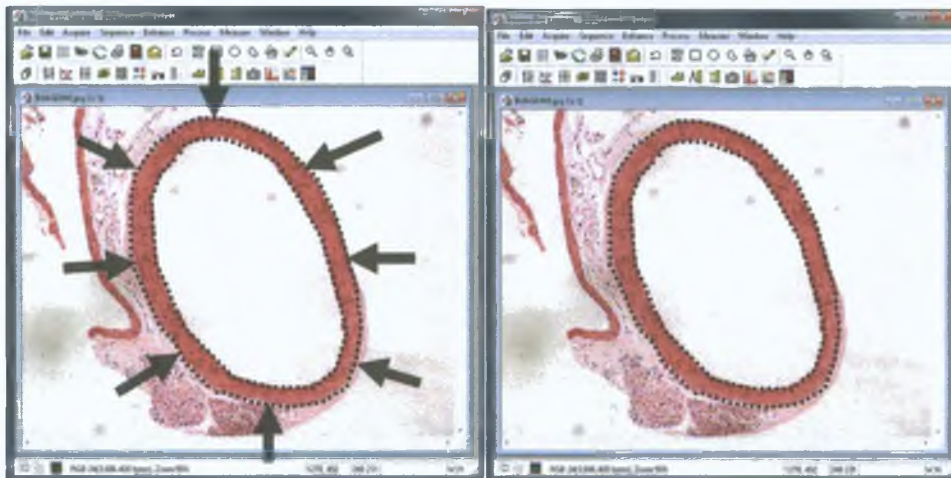
At the end of the cardiac catheterization, the catheter was carefully removed. The mice were euthanized with an overdose of intra-cardiac sodium pentobarbital. The mice then underwent cardiac puncture, obtaining a 0.8ml blood sample, which was saved for further studies. The heart and aorta (to the level of the diaphragm) were excised en bloc and fixed in 10% buffered formalin for 24 hours followed by processing for paraffin embedding. 5 micrometer sections of the aortic root were cut to achieve circular cross sections. The lungs were also excised individually. Tissues were fixed in 10% buffered formalin overnight, processed for paraffin embedment and sectioned at 5 micrometers. These slides were then stained with haematoxylin and eosin. Sectioning and staining were performed by the Department of Pathology, RCSI.

Haematoxylin and eosin stains were used for stereology. Images were photographed (Nikon Coolscope, Nikon) and image analysis software (Image Pro Express, Media Cybernetics) used to measure the thickness of the medial layer of the aortic root.



A

B



C

D

Figure 2.4 A - D. A, image of aortic cross-section loaded into Image-Pro Express® for analysis. B, inner aspect of aortic medial wall plotted, with more than 40 points identified with “image wizard” assistance. C, outer aspect of aortic medial wall plotted, with more than 40 points identified, again with “image wizard” assistance. D, with both aspects of aortic medial wall identified, the software calculates the average distance between the two line, which relates to the average thickness of the aortic medial layer.

The V-VG stain for elastic tissue content of the aortic root was used to assess the degree of fragmentation of the elastic fibres. A modification of a previously published technique was used to quantify aortic pathology (Habashi, Judge *et al.* 2006) . Two independent observers blinded to the genotype and treatment group scored each slide using an arbitrary scoring system which counted the number of “islands of damage” within an aortic cross-section from each mouse. An “island of damage” was defined as an isolated area of aortic wall where 2 adjacent elastic fibres were fragmented with interposed excessive connective tissue matrix.

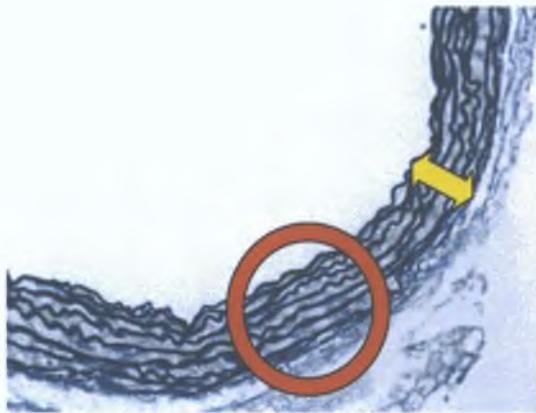


Figure 2.5: Light microscopy image: Verhoeff-Van Gieson stained cross-section of aortic root of a wild-type mouse at 8 months, magnification x10. Normal aortic wall is displayed (yellow arrows) with the usual arrangement of elastin (red circle).

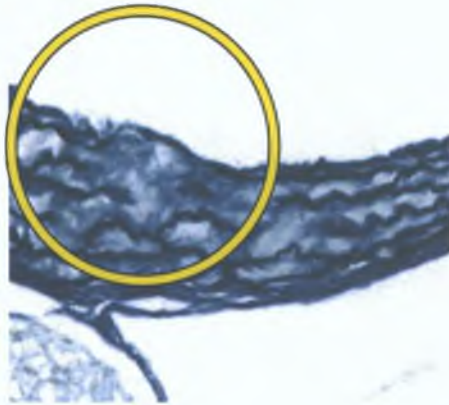


Figure 2.6: Light microscopy image: Verhoeff-Van Gieson stained cross-section of aortic root of a “Marfan” mouse at 8 months, magnification x20, displaying an island of damage (yellow circle). The aortic wall is thickened with loss of the usual arrangement of elastin.

Aortic root sections were also stained with Alcian blue stain for collagen content.

2.1.7 Electron Microscopy protocol

Examination of the aortic tissue specimens with electron microscopy was conducted in collaboration with the Department of Anatomy in the National University of Ireland in Galway. The aortic root was dissected out and immersion fixed in primary fixative, 2% Glutaraldehyde + 2% Paraformaldehyde in 0.1M Sodium Cacodylate/ HCl buffer pH7.2. They were stored in the primary fixative until delivery to the Anatomy Department, NUI Galway. Members of the Department of Anatomy of NUI Galway conducted the secondary fixation and processing of the aortic tissue samples, followed by imaging at an ultra-structural level and subsequent stereological quantification of the cell organelles.

Samples were rinsed in freshly prepared 0.2M Sodium Cacodylate/HCl Buffer pH7.2 (3 ×10 mins). Samples were then immersion fixed in secondary fixative, 1% Osmium Tetroxide in 0.1M Sodium Cacodylate/ HCl buffer pH7.2 (2 hrs). Following fixation, samples were dehydrated through a series of graded alcohols (40%, 50%, 70%, 80%, 90%, 95% and 100%) and routinely embedded in an Agar Low Viscosity Resin.

Histological Protocol:

Light microscopy images were taken to confirm aortic root samples without the presence of artefact. Semi-thin sections (0.75 µm thick) were cut using a glass knife and a Reichert-Jung Ultracut ultramicrotome, (Boeckeler Instruments, Inc., Arizona, U.S.). The sections were placed on glass slides and stained for 8 seconds with toluidine blue. Sections were examined on a Leica Bright Field Microscope Serial#14003 connected to a computer with Leica Application Suite microscope software, (Leica Microsystems Inc., Bannockburn, U.S.). Several images were taken of each tissue sample at ×10 and × 40 objective magnifications, two were chosen from each sample on which to carry out stereological analysis. For TEM, ultra-thin sections (0.5 µm) were cut using a diamond knife and a Reichert-Jung UltracutE ultramicrotome. The sections were placed on 200 µm mesh copper grids and stained with uranyl acetate and lead citrate using a Leica EM AC20 Autocontraster, (Leica Microsystems Inc., Bannockburn, U.S.). Sections were examined on a Hitachi H7000 Transmission Electron Microscope, (Hitachi High Technologies America, Inc., California, U.S.) at an accelerating voltage of 75kV. Several images were taken of each tissue sample at 5,000 and 20,000 magnifications, six were chosen from each sample on which to carry out stereological analysis.

Stereological parameters investigated from images obtained by TEM

The volume of smooth muscle cells was estimated using a variation of the “Nucleator” principle as described in (Dockery *et al.*, 1997). Twenty smooth muscle cells were chosen from images of each animal at final magnification $\times 310$. The profile of each smooth muscle cell was traced and a 4-way nucleator applied. The distance from the nucleus of the cell to the cell membrane was measured. This was cubed and the mean multiplied by $4\pi/3$, to give an estimate of the individual cell volumes. This gave an estimate of the number-weighted mean smooth muscle cell volume for each animal in all groups (Dockery, Tang *et al.* 1997).

Surface density (S_v) of rough endoplasmic reticulum in smooth muscle cells was estimated using an intersect measuring technique on images at a final magnification $\times 34,560$. A stereological grid was applied to the images in a random orientation. By counting all intersects hitting the object of interest and applying the formula:

$$S_v = 2 \times I/L$$

where I = the number of intersects and L = the total length of test line applied (Dockery *et al.*, 1991), an unbiased estimate of rough endoplasmic reticulum in smooth muscle cells was determined.

$V_v \text{ RER: cell}$ (where $V_v \text{ rER: cell}$ is the volume fraction of rough endoplasmic reticulum as compared to the volume of the cell) of smooth muscle cells was estimated on images at a final magnification of $\times 34,560$ by randomly applying a stereological grid onto the images using a simple point counting method and the formula:

$$V_v = P(\text{rER}) / P(\text{cytoplasm})$$

where $P(\text{RER})$ was the points that hit the cisternae of rough endoplasmic reticulum and $P(\text{cytoplasm})$ was the points that hit the cytoplasm of SMC (Mayhew 1991). $V_v \text{ Nucleus: cell}$ (where $V_v \text{ Nucleus: cell}$ is the volume fraction of the nucleus as compared to the volume

of the cell) of smooth muscle cells was estimated on images at a final magnification of $\times 8,640$ by randomly applying a stereological grid onto the images using a simple point counting method and the formula:

$$V_v = P(\text{nucleus}) / P(\text{cell})$$

Where $P(\text{nucleus})$ was the number of test points falling on the smooth muscle cell nucleus and $P(\text{cell})$ was the number of test points falling on the smooth muscle cells. (Mayhew 1991)

Because the volume of the smooth muscle cells was known it was possible to estimate the absolute mean surface area (SA) of rough endoplasmic reticulum and the absolute mean volume of rough endoplasmic reticulum in smooth muscle cells.

Absolute SA (surface area) of rough endoplasmic reticulum *in* smooth muscle cells was estimated by multiplying the V_v rough endoplasmic reticulum in smooth muscle cells by the volume of the smooth muscle cell.

Absolute volume RER *in* smooth muscle cells was estimated by multiplying the S_v rough endoplasmic reticulum in smooth muscle cells by the volume of the smooth muscle cells.

2.2 Ethical approval and animal care

A genetically modified murine model of Marfan syndrome accurately replicates aneurysmal disease of the thoracic aorta. The animals were survived for 8 months from birth. Mice with this mutation remain asymptomatic during this period with an extremely low rate of dissection or rupture of the aorta. Using a model with this level of sophistication facilitates using a smaller number of animals, as each affected animal will have a more predictable natural history. This in turn means that a lower number of animals are required to observe potential therapeutic benefits. Multiple modalities of measurements, including non-invasive measurements were employed, which has the

effect of further reducing the number of animal required. Non-invasive measurements also mean less discomfort to the animals during the study. Procedures were conducted with anaesthesia expertise provided by small animal veterinarians, to ensure the highest levels of animal care.

All animals were housed in a licensed biomedical research facility (Royal College of Surgeons in Ireland, Department of Surgery, Beaumont Hospital) and all procedures were carried out under license from the Department of Health and Children, Ireland. Ethical approval was obtained from the Royal College of Surgeons in Ireland Research Ethics Committee. Appendix 1: 1. Ethical approval, contains a copy of the letter from the Royal College of Surgeons in Ireland Research Ethics Committee granting ethical approval, code REC 099, providing institutional support for the ethical considerations in relation to the use of animals in this research study. An extension to this approval was sought from the committee.

2.3 Statistical Analysis

Statistical analysis was conducted by using the software package: StatsDirect statistical software version 2.7.8, (Cheshire, U.K.). Statistical analysis included, Analysis of Variance, ANOVA, with Bonferonni comparisons, (used to compare the means of two or more groups), generate p-values, estimate standard error of the mean, medians, interquartile ranges and confidence intervals. The statistical package was also used to graph these statistics. The threshold for statistical significance used in these studies was $p \leq 0.05$.

2.4 References

- Dietz, H. C., G. R. Cutting, *et al.* (1991). "Marfan syndrome caused by a recurrent de novo missense mutation in the fibrillin gene." Nature **352**(6333): 337-339.
- Dockery, P., Y. Tang, *et al.* (1997). "Neuron volume in the ventral horn in Wobbler mouse motoneuron disease: a light microscope stereological study." J Anat **191** (Pt 1): 89-98.
- Habashi, J. P., D. P. Judge, *et al.* (2006). "Losartan, an AT1 antagonist, prevents aortic aneurysm in a mouse model of Marfan syndrome." Science **312**(5770): 117-121.
- Judge, D. P., N. J. Biery, *et al.* (2004). "Evidence for a critical contribution of haploinsufficiency in the complex pathogenesis of Marfan syndrome." J Clin Invest **114**(2): 172-181.
- Liu, J. and D. F. Rigel (2009). "Echocardiographic examination in rats and mice." Methods Mol Biol **573**: 139-155.
- Mayhew, T. M. (1991). "The new stereological methods for interpreting functional morphology from slices of cells and organs." Exp Physiol **76**(5): 639-665.
- Neilan, T. G., G. A. Doherty, *et al.* (2006). "Disruption of COX-2 modulates gene expression and the cardiac injury response to doxorubicin." Am J Physiol Heart Circ Physiol **291**(2): H532-536.

Chapter 3

Natural history of Marfan syndrome

3.1 Introduction

As discussed, Marfan syndrome is a multi-system disease. The most life threatening of these is related to aortic pathology. The aorta progressively dilates, eventually becoming aneurysmal. This aneurysmal aorta then is at a greatly increased risk of rupture or dissections, both of which have an extremely high mortality and if one survives, a significant morbidity. This poor survival was demonstrated in a series of 257 patients with Marfan syndrome, published in 1972. The average age of death for the 72 deceased patients was 32 years. 80% of the known causes of death were due to aortic dilatation and its consequences.(Murdoch, Walker *et al.* 1972) A study published in 1989 showed that one third of patients who had not yet undergone surgery, had evidence of aortic dissection when cardiac catheterization was conducted.(Marsalese, Moodie *et al.* 1989) This same study showed that 61% of known deaths were due to aortic dissection or rupture or sudden cardiac death.(Marsalese, Moodie *et al.* 1989) The tissue of the aorta itself may be diseased (which may either cause or be a result of the aneurysm). The aneurysm occurs at the level of the sinotubular junction.(Shores, Berger *et al.* 1994) This is the area where the coronary arteries originate, at the most proximal part of the aorta, the aortic root.

volume of blood ejected during systolic contraction (stroke volume) and vice-versa. This facilitates synchronization of the cardiac output with venous return.

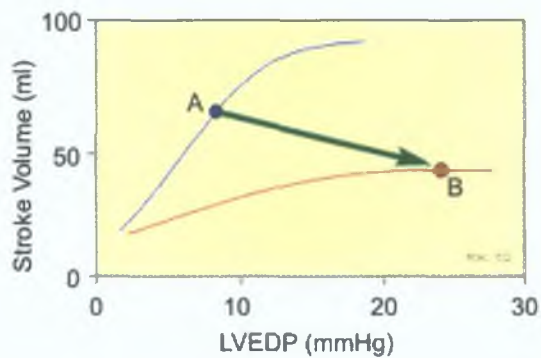


Figure 3.2: The Frank-Starling relationship showing the effects of heart failure (ventricular systolic dysfunction, loss of inotropy) on stroke volume and ventricular preload (left ventricular end-diastolic pressure, LVEDP). Point A, control point; Point B, ventricular failure.

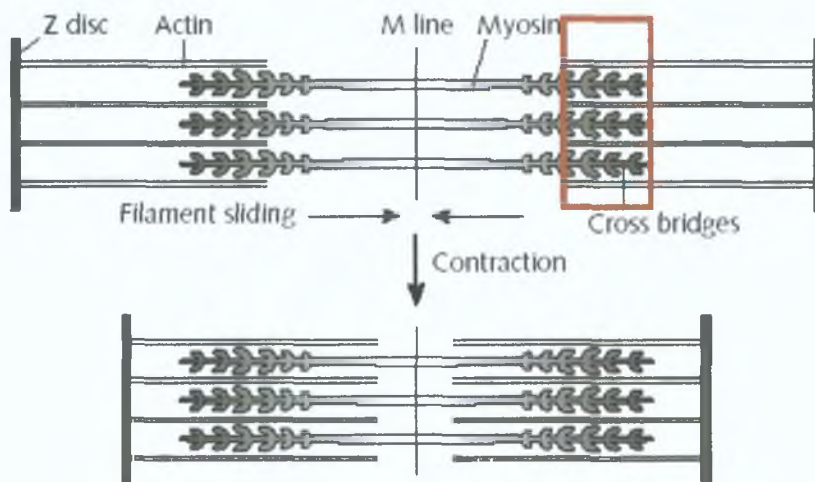


Figure 3.3: Schematic diagram of a single sarcomere: (above) in relaxation, with area of overlap outlined in red, of actin and myosin filaments; (below) shortened during contraction.

As the left ventricle fills with more blood than usual, the force of each contraction of the cardiac muscle increases. This is because each cardiac muscle fibre experiences an increased load. Stretching of the cardiac muscle fibre augments cardiac muscle contraction by increasing the affinity of troponin C for calcium. This causes a greater number of actin-myosin cross-bridges to form within the muscle fibres. The force that any single cardiac muscle fibre generates is proportional to the initial sarcomere length (also known as preload), and the stretch on individual fibres is related to End Diastolic Volume of the ventricle. The optimal initial length of the sarcomere is 1.6 to 2.2 μm . With increasing end diastolic volume, secondary to aortic incompetence, there is less overlap of the thick and thin filaments and so a less forceful contraction. This will in turn, further increase End Diastolic Volume within the Ventricle (left ventricle in this case). The cardiac muscle is shifted to far left, on the Frank-Starling Curve and results in continued strain and progressive dilation of the left ventricle. Over time the left ventricle which continues to function inefficiently, cannot accommodate to changes in demand and starts to fail. On the subcellular level, this phenomenon might be explained by a failure of the myofibrils to increase the Ca^{2+} sensitivity after an increase of the sarcomere length (Schwinger, Bohm *et al.* 1994).

On a cardiovascular level, as left ventricular pressure decreases in diastole below aortic pressure, the aortic valve is not able to close, the regurgitant fraction, regurgitates back through the aortic valve and causes a decrease in the diastolic blood pressure in the aorta. The sympathetic nervous system via the renin-angiotensin-aldosterone axis of the kidneys compensates for reduced cardiac output. As diastolic pressure is reduced systolic blood pressure is normalized and sometimes elevated. Catecholamines increase heart rate and

contractility, thereby increasing cardiac output. Chronic aortic regurgitation causes cardiac remodelling with resultant heart failure. Concentric left ventricular hypertrophy is due to the increased left ventricular systolic pressures associated with aortic regurgitation. Eccentric hypertrophy is due to volume overload caused by the regurgitant fraction. The patient experiences increased dyspnoea, orthopnoea, paroxysmal nocturnal dyspnoea and fatigue. The patient may also experience wheezing or “cardiac asthma.”(Fishman 1989)



Figure 3.4: Illustration of regurgitant flow of blood through an incompetent aortic valve.

The timing and severity of which these events occur can vary from patient to patient. This can range from a slow, progressive left ventricular failure secondary to aortic incompetence to an acute aortic dissection, with no way to accurately predict which pattern will affect each patient. Patients require serial echocardiography and assessment of the aortic root diameter.

In order to improve medical management of patients who have Marfan syndrome and to develop new strategies to attenuate, slow or ameliorate disease progression, a complete

understanding of the pattern, timing and underlying mechanisms of disease is of vital importance.

Historically, because fibrillin-1 is present in tissues affected by Marfan syndrome, it was considered that the underlying defect in fibrillin-1 led to a primary structural weakness in this connective tissue protein. Because of recent discoveries, this concept has come into question. Transforming Growth Factor beta (TGF- β) dysregulation has become central to the current concept of the underlying mechanism of disease and proposed treatment. However, the mechanism of disease has yet to be completely defined.

The aim of this research therefore was to establish the pattern, extent, timing and other aspects of the underlying mechanism of disease in a model extensively described in the literature as suitable for the study of Marfan syndrome.

3.2 Materials and Methods

A pair of male C1039G Marfan mice was cross bred with C57Bl6 females. Genetic analysis of the offspring was conducted. Male mice identified to have the C1039G mutation were entered into the study. Thirty-five C1039G mice were entered into the natural history group. Forty-five normal, "C57 black 6 mice", were entered into the study for comparison.

The protocol used was based on the literature descriptions of the models used in Johns Hopkins University. Each animal received food and water ad-libitum. Aortic root diameter was assessed in-vivo, at 3 months and 8 months for evidence of established of progression of aneurysmal dilatation, by trans-thoracic echocardiography as outlined in the materials and methods chapter. Aortic root pathology was assessed histologically

using haematoxylin and eosin staining and Verhoeff-von Gieson staining. Animals were euthanized. Samples of aortic root were harvested at sequential periods for histological examination.

Animals were separated into ten groups, five groups of normal mice and five groups of Marfan mice. One group from each was euthanized at 6 weeks, 3 months, 4.5 months, 6 months and 8 months. Aortic root thickness was assessed with Haematoxylin and Eosin staining. Architecture of the aortic media at the level of the aortic root was assessed by staining sections with Verhoeff-von Gieson stain. The aortic wall architectural score is based on number of islands of damage, per full aortic root cross section. An island of damage is defined as an area where there are two or more disrupted elastic lamellae with associated thickening of the aortic media.

Table 3.1: Schedule for histological analysis to assess natural history of aortic disease in Marfan syndrome with comparison to normal aortic tissue.

Time point	6 weeks	3 months	4.5 months	6 months	8 months
Haematoxylin and Eosin	Normal(n=5)) Marfan(n=5)	Normal(n=5)) Marfan(n=5)	Normal(n=5)) Marfan(n=5)	Normal(n=5)) Marfan(n=5)	Normal(n=5)) Marfan(n=5)
Verhoeff von Gieson	Normal(n=5)) Marfan(n=5)	Normal(n=5)) Marfan(n=5)	Normal(n=5)) Marfan(n=5)	Normal(n=5)) Marfan(n=5)	Normal(n=5)) Marfan(n=5)

Cardiac function was assessed using haemodynamic variables cardiac catheter recordings of dP/dt maximum as a measure of left ventricular systolic function at 8 months. The

model used is too small and the technique too demanding to assess this measurement at earlier time points.

Aortic valve function was assessed using catheter recordings of systolic and diastolic blood pressure at eight months. Assessment of the aortic valve closure was made by measuring dP/dt maximum of the downslope of the aortic trace (immediately after the peak systolic pressure and before the minimum diastolic value reached).

Samples of aortic root were harvested at 8 months for ultra-structural examination with electron microscopy. Measurements of aortic vascular smooth muscle cells were taken. The volume of rough endoplasmic reticulum was measured. The volume of the cisternae within the Golgi-apparatus was measured. The volumes of mitochondria were also measured.

3.3 Results

Results are followed by +/- standard error of the mean in brackets.

3.3.1 Aortic Root Diameter

Aortic root diameter was measured using trans-thoracic echocardiography. In the group containing normal mice (n= 20), the mean aortic root diameter grew from 0.132 (+/- 0.001) cm at 3 months to 0.161(+/-0.001) cm at 8 months (Figure 3.5). This is an increase of 0.0287(+/-0.004) cm over the 5 month period, a 21.7% increase in the aortic root diameter. The mean aortic root diameter of the group of Marfan mice, 0.165 (+/- 0.002) cm, was already enlarged when measured at 3 months of age. This was an increase of 0.033cm compared to the mean of the normal group at the same age (Figure 3.5). The

average aortic root diameter in the Marfan group was increased by 25%, when compared to the normal group. Therefore, this model of Marfan syndrome had established dilatation of the aortic root at 3 months of age. The mean aortic root diameter increased with growth of the mice, in the normal group to 0.161(+/-0.001) cm at 8 months. This was an average increase of 0.0287cm, or 21.7% in this group. This would be considered normal growth.

The mean aortic root diameter in the Marfan group was increased from 0.165(+/-0.001) cm at 3 months to 0.252(+/-0.004) cm at 8 months (Figure 3.5). This was an increase of 0.0869cm, or 53.9% in the mean aortic root diameter over the 5 month period. Compared to the normal group at 8 months, the mean aortic root diameter was 0.091cm larger, or 56.5% larger than the normal group ($p<0.0001$).

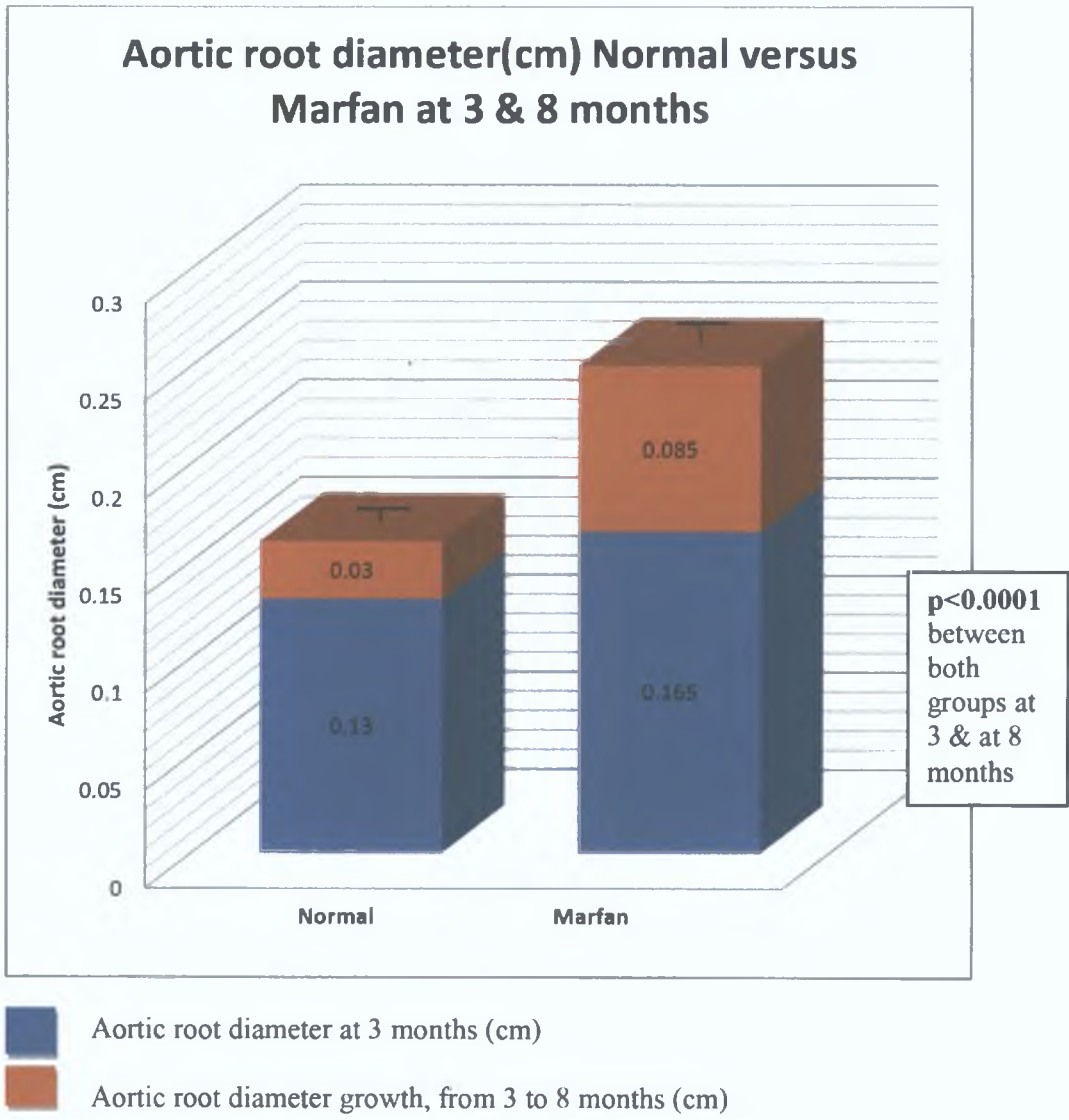


Figure 3.5: Comparing Normal & Marfan Aortic root diameter (cm) at two time-points, 3 and 8 months.

3.3.2 Cardiac catheterization results

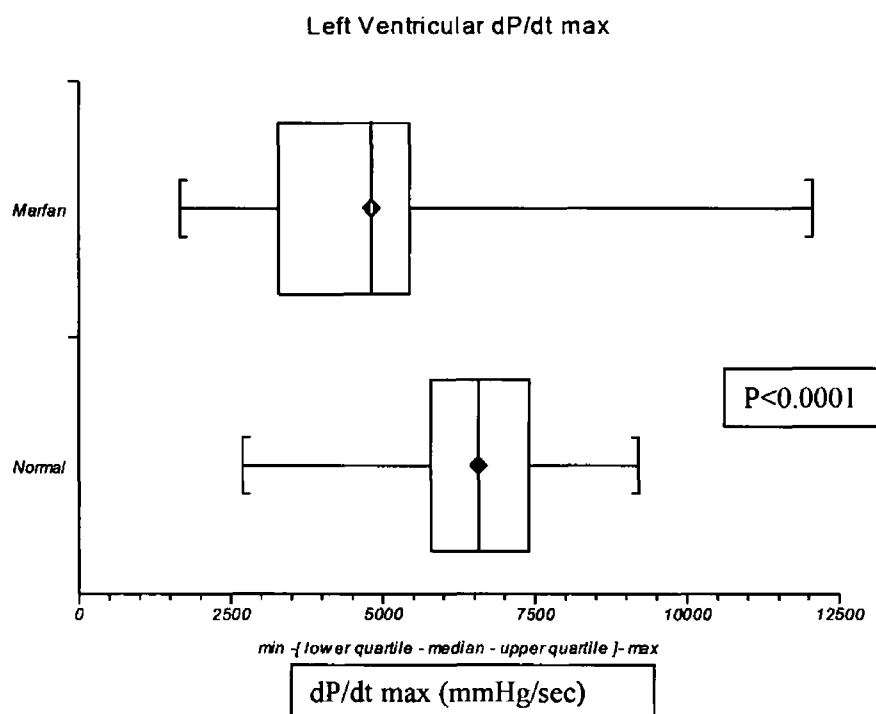


Figure 3.6: Left ventricular dP/dt max, comparing mean values of normal and of Marfan groups.

There was a reduction in the left ventricular dP/dt maximum in the Marfan group, 4793(+/- 172.6) mmHg/sec, when compared with the normal group, 6574 (+/-257.3) mmHg/sec, ($p < 0.0001$), (Figure 3.6). This was a 27% reduction in contractility. This is a statistically significant result.

As discussed previously in this chapter in relation to the Frank-Starling mechanism, changes in filling pressure or pre-load secondary to anaesthesia, will affect cardiac contractility. There are a number of factors contributing to variation in subject to subject pre-load, such as hydration status, response to anaesthetic, depth of anaesthesia and vascular tone (which could relate to pharmaceutical therapy). In an attempt to normalise for this we calculated the left ventricular contractility index. The left ventricular

contractility index is the left ventricular dP/dt max divided by the left ventricular end diastolic pressure.

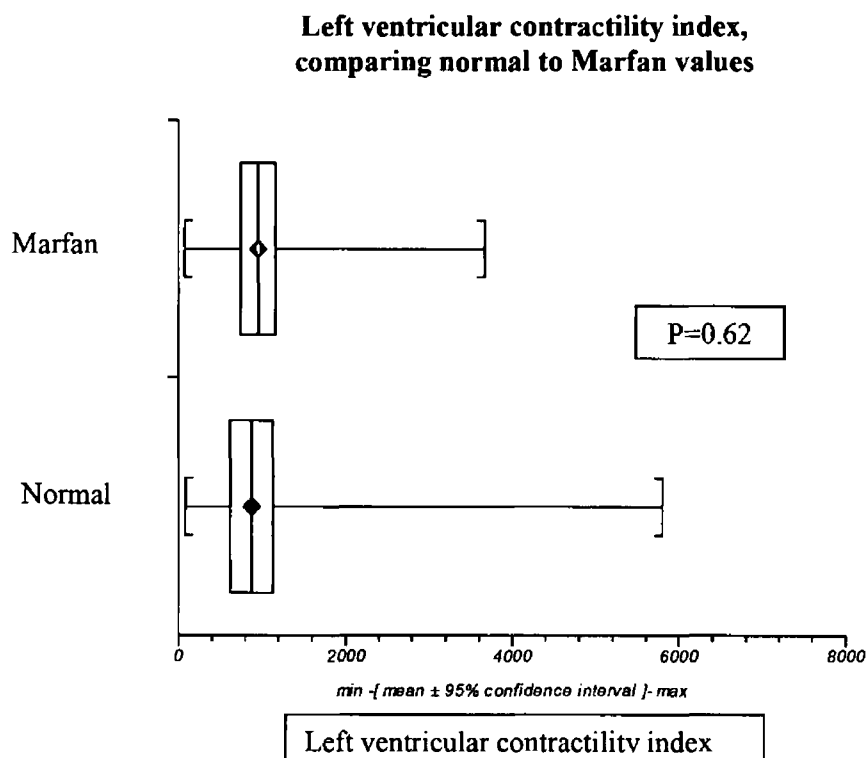


Figure 3.7: Left ventricular contractility index, comparing Normal to Marfan Values.

The mean contractility index for the normal group is 876(+/-129.9). The mean contractility index for the Marfan group is 957(+/-102.9), (Figure 3.7). The p-value for comparison between the two groups is 0.62, which shows that there is no statistical difference, between the two for this variable. In both Figures 3.6 and 3.7 the range is broad in both groups and this affects statistical significance negatively. Anaesthesia using a combination of Ketamine and Xylazine is well known to be one of the most reliable for inducing relaxation, sedation and analgesia in mice when assessing cardiac

function.(Hart, Burnett *et al.* 2001) Unfortunately it is also well known for inducing bradycardia. Bradycardia would affect left ventricular dP/dt_{max} and would be a variable which would increase the range of measurements taken. In an attempt to control for variability of left ventricular dP/dt_{max} , the left ventricular contractility index was calculated, though the range of measurements remains high (Figure 3.7).

Pulse Pressure

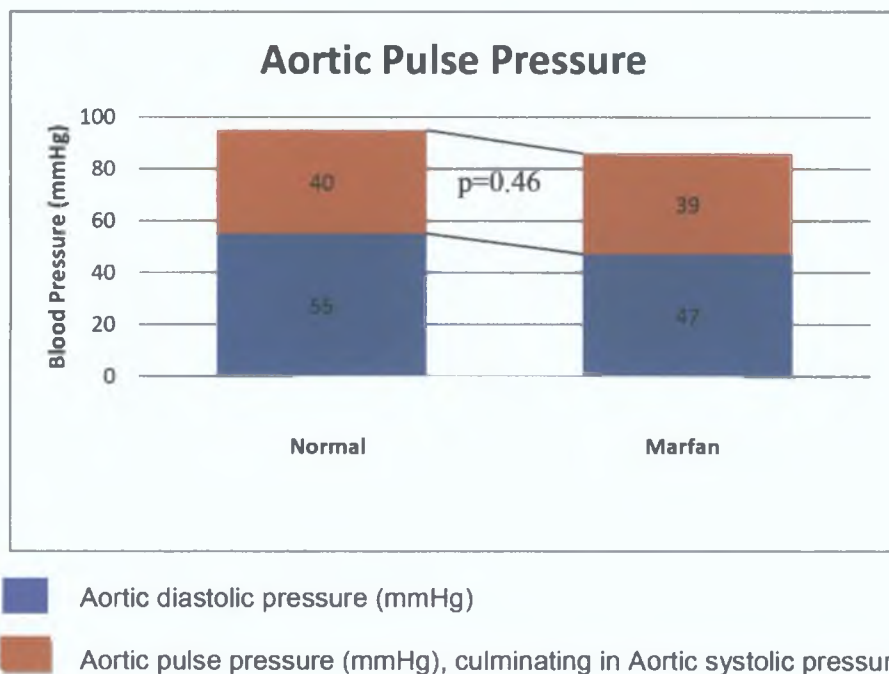


Figure 3.8: Comparing Average aortic pulse pressure between Normal and Marfan Groups. The aortic diastolic pressure is noted in blue, with the aortic systolic pressure noted by red, with pulse pressure documented within the red section of histogram. Lines joining systolic and diastolic values convey their similarity.

The mean pulse pressure for the normal group is 40.7 (+/- 0.66) mmHg and the mean for the Marfan group is 39.7 (+/- 1.13) mmHg, (Figure 3.8). There is very little difference in the pulse pressure between the two groups. 1mmHg would not be clinically significant even if it was statistically significant.

Analysis of the Aortic dicrotic notch.

The aortic pulse has a positive inflection after peak systolic pressure during diastole. It is caused by the rebound impulse due to the closure of the aortic valves.

The maximum slope of the down-stroke of the aortic pressure waveform following peak systolic pressure was measured. A positive result when the maximum slope was measured reflected a positive inflection (which represents a change in pressure secondary to aortic valve coaptation), (Figure3.9). A negative result when the maximum slope was measured, reflected an absence of a positive inflection (which may represent a failure of effective aortic valve coaptation) and so identified the presence of aortic incompetence (Figure 3.10). The presence of aortic insufficiency (incompetence) may be the cause of a reduction in left ventricular dP/dt max.

Table 3.2: Comparison of the aortic dicrotic notch in Marfan and normal aortic pressure tracing

Phenotype	Aortic notch absent	Total	Percentage
Normal	0	20	0%
Marfan	8	22	36.4%

The aortic valve was competent in all normal controls, as the aortic notch was present in all twenty of the group, (Table 3.2). Aortic incompetence was present in 36.4% of aortic pressure tracings taken in untreated Marfan mice, (Table 3.2).

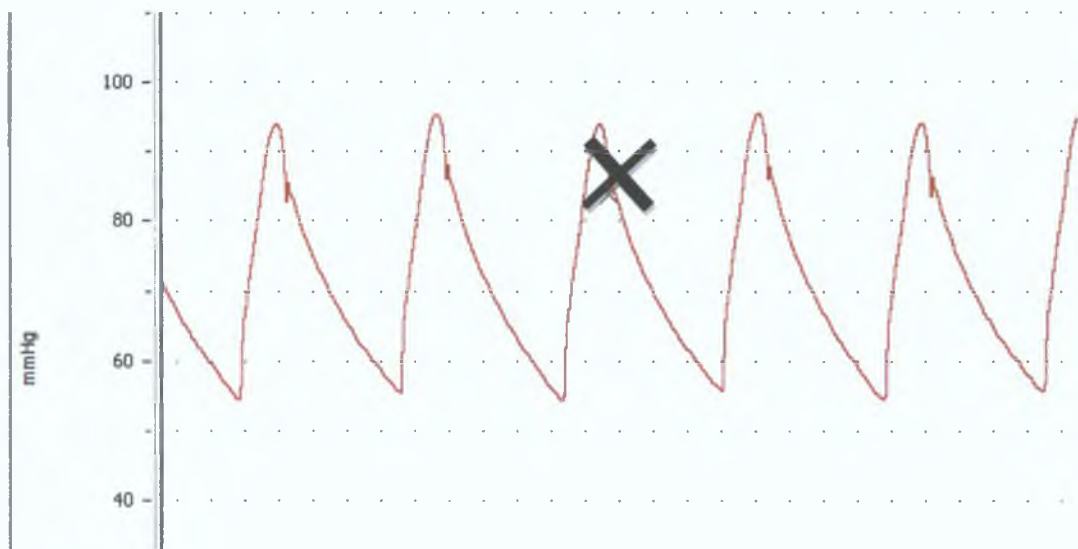


Figure 3.9: Aortic pressure trace, taken with Millar pressure transducer. It shows the aortic pulse pressure with aortic dirotic notch, present on down-stroke of wave form and identified with an X.



Figure 3.10: Aortic pressure trace, taken with Millar pressure transducer. It shows the aortic pulse pressure with absence of the aortic dirotic notch, which is normally present on down-stroke of wave form (yellow circle).

3.3.3 Histology

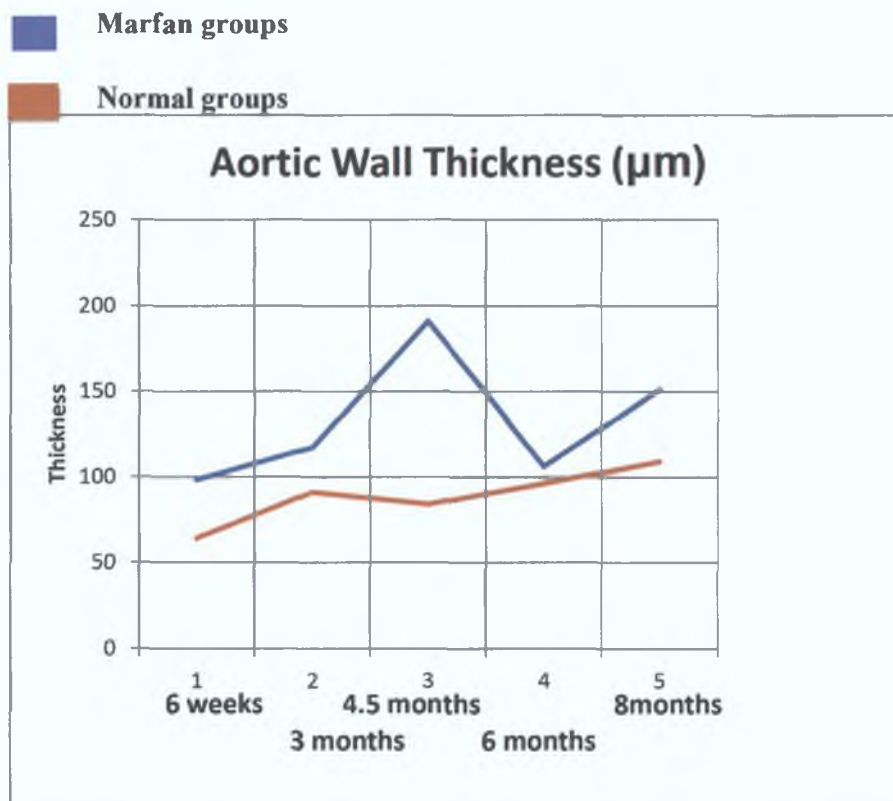


Figure 3.11: Natural history of aortic wall thickness (μm) comparing normal to Marfan at different time-points. $N = 60$. Mean standard deviation of normal group = $14.4\mu\text{m}$ and Marfan group = $60.7\mu\text{m}$. There is a fluctuation in the trend at 4.5 months.

One of the values for aortic wall thickness in the 4.5 month group was more than 3 standard deviations outside the mean for the rest of the values (Figure 3.11). This one observation was removed from the data, to gain more meaningful information from the groups (Figure 3.12).

- Marfan groups
- Normal groups

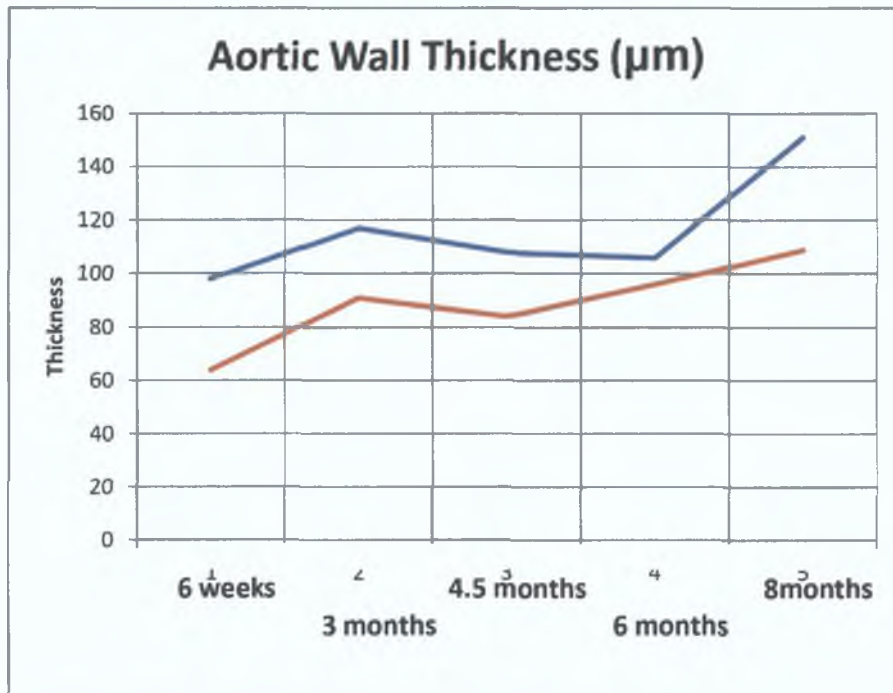


Figure 3.12: Natural history of aortic wall thickness (µm) comparing normal to Marfan at different time-points (with outlier removed). N = 59. Mean standard deviation of normal group = 14.4µm, and Marfan group = 31.5µm.

By removing one outlier from the 4.5 month group, the graph shows an overall increase in the aortic wall thickness with age in both groups. The marfan groups have consistently higher values at each time point, with $p < 0.01$ when an analysis of variance with Bonferroni corrections.

Table 3.3: Aortic wall thickness in normal & marfan subjects at consecutive time-points (without outlier).

	<i>6 weeks</i>	<i>3 months</i>	<i>4.5 months</i>	<i>6 months</i>	<i>8 months</i>
Normal					
Mean	64.69	91.99	84.14	96.482	109.85
+/-std deviation	11.5	23.5	4.4	18.9	13.7
Marfan					
Mean	98.612	117.62	108.55	106.266	151.68
+/-std deviation	17.2	35.8	42	38.3	24.2

The aortic wall was thinnest at 6 weeks in both groups. The mean aortic wall thickness in normal subjects increased from a low of 64.69 μm (+/-5.2), to its thickest at 8 months of 109.85 μm (+/-6.1) (Table 3.3). It rose steadily, following an initial elevated value of 91.99 μm (+/- 10.5), rising from 84 μm at 4.5 months, 96 μm (+/- 8.4) at 6 months & finally 109 μm (+/- 6.1) at 8 months. The aortic wall in Marfan syndrome was thicker than normal aorta wall at 6 weeks, 98.6 μm (+/- 7.7). In fact it is 53% thicker than normal at this stage. There was again an initial elevation of the value at 3 months, 117 μm (+/- 15.9). After this the trend rose from the 6 week value to 108.5 μm (+/- 21) at 4.5 months, 106 μm (+/- 17.1) at 6 months to the thickest value of 151 μm (+/- 7.7) at 8 months. The marfan aortic wall was thicker than normal aortic wall at every time-point measured. At 8 months, the wall was 38% thicker than normal. The aortic wall was found to be significantly thickened at the earliest time-point measured (6weeks), and this trend followed as the aortic wall grew in the normal context, so too did the marfan aorta, though with ongoing, significant thickening (Figure 3.12). This thickening was pathological, as with more thickening, the aortic wall became less compliant.

- Marfan groups
- Normal groups

Measure of architectural integrity

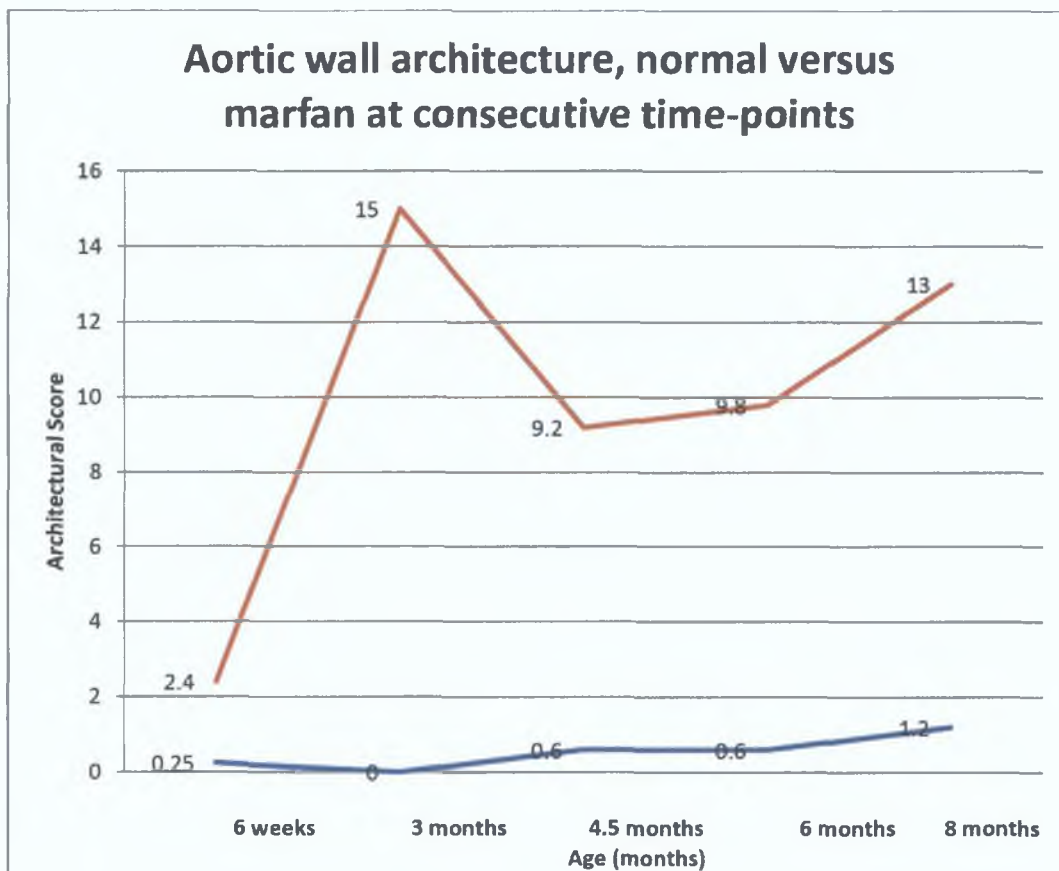


Figure 3.13: Natural history of aortic wall architecture, comparing normal to Marfan at different time-points. N = 53. Mean standard deviation, of normal group = 0.79, and Marfan group = 10.1. There is a fluctuation in the trend at 3 months.

There was one value in the 3 month group which lay more than 3 standard deviations outside the mean for the rest of the values (Figure 3.13). By removing this outlier, a

different mouse than in discussed in relation to aortic wall thickness (figure 3.11), the data was more representative. The graph now looks like Figure 3.14.

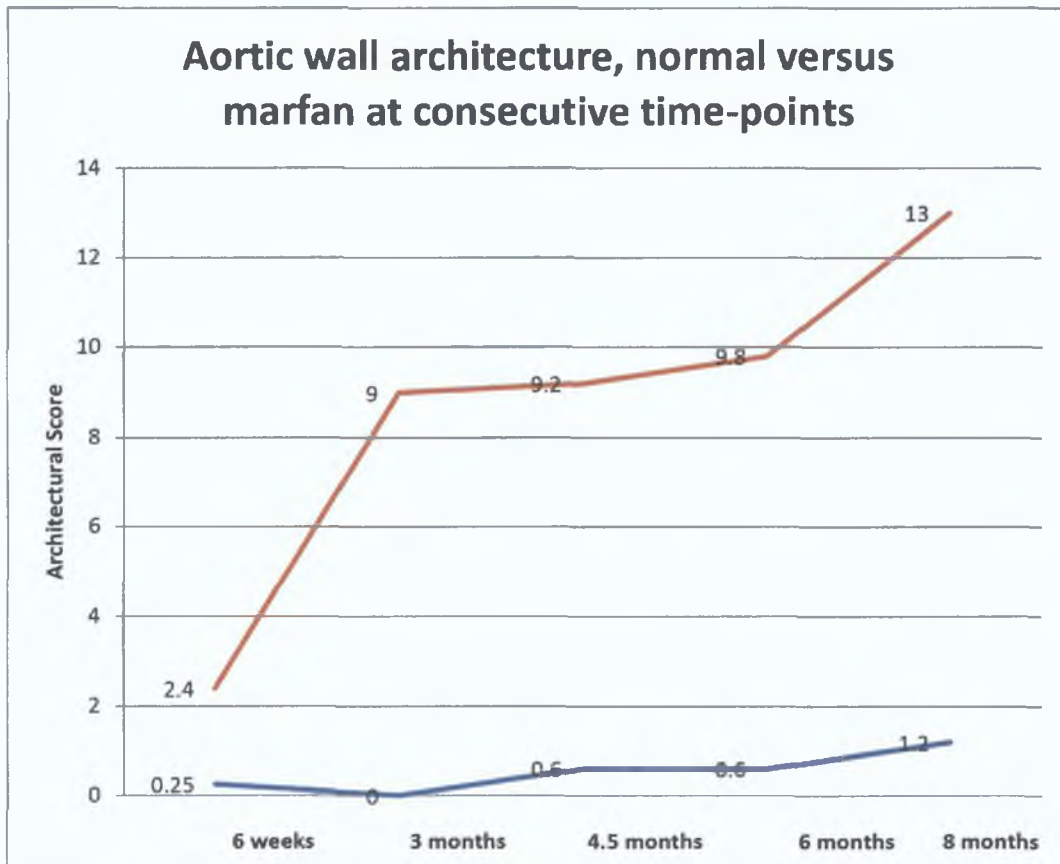
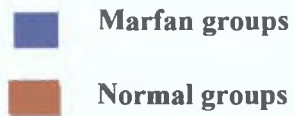


Figure 3.14: Aortic wall architecture, normal versus marfan at consecutive time points, with outlier removed from the data. N = 52. Mean standard deviation, of normal group = 0.79, and Marfan group = 8.5. The graph shows an overall increase in the aortic wall thickness with age in both groups. The marfan groups have consistently higher values at each time point.

The aortic wall architecture was assessed at 5 different time-points, in each group. In the normal group showed consistently low architectural scores, starting a 0.25 (+/- 0.25) at 6 weeks, 0 at 3 months, 0.6 (+/- 0.4) at 4.5 months and 6 months, then rose slightly to 1.2 (+/- 0.49) at 8 months, (Figure 3.14). On the other hand, the 6 week marfan group showed an initial score of 2.4 (+/- 1.9), which was significantly higher than normal at this time point. There was a sharp rise between 6 weeks and 3 months in the marfan group, with the architectural score rising to 9 (+/- 3). This was a 3.75 fold rise from an already elevated value at 6 weeks. A lot of damage had taken place at this stage. The values then rose very slowly to 9.2 (+/- 4.3) at 4.5 months and 9.8 (+/-6) at 6 months. There was a further steep rise to 13 (+/- 2.6) at 8 months in this marfan group. This was 10.8 times the value of the normal group at this age. Overall, the two patterns were widely disparate with the normal group having consistently low values and the marfan group rising quickly, remaining elevated and continuing to rise, (Figure 3.14).

Elastin Volume

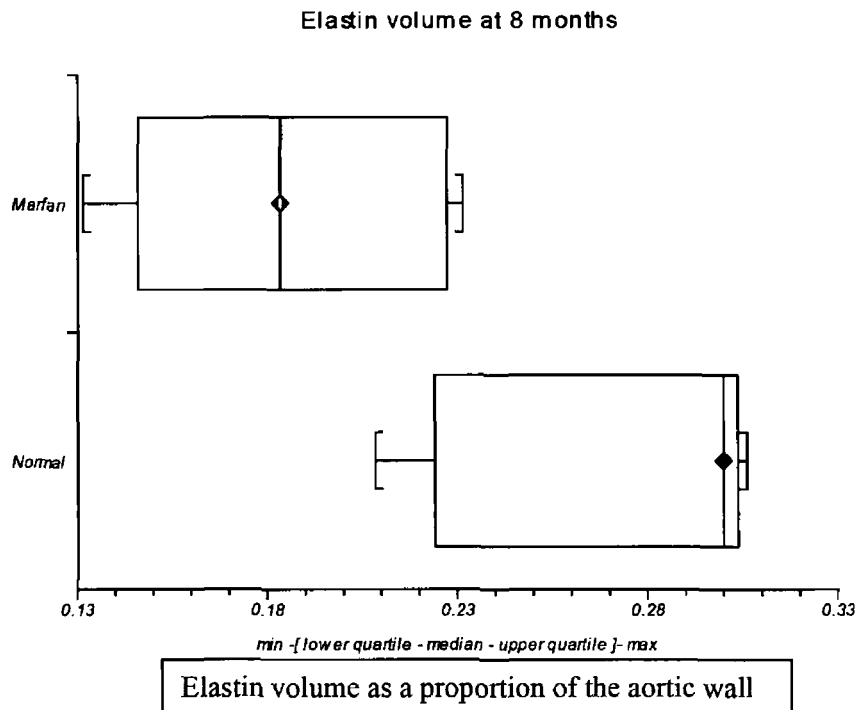


Figure 3.15: Mean elastin volume as a proportion of the aortic wall at 8 months in normal and Marfan groups. This shows that elastin volume is greatly reduced in the Marfan group compared with the normal group.

Elastin volume was 0.271 (+/- 0.02) of the aortic wall, where Marfan aortic wall thickness had a greatly reduced level of elastin at 0.1858 (+/- 0.01), (Figure 3.15). Despite a range in values, there remains a statistically significant difference between the two groups, $p = 0.0143$. The loss of elastin in the Marfan group was associated with a high degree of architectural damage seen at eight months in the Marfan group.

3.3.4 Electron-microscopy of Aortic Wall

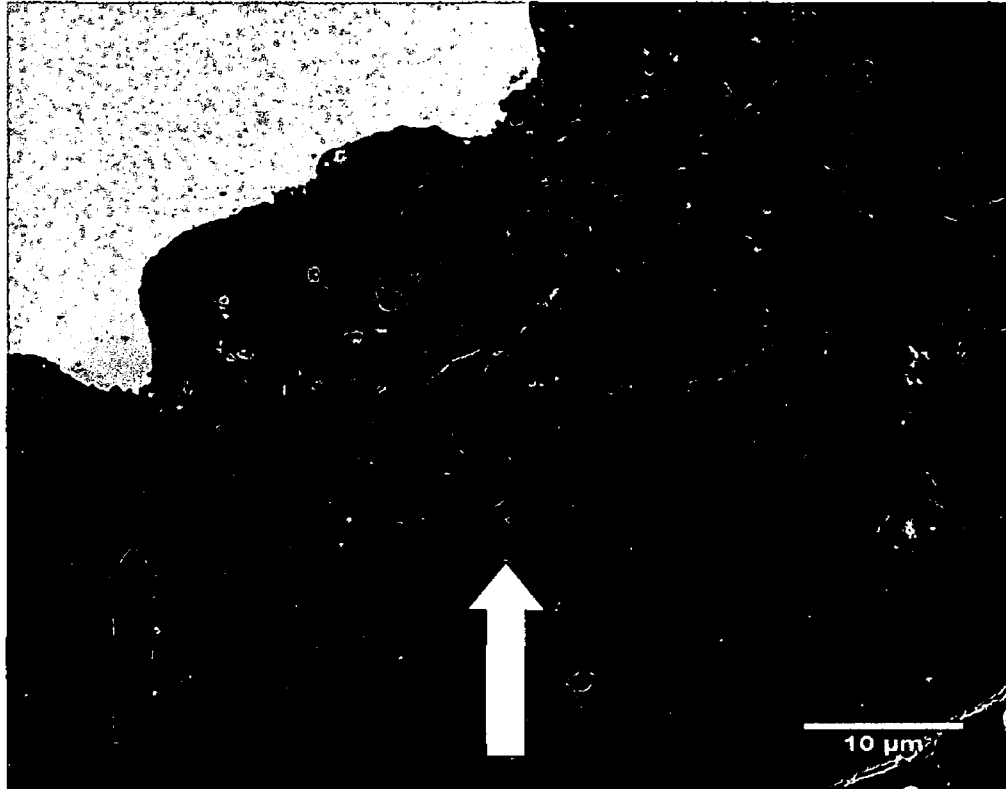


Figure 3.16: Transmission electron micrograph of a uranyl acetate and lead citrate stained resin section of the tunica media showing concentric bands of elastic lamellae (white arrow) interspersed with SMCs (black arrow). Tissue: normal mouse aortic root. Scale bar: 10 μm.

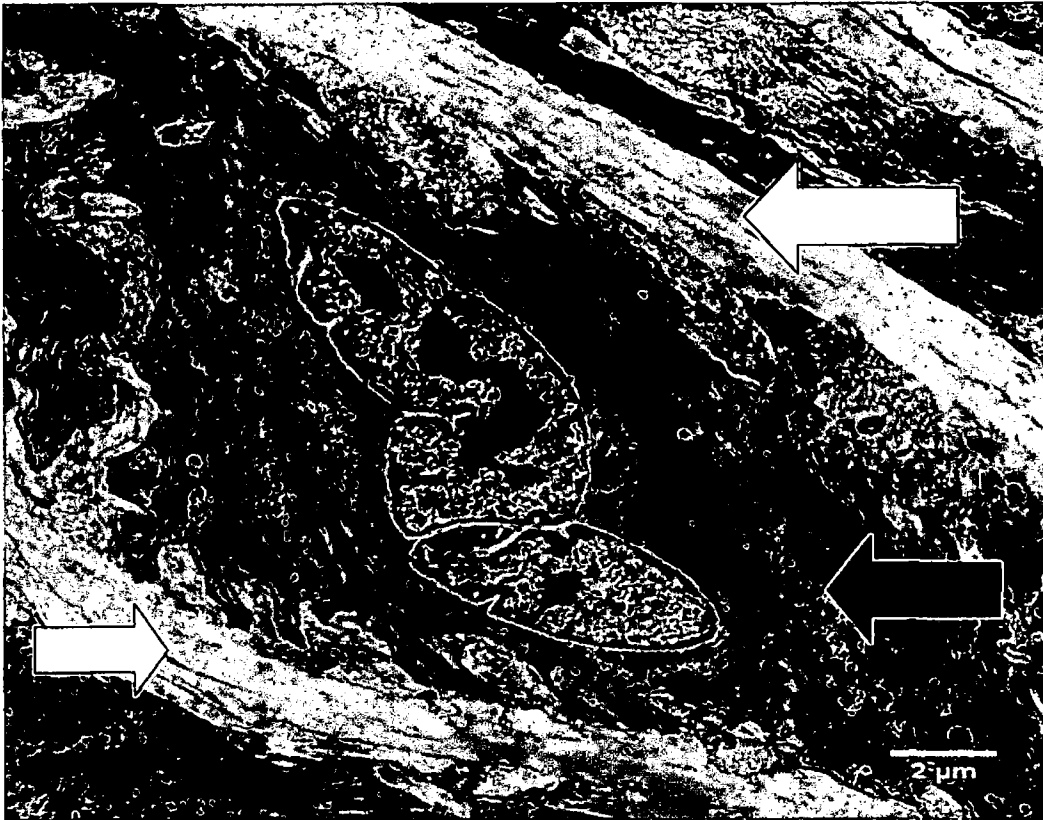


Figure 3.17: Transmission electron micrograph of a uranyl acetate and lead citrate stained resin section of a SMC (black arrow), lying between two elastic lamellae (white arrow). Tissue: normal mouse aortic root. Scale bar: 2 μ m.

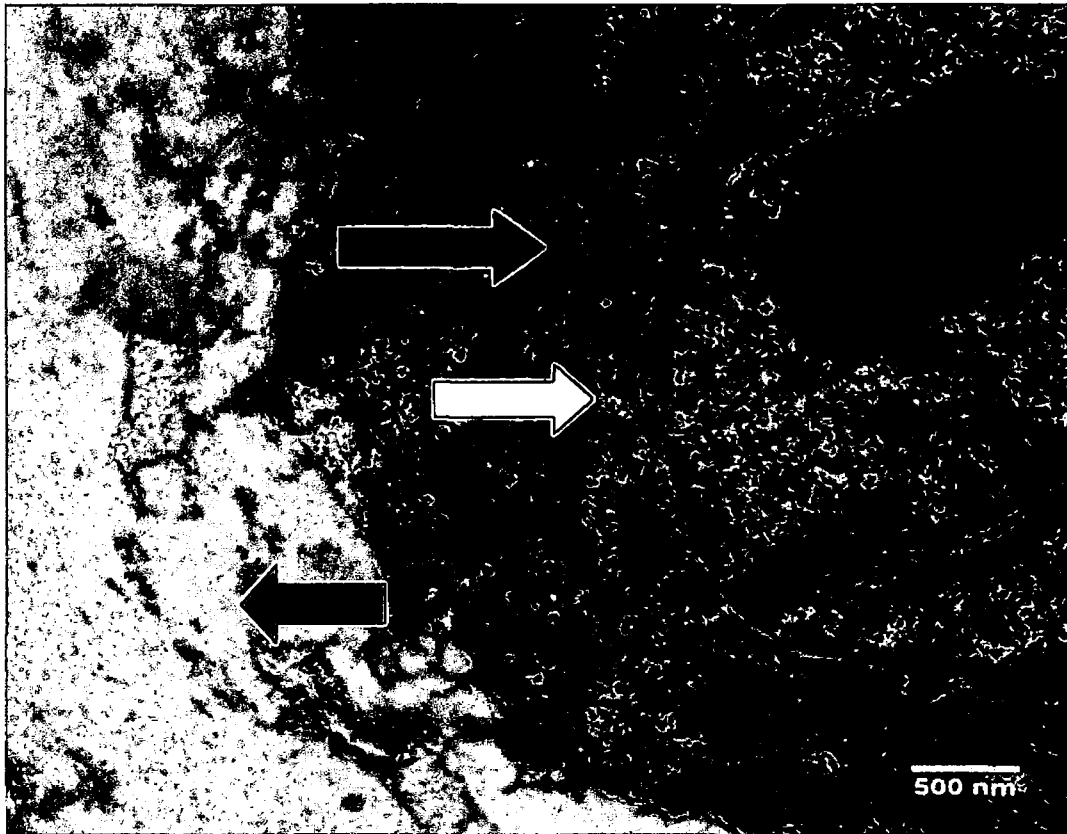


Figure 3.18: Transmission electron micrograph of a uranyl acetate and lead citrate stained resin section of a SMC with small amount of RER (white arrow) and mitochondria (black arrow) in cytoplasm, lying beside an elastic lamella (blue arrow). Tissue: normal mouse aortic root. Scale bar: 500nm.

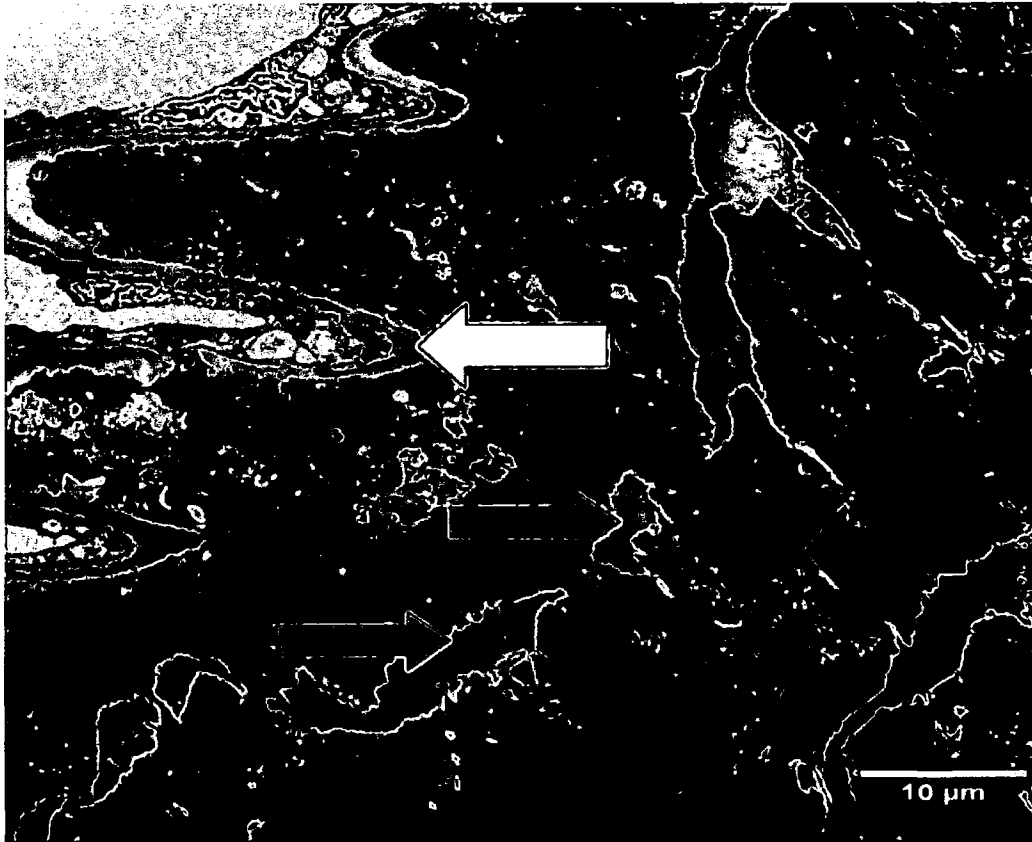


Figure 3.19: Transmission electron micrograph of a uranyl acetate and lead citrate stained resin section showing an intact internal elastic lamella (white arrow) above a fragmented elastic lamella (blue arrows), with interspersed SMCs (black arrow) within the tunica media. Tissue: Marfan mouse aortic root. Scale bar: 10μm.



Figure 3.20: Transmission electron micrograph of a uranyl acetate and lead citrate stained resin section showing the tunica media with a broken internal elastic lamella (blue arrows) and disorganised SMCs (black arrows). Tissue: Marfan mouse aortic root. Scale bar: 5µm.

In figure 3.20, loss of the tunica intima is observed. This could be an artefact in relation to slide preparation, though impairment of the tunica intima has been observed with vacuolisation, thinning, intercellular fissuring and loss of function of this layer.(Sheremet'eva, Ivanova *et al.* 2004)

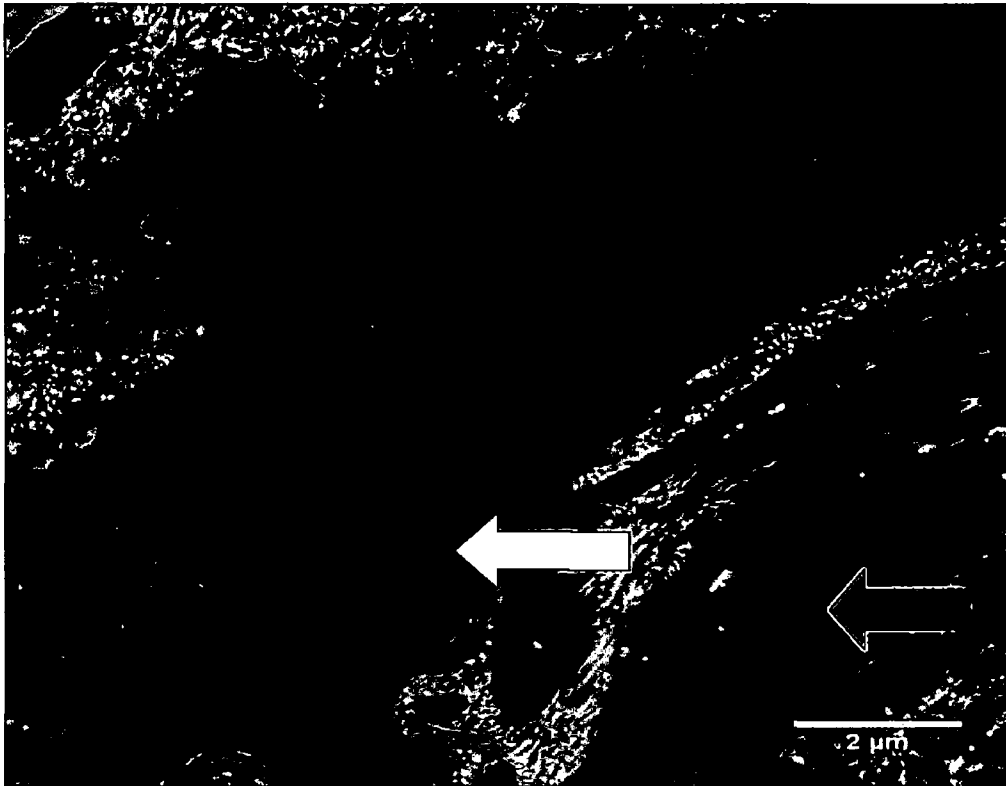


Figure 3.21: Transmission electron micrograph of a uranyl acetate and lead citrate stained resin section showing a SMC with RER (white arrow) and elastic fibre (blue arrow). Tissue: Marfan mouse aortic root. Scale bar: 2µm.

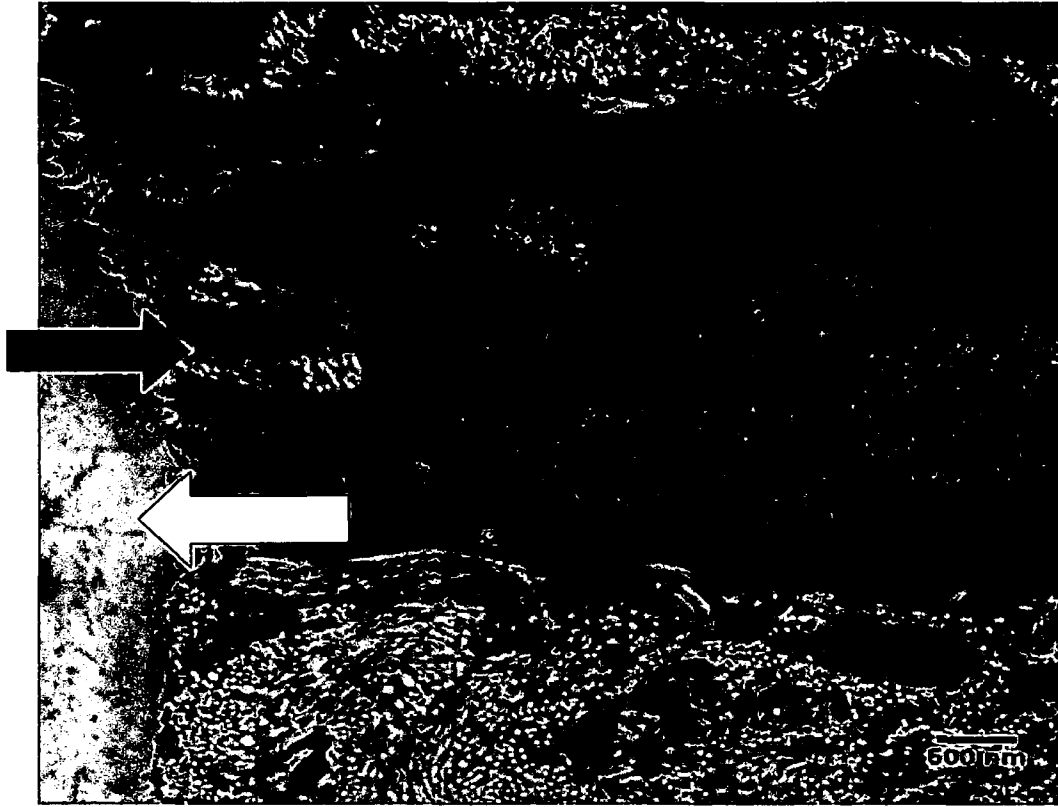


Figure 3.22: Transmission electron micrograph of a uranyl acetate and lead citrate stained resin section of a SMC (black arrow) attached to elastic fibre (white arrow).

Tissue: Marfan mouse aortic root. Scale bar: 500nm.

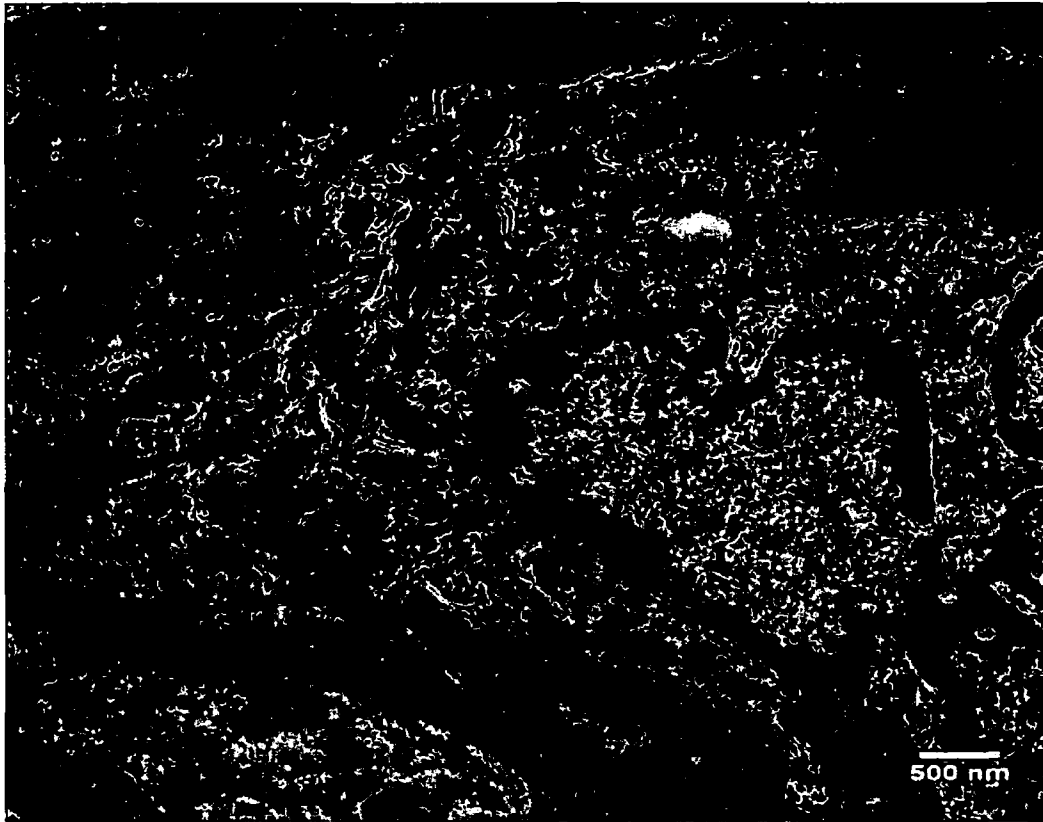


Figure 3.23: Transmission electron micrograph of a uranyl acetate and lead citrate stained resin section of a SMC with cell nucleus (white asterisk) surrounded by RER (white arrow) and mitochondria (black arrow). Tissue: Marfan mouse aortic root. Scale bar: 500nm.

Assessment of intra-nuclear activity by ultrastructural examination with electron microscopy

Euchromatin is a lightly packed form of chromatin (DNA, RNA and protein) that is rich in gene concentration, and is often (but not always) under active transcription. Euchromatin participates in the active transcription of DNA to mRNA products. The unfolded structure allows gene regulatory proteins and RNA polymerase complexes to bind to the DNA sequence, which can then initiate the transcription process. Not all

euchromatin is necessarily transcribed, but in general that which is not is transformed into heterochromatin to protect the genes while they are not in use. There is therefore a direct link to how actively productive a cell is and the amount of euchromatin that can be found in its nucleus. It is thought that the cell uses transformation from euchromatin into heterochromatin as a method of controlling gene expression and replication, since such processes behave differently on densely compacted chromatin, known as the “accessibility hypothesis”. One example of constitutive euchromatin that is “always turned on” is housekeeping genes, which code for the proteins needed for basic functions of cell survival. Euchromatin comprises the most active portion of the genome within the cell nucleus.

When the mean volume of euchromatin was measured (of the aortic smooth muscle cell nucleus) there was no statistical difference between normal, 0.59 (+/- 0.01) and Marfan nuclei, 0.61 (+/- 0.01). When the mean levels of heterochromatin were measured, of the aortic smooth muscle cell nucleus, there was no statistical difference between normal, 0.318 (+/- 0.02), and Marfan, 0.298 (+/- 0.01). P-values are > 0.4 in these cases.

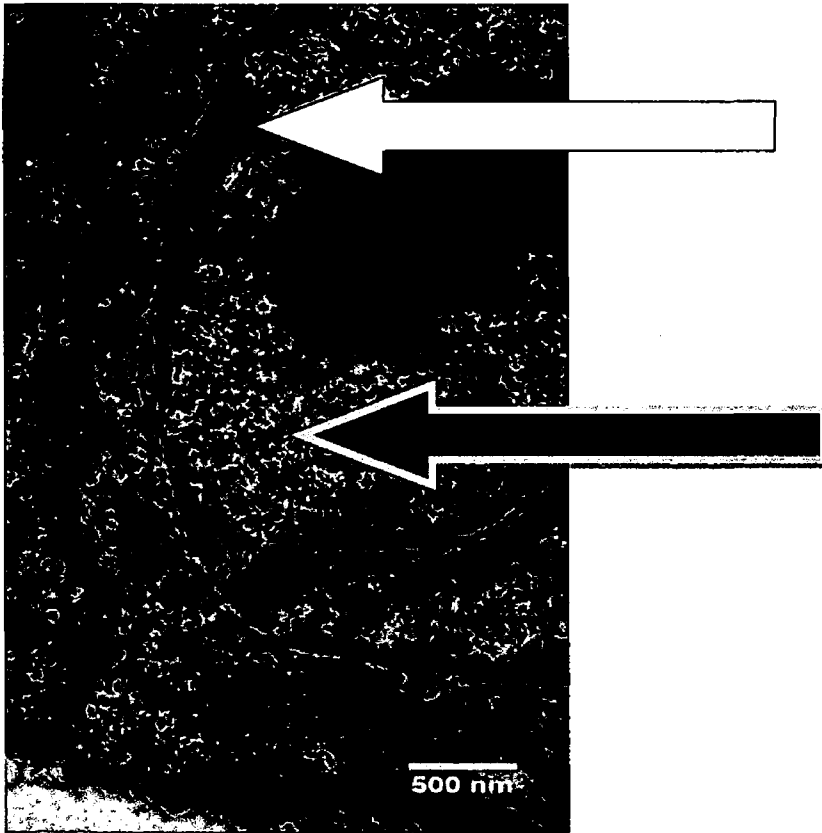


Figure 3.24: Electron photomicrograph of a nucleus of an aortic smooth muscle cell showing euchromatin (black arrow) and heterochromatin (white arrow).

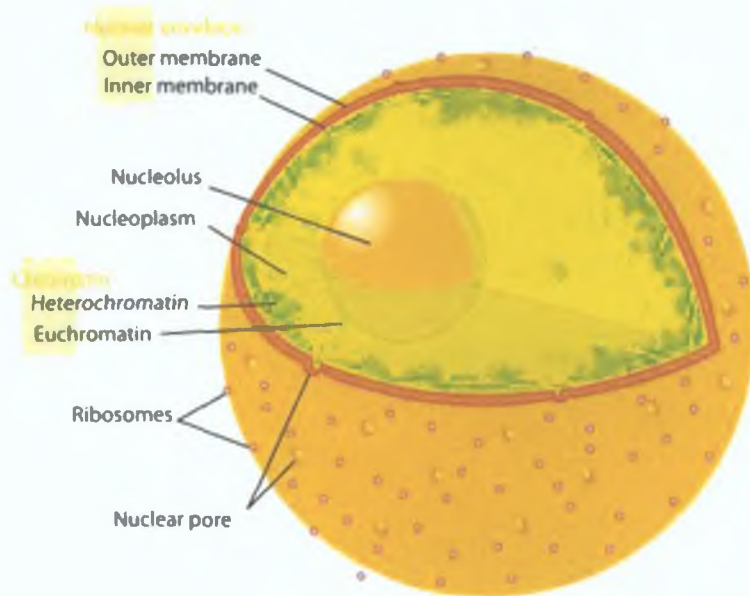


Figure 3.25: Diagram of a nucleus of cell showing euchromatin and heterochromatin. (Diagram by Mariana Ruiz Villarreal, permission granted by artist)

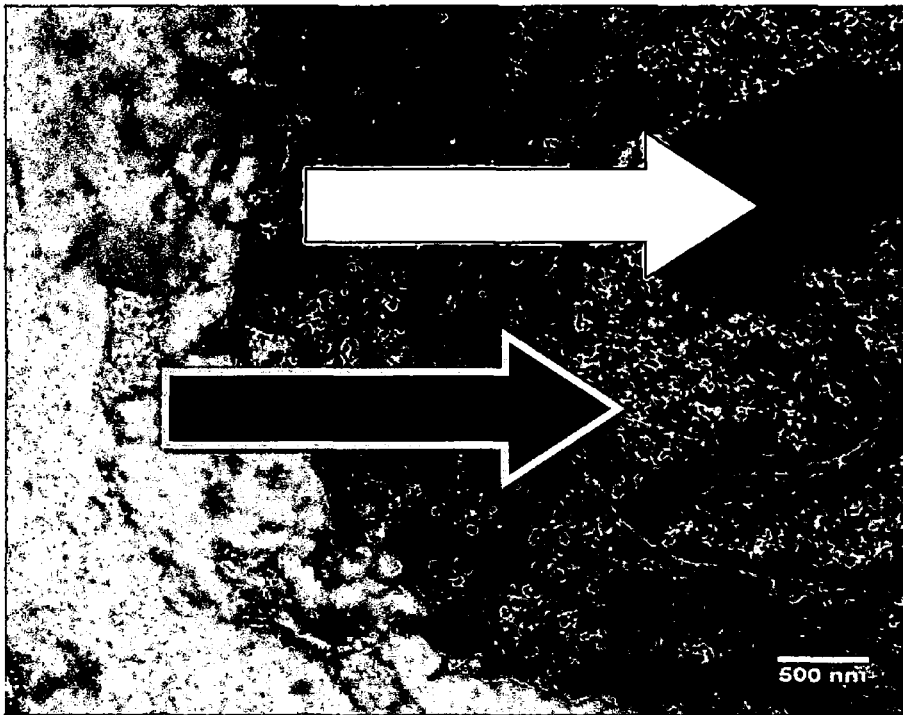


Figure 3.26: Electron photomicrograph of an aortic smooth muscle cell showing a nucleus (black arrow) and nucleolus (white arrow) within.

The nucleolus (also called nucleole) is a non-membrane bound structure composed of proteins and nucleic acids found within the nucleus. Ribosomal RNA (rRNA) is transcribed and assembled within the nucleolus. The nucleolus ultra-structure can be visualized with an electron microscope. There is no statistical difference between the mean volume of the nucleolus (as a proportion of the nucleus), in the normal aortic smooth muscle cell (0.0846) and the Marfan aortic smooth muscle cell (0.0853).

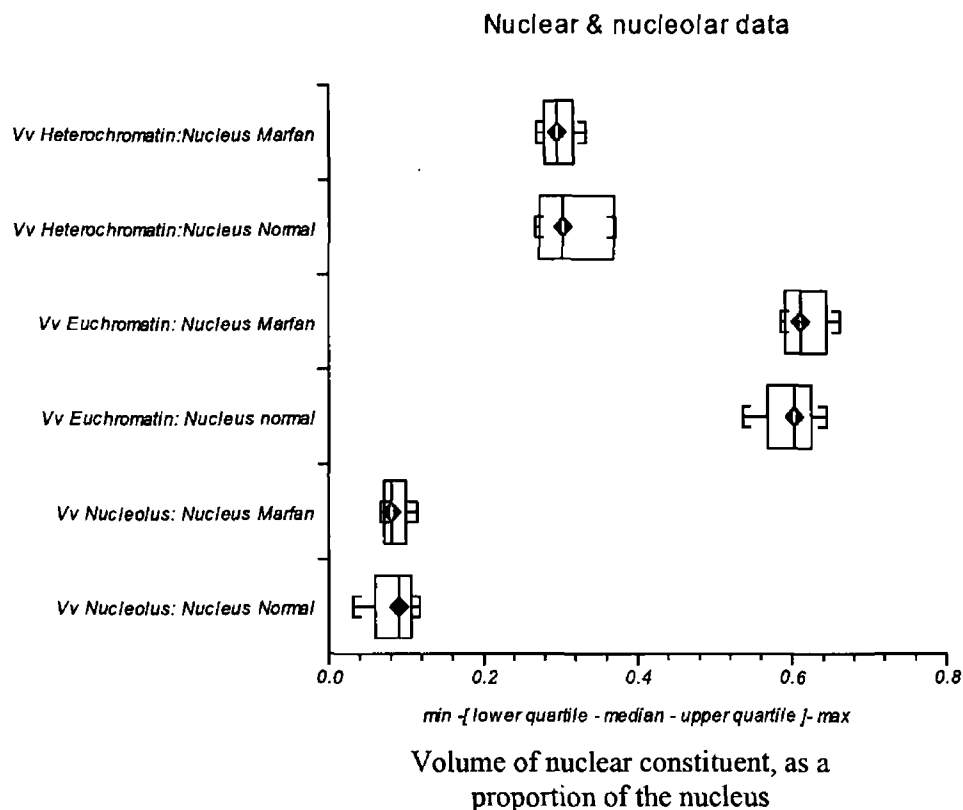


Figure 3.27: Nuclear & Nucleolar data, normal and Marfan groups at 8 months. Heterochromatin volume (as a proportion of the nucleus) in Marfan group is similar to normal. Euchromatin volume (as a proportion of the nucleus) in Marfan group is similar to normal. Nucleolar volume (as a proportion of the nucleus) in Marfan group is similar to normal.

Mitochondria are a membrane-enclosed organelle found in most eukaryotic cells. These organelles range from 0.5 to 10 micrometers (μm) in diameter. Mitochondria are sometimes described as "cellular power plants" because they generate most of the cell's supply of adenosine triphosphate (ATP), used as a source of chemical energy. In addition to supplying cellular energy, mitochondria are involved in a range of other processes,

such as signalling, cellular differentiation, cell death, as well as the control of the cell cycle and cell growth. Mitochondria have been implicated in several human diseases, including mitochondrial disorders and cardiac dysfunction.

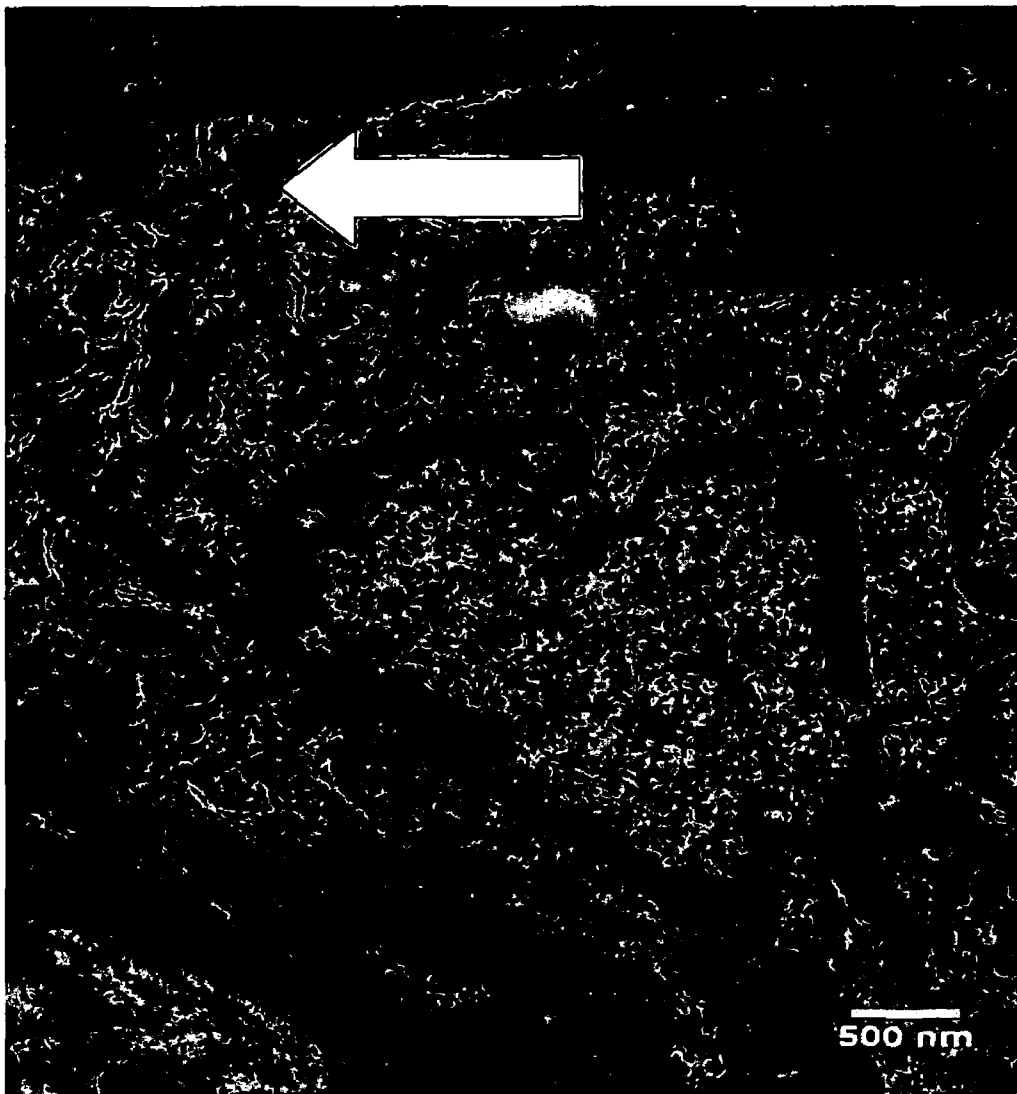


Figure 3.28: Electron photomicrograph of cell organelles within an aortic smooth muscle cell. Mitochondria are present; one mitochondrion is displayed by a white arrow.

As noted in a prior electron-microscopy study of Marfan aorta, we also noted in our study that there were an increased amount of mitochondria in the aortic smooth muscle cells in Marfan aortic smooth muscle compared to normal aortic smooth muscle.(Scheck 1979) The volume of mitochondria as a proportion of the cytoplasm was increased in Marfan aorta, 0.108 (+/- 0.01), as compared to normal aortic tissue, 0.07 (+/- 0.01). Though the $p = 0.089$, it comes close to statistical significance. The number of individual mitochondria was not quantified separately, as a stereological technique was used to measure the volume of the cell and the volume of which contained mitochondria. The number of mitochondria could be estimated from the volume of mitochondria per cell, though the accuracy of this calculation has not been validated.

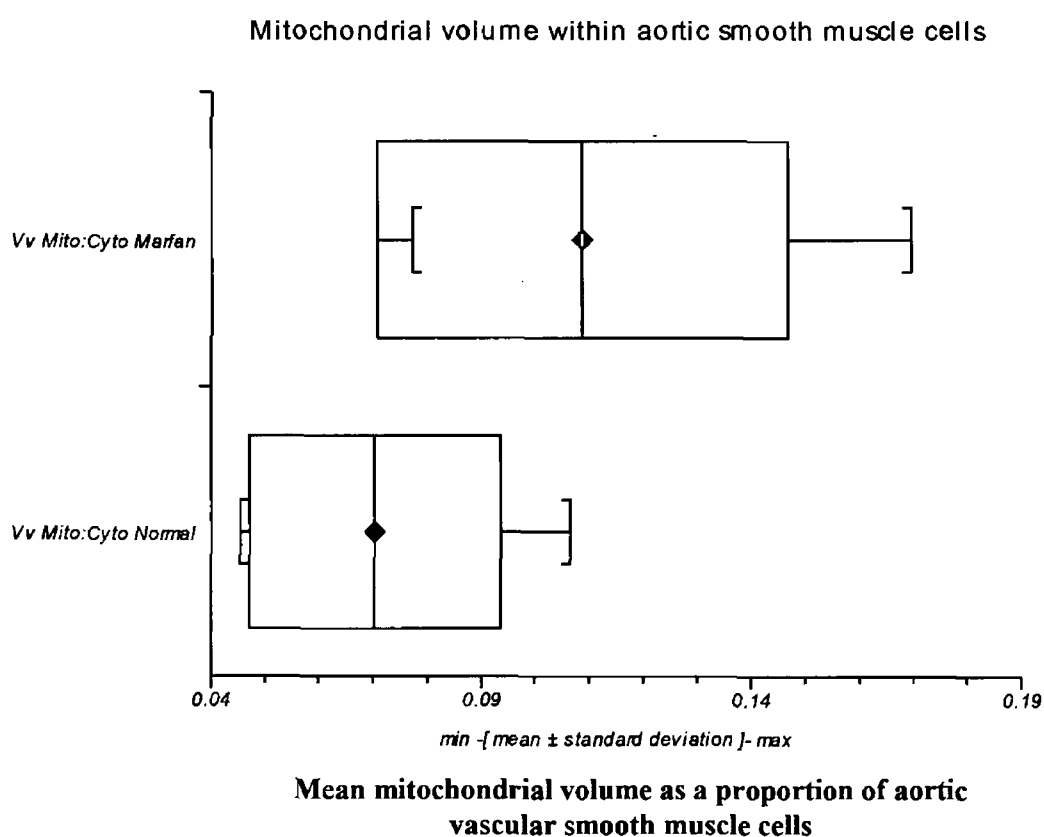


Figure 3.29: Mean mitochondrial volume as a proportion of aortic vascular smooth muscle cells. A comparison between normal and Marfan aortic root tissue.

Rough Endoplasmic Reticulum, as a proportion of the cytoplasm was greatly increased in Marfan groups, 0.0346, compared to normal groups, 0.0091, ($p = 0.0005$), which is displayed in the graph below. The difference in smooth endoplasmic reticulum approached significance at $p = 0.06$, though unexpectedly extremely small volumes were noted in the normal group, the value measure was equal to zero. The Marfan group, 0.0016, also had very small volumes.

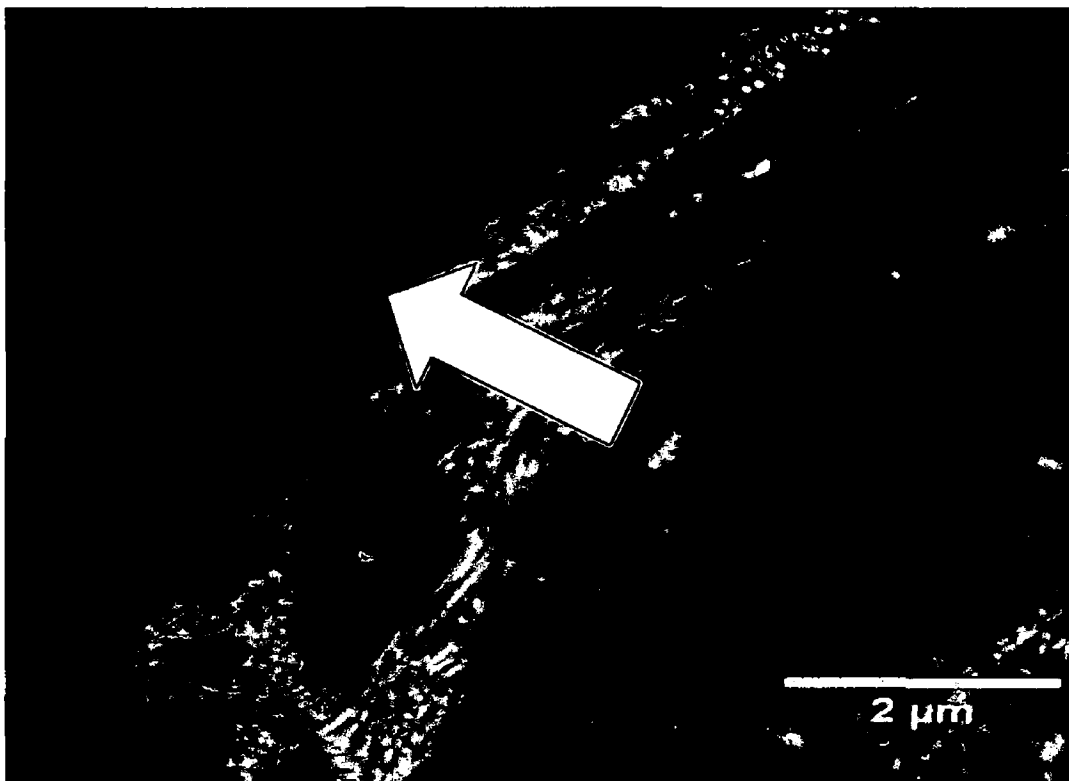


Figure 3.30: Electron photomicrograph of cell organelles within an aortic smooth muscle cell from the normal, control group. Rough Endoplasmic Reticulum are present, one area displayed by a white arrow.

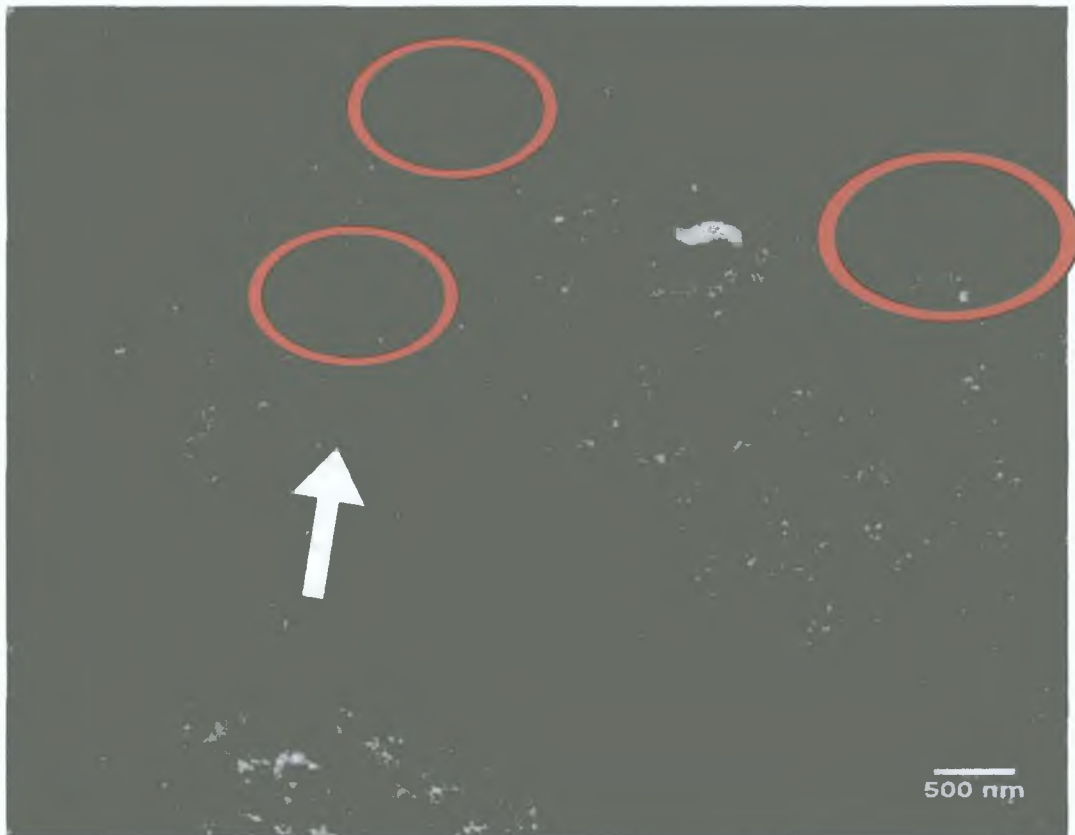
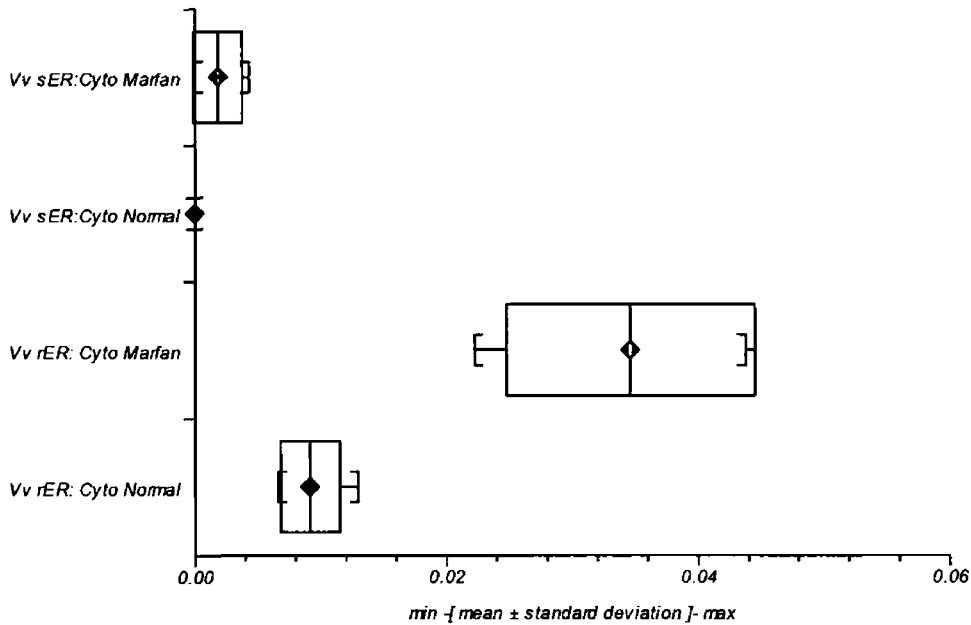


Figure 3.31: Electron photomicrograph of cell organelles within an aortic smooth muscle cell from the Marfan group. Rough Endoplasmic Reticulum is present, one area displayed by a white arrow and other areas encircled in pink.

rough & smooth Endoplasmic Reticulum in Normal & Marfan Aortic smooth musc



Volume of Endoplasmic Reticulum as a proportion of aortic smooth muscle

Figure 3.32: Mean volume of rough Endoplasmic Reticulum compared to smooth Endoplasmic Reticulum, as a proportion of normal or Marfan aortic vascular smooth muscle cytoplasm.

There was almost no Golgi apparatus measured as a proportion of the aortic smooth muscle cytoplasm in the normal group, the value measured was equal to zero. In comparison to this, the amount of Golgi apparatus (i.e. the mean volume of Golgi apparatus measured as a proportion of the aortic smooth muscle cytoplasm) in the Marfan group measured was 0.0016, as a proportion of the cytoplasm (estimated std. error of the mean = 0.00071). This did not meet the criteria for statistical significance.

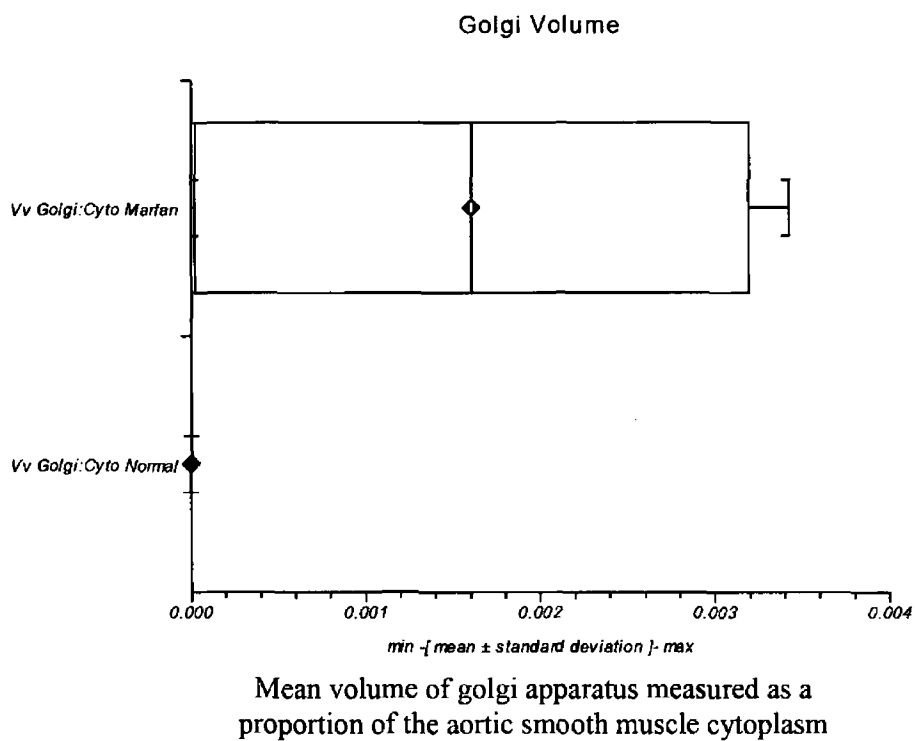


Figure 3.33: Mean volume of Golgi apparatus measured as a proportion of the aortic smooth muscle cytoplasm, normal compared to the Marfan group.

Light microscopy images, of the course of the natural history in normal and Marfan aortic root.

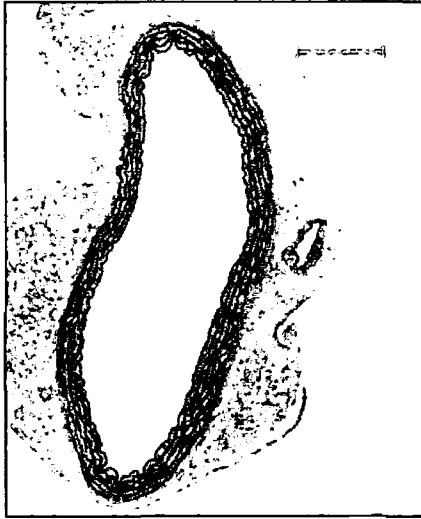


Figure 3.34: Light microscopy image: haematoxylin and eosin stained cross-section of aortic root of wild-type mouse at 6 weeks, magnification x10.



Figure 3.35: Light microscopy image: haematoxylin and eosin stained cross-section of aortic root of wild-type mouse at 3 months, magnification x40.

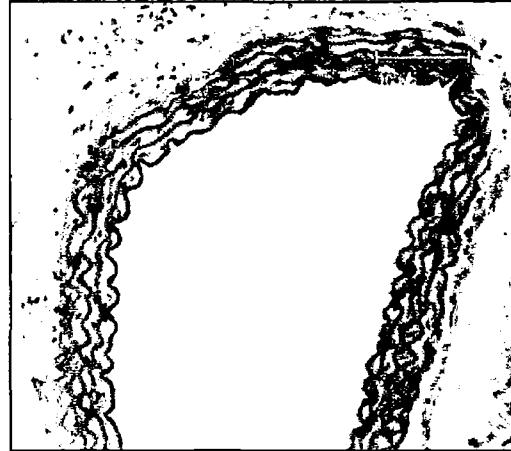


Figure 3.36: Light microscopy image: haematoxylin and eosin stained cross-section of aortic root of wild-type mouse at 3 months, magnification x20.

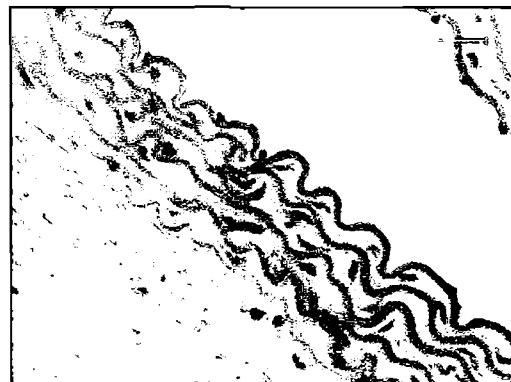


Figure 3.37: Light microscopy image: haematoxylin and eosin stained cross-section of aortic root of wild-type mouse at 4.5 months, magnification x40.

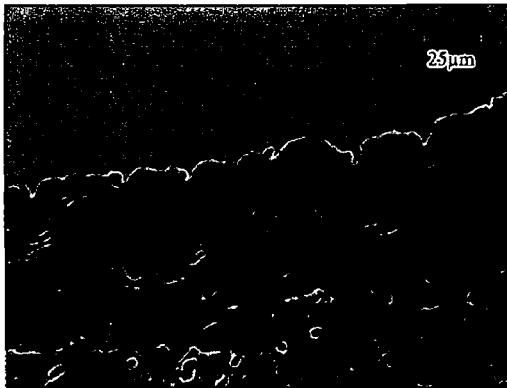


Figure 3.38: Light microscopy image: haematoxylin and eosin stained cross-section of aortic root of wild-type mouse at 6 months, magnification x40.

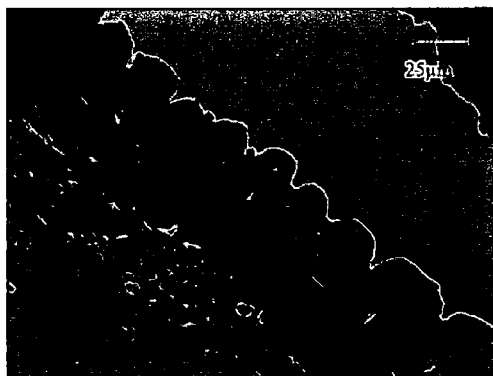


Figure 3.39: Light microscopy image: haematoxylin and eosin stained cross-section of aortic root of wild-type mouse at 8 months, magnification x40.

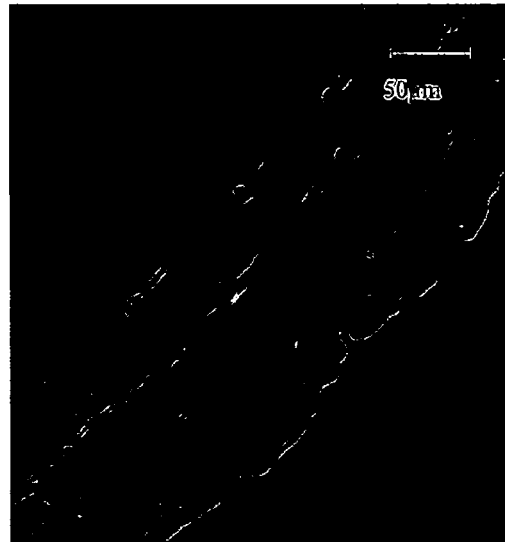


Figure 3.40: Light microscopy image: haematoxylin and eosin stained cross-section of aortic root of wild-type mouse at 8 months, magnification x40.

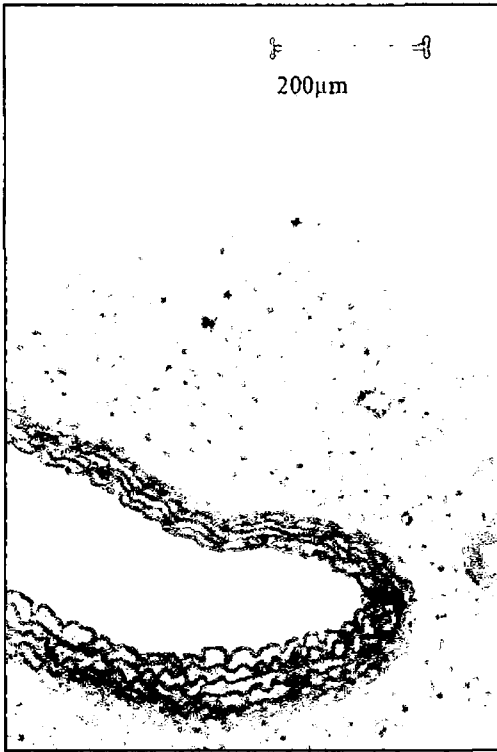


Figure 3.41: Light microscopy image: haematoxylin and eosin stained cross-section of aortic root of “Marfan” mouse at 6 weeks, magnification x10.

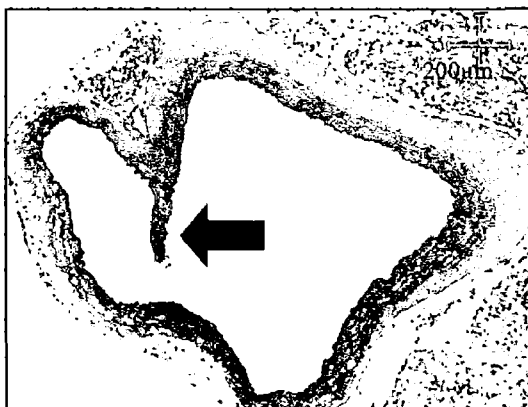


Figure 3.42: Light microscopy image: haematoxylin and eosin stained cross-section of aortic root of “Marfan” mouse at 6 weeks, magnification x10. Aortic valve cusp present (black arrow).



Figure 3.43: Light microscopy image: haematoxylin and eosin stained cross-section of aortic root of “Marfan” mouse at 3 months, magnification x10. Early evidence of aberrant aortic wall is present.

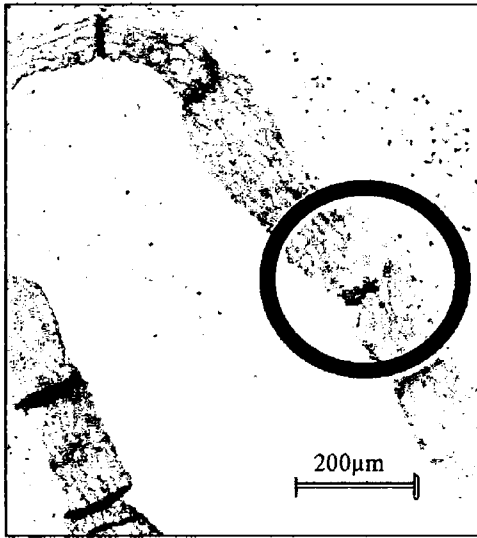


Figure 3.44: Light microscopy image: haematoxylin and eosin stained cross-section of aortic root of “Marfan” mouse at 4.5 months, magnification x10. Loss of usual arrangement of elastin is evident (black circle).

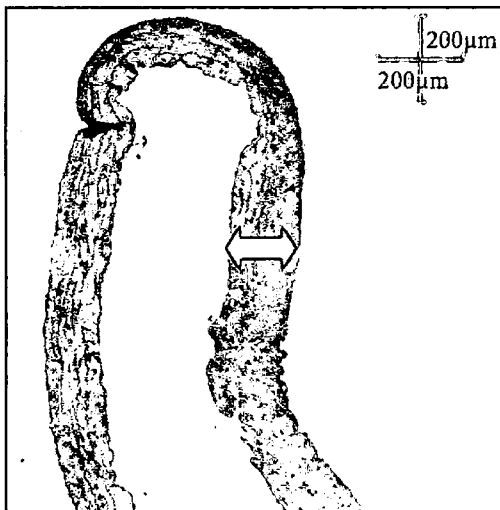


Figure 3.45: Light microscopy image: haematoxylin and eosin stained cross-section of aortic root of “Marfan” mouse at 6 months, magnification x10. Evidence of progressive aberrant aortic wall thickening is present (yellow arrows).



Figure 3.46: Light microscopy image: haematoxylin and eosin stained cross-section of aortic root of “Marfan” mouse at 8 months, magnification x10. Thickened aortic wall is evident with loss of the uniform vascular smooth muscle cell arrangement.

Light microscopy images of haematoxylin and eosin stained cross-sections of normal murine aortic wall, at the level of the aortic root, are shown in figures 3.34 to 3.39. They display the change in the appearance of the aortic wall through the course of development from 6 weeks (figure 3.34), 3 months (figure 3.35 & 3.36), 4.5 months (figure 3.37), 6 months (figure 3.38) and at 8 months (figure 3.39 & 3.40). The normal aorta, at the level of the aortic root, has to accommodate an ever increasing circulating volume of blood as the mouse develops and grows. The larger volume of blood is accommodated by increasing the diameter of the aorta, which is evident in figures 3.34 to 3.40. By referring to the law of La Place, the greater the radius of the vessel, the greater the transmural pressure across the wall. The wall develops and becomes slightly thicker to accommodate to the tension on the wall of the vessel, from having tightly compact elastin fibres with little space in between fibres, at 6 weeks (figure 3.34) and 4.5 months (figure 3.37), to developing a slightly thicker appearance with more substantial space between the fibres at 6 (figure 3.38) and 8 months (figure 3.40). Throughout the course of development we can see the smooth uniform arrangement of smooth muscle cells between the elastin fibres remains a feature.

In contrast to the normal maturation of the aortic wall, the pathological changes present during development of the Marfan aortic wall are displayed in light microscopy images of haematoxylin and eosin stained cross-sections of Marfan, murine aortic wall, at the level of the aortic root in figures 3.41 to 3.46. At 6 weeks, the elastin fibres are tightly compact with a “wavy,” uniform smooth pattern (figures 3.41 and 3.42). There is evidence of early abnormal thickening of the aortic wall at 3 months (figure 3.43) and loss of the usual

uniform arrangement of elastin fibres at 4.5 months (figure 3.44). There is evidence of established abnormal thickening of the aortic wall present at 6 months (figure 3.45) and this persists at 8 months (figure 3.46).

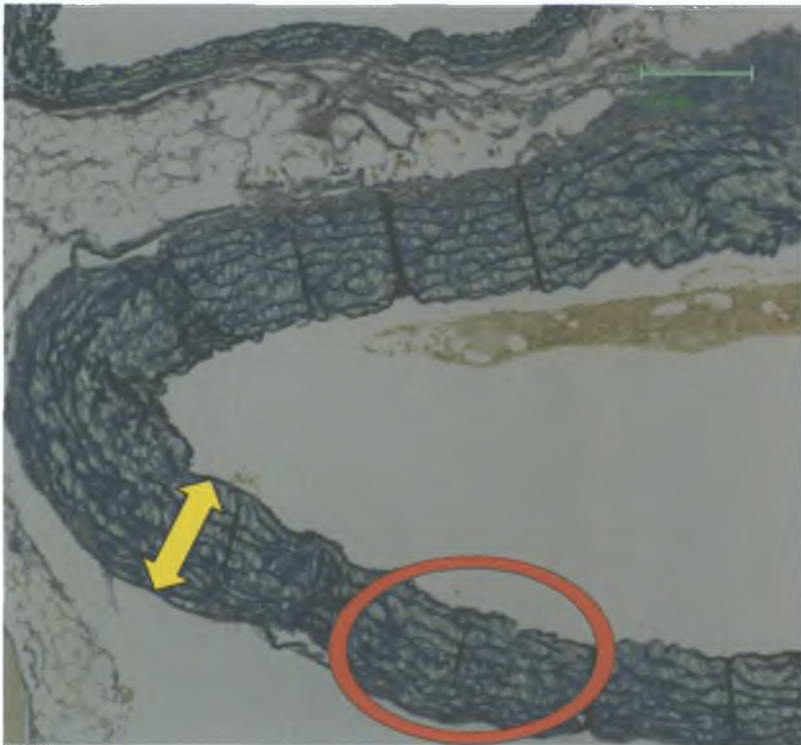


Figure 3.47: Light microscopy image: Verhoeff-Van Gieson stained cross-section of aortic root of “Marfan” mouse at 8 months, magnification x10. The aortic wall is thickened (yellow arrows) with loss of the usual arrangement of elastin (red circle).

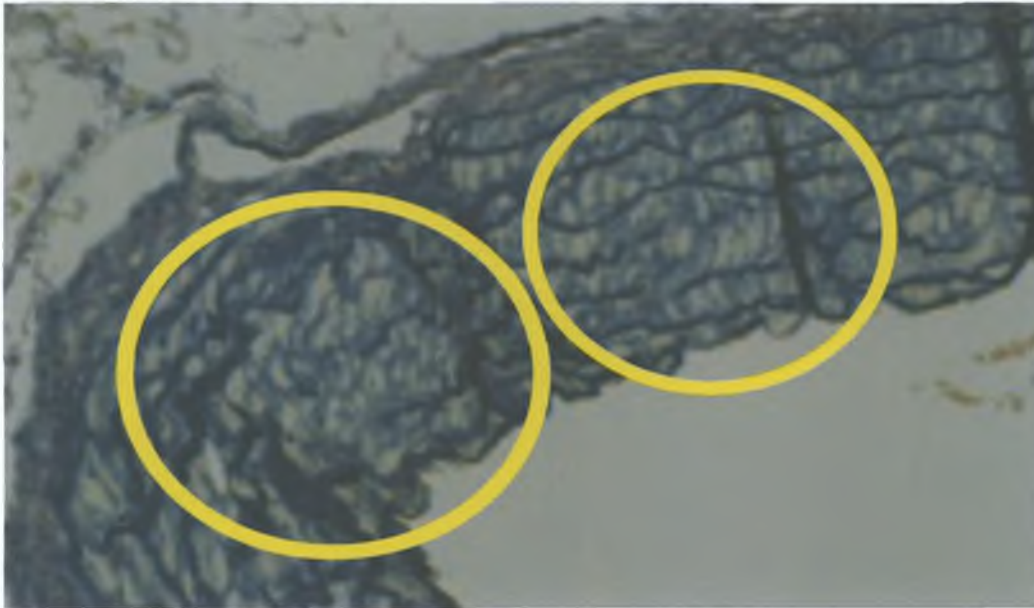


Figure 3.48: Light microscopy image: Verhoeff-Van Gieson stained cross-section of aortic root of “Marfan” mouse at 8 months, magnification x20. At a higher magnification view, this displays two islands of damage, encircled (yellow).

Light microscopy images of Verhoeff-Van Gieson stained cross-sections of murine Marfan aortic root at 8 months, display both aortic wall thickening and loss of the usual arrangement of elastin in figure 3.47. A higher power light microscopy image displays two areas where there is loss of continuity of, two or more, separate elastin fibres in close proximity, also called “islands of damage” (figure 3.48).

3.4 Discussion

Mean values and standard deviations were established for a normal murine aorta root diameter at 3 and 8 months. Mean values and standard deviations were also established for a murine Marfan model aorta root diameter at 3 and 8 months. The Marfan aortic root were found to be dilated by 25% at 3 months and developed aneurysmal disease with a growth rate of 53% over a 5 month period. This is similar to the initial studies published by our collaborators, showing a 14% increase in the diameter of the aortic root at 7 weeks of age between normal and Marfan mice.(Habashi, Judge *et al.* 2006) There was a 27% increase in the size of the aortic root in Marfan mice compared to normal controls at 3 months, in a study conducted by Chung *et al.* (Chung, Yang *et al.* 2008) The growth rate in our study was 3 times the growth rate of normal aortic root diameter in Marfan mice, which was similar to that of Habashi *et al.*(Habashi, Judge *et al.* 2006) The mean aortic root diameter of Marfan mice had aneurysmal aortas 56.5% wider than normal controls at 8 months, which is even greater than the 36% difference observed by Habashi *et al.*(Habashi, Judge *et al.* 2006) and the 32% difference seen by Chung *et al.* (Chung, Yang *et al.* 2008) The extent of aneurysmal dilatation in this study is comparable to other studies being conducted internationally.

Myocardial function was assessed in both normal and Marfan groups. Left ventricular function can be reduced in Marfan Syndrome prior to established valvular disease(Kiotsekoglou, Bajpai *et al.* 2008). Left ventricular dP/dt maximum was measured and shown to be reduced by 27% compared to normal. Using a contractility index of left ventricular function did not discriminate between the two groups. In 2003, a cohort of patients with Marfan syndrome in the Mayo clinic with no or mild aortic or mitral regurgitation, had, in general, no evidence of left ventricular impairment in the absence of significant valvular disease.(Chatrath, Beauchesne *et al.* 2003) Though in 2006, evidence of

mild but significant impairment of left ventricular systolic & diastolic function, was found in a cohort of Marfan patients unrelated to valvular disease.(De Backer, Devos *et al.* 2006) Aortic pulse pressure was measured to assess for evidence of aortic insufficiency. There was no clinically significant widening of the aortic pulse pressure in either group. If there was a significant widening of the aortic pulse pressure in the Marfan group this would have supported evidence of severe aortic insufficiency.(Hamby, Gulotta *et al.* 1968) The aortic dirotic notch, which reflects failure of coaptation, is a more subtle sign of aortic insufficiency.(Hamby, Gulotta *et al.* 1968) This was present in 36% of the Marfan group. This finding would reflect aortic annular dilatation secondary to aortic root dilatation as measured by echocardiography, as patients with aneurysms of the ascending aorta or aortic root, frequently have aortic valve insufficiency despite having normal valve leaflets.(David, Feindel *et al.* 1995) These results displayed in Figure 3.5 and discussed in Section 3.3.1

Ongoing aortic insufficiency would cause impairment of left ventricular function. Reduced left ventricular function would be reflected by reduced left ventricular contractility. As mentioned above, there is evidence of ventricular dysfunction and it is likely that this is secondary to aortic insufficiency, though there could be a primary Marfan related cardiomyopathy which could be an alternate primary cause. (Alpendurada, Wong *et al.* 2010) Histological analysis showed progressive aberrant thickening of the aortic wall at the level of the aortic root. The progressive thickening occurred with a similar pattern to the normal growth pattern in the wild-type group. Thickening was found to be established early in the disease and continue to develop over the first 3 months of life. There was a second rapid increase in thickening from 6 to 8 months after a plateau phase. Other studies have observed a similar findings with regard to aortic wall thickness increased by 50%.(Habashi, Judge *et al.* 2006) This was initially thought to be related to a second phase of inflammation, brought about by recruitment of neutrophils, as matrix metalloproteinase-9 levels are elevated in

Marfan aortic root tissue (Ikonomidis, Jones *et al.* 2006) and Matrix metalloprotease-9 is also called neutrophil elastase, and there is growing evidence that it is involved in remodelling of vessels. (Dollery, Owen *et al.* 2003) A neutrophilic infiltrate was not observed in our specimens at 8 months. This suggests that, the pathological process maybe, related to an ongoing interaction between the aortic vascular smooth muscle cells and the intercellular matrix of the aortic wall.

Progressive loss of the architectural integrity of the aortic wall at the level of the aortic root was observed in the Marfan group. There was some evidence of disruption of the elastic fibre architecture at 6 weeks in the Marfan group. Other groups also found evidence of loss of architectural integrity with fragmentation of the elastic lamellae.(Habashi, Judge *et al.* 2006; Chung, Yang *et al.* 2008) There was a dramatic rise in the amount of “islands of damage” in the six week period between 6 weeks and 3 months of age. This was followed by a plateau phase, until the period between 6 and 8 months where there was a second rise in the amount of disruption. The timing of both aberrant thickening and architectural disruption are similar in the Marfan group, suggesting that these are both consequences of the same mechanism. Elastin volume was reduced in the Marfan group along with increased elastin disruption.

Ultra-structural analysis showed no evidence that there was an appreciable difference in the amount of nucleus available for transcription as the proportion of heterochromatin or euchromatin, within the cell nucleus was unchanged. There was no ultra-structural evidence that an overall increased amount of ribosomal RNA was being transcribed, as there was no difference between nucleolar size in each group. The amount of rough Endoplasmic Reticulum was increased greatly, proving that there is an increased amount of protein production within the aortic vascular smooth muscle and this correlates with the histological findings and the aortic root dilatation in the Marfan group. Mitochondrial volumes were greatly increased in the Marfan group, which reflects greater activity of the cell and they are

localized close to the rough Endoplasmic Reticulum reflecting the increased activity of the rough Endoplasmic Reticulum. The Marfan aortic vascular smooth muscle showed a trend toward having an increased volume of rough Endoplasmic Reticulum compared to normal aortic vascular smooth muscle cells. The Golgi volume was also increased in the Marfan group, which reflects a great amount of transportation of proteins through the cell for transport out of the cell. The excessive protein production within the aortic vascular smooth muscle cell, is associated with increased transportation of these proteins out of the cell, and in turn was associated with histological changes within the aortic wall itself and the overall dilatation of the lumen of this structure. Increased prominence of synthetic organelles have been noted within aortic vascular smooth muscle cells in a mouse homozygous for a targeted hypomorphic allele of fibrillin-1, with prominence of Golgi apparatus, endoplasmic reticulum and cytoplasmic vacuoles.(Bunton, Biery *et al.* 2001)

Observations have been made which are comparable to other studies published to show a significant differences between echocardiographic, invasive left ventricular assessment, histologic and ultrastructural aspects of Marfan syndrome recapitulated by the C1039G Marfan mouse. These results document the natural history and form integral pieces of the puzzle in understanding the pathophysiology of Marfan syndrome.

3.5 References

- Alpendurada, F., J. Wong, et al. (2010). "Evidence for Marfan cardiomyopathy." Eur J Heart Fail 12(10): 1085-1091.
- Bunton, T. E., N. J. Biery, et al. (2001). "Phenotypic alteration of vascular smooth muscle cells precedes elastolysis in a mouse model of Marfan syndrome." Circ Res 88(1): 37-43.
- Chatrath, R., L. M. Beauchesne, et al. (2003). "Left ventricular function in the Marfan syndrome without significant valvular regurgitation." Am J Cardiol 91(7): 914-916.
- Chung, A. W., H. H. Yang, et al. (2008). "Long-term doxycycline is more effective than atenolol to prevent thoracic aortic aneurysm in marfan syndrome through the inhibition of matrix metalloproteinase-2 and -9." Circ Res 102(8): e73-85.
- David, T. E., C. M. Feindel, et al. (1995). "Repair of the aortic valve in patients with aortic insufficiency and aortic root aneurysm." J Thorac Cardiovasc Surg 109(2): 345-351; discussion 351-342.
- De Backer, J. F., D. Devos, et al. (2006). "Primary impairment of left ventricular function in Marfan syndrome." Int J Cardiol 112(3): 353-358.
- Dollery, C. M., C. A. Owen, et al. (2003). "Neutrophil elastase in human atherosclerotic plaques: production by macrophages." Circulation 107(22): 2829-2836.
- Finkbohner, R., D. Johnston, et al. (1995). "Marfan syndrome. Long-term survival and complications after aortic aneurysm repair." Circulation 91(3): 728-733.
- Fishman, A. P. (1989). "Cardiac asthma--a fresh look at an old wheeze." N Engl J Med 320(20): 1346-1348.
- Habashi, J. P., D. P. Judge, et al. (2006). "Losartan, an AT1 antagonist, prevents aortic aneurysm in a mouse model of Marfan syndrome." Science 312(5770): 117-121.
- Hamby, R. I., S. J. Gulotta, et al. (1968). "Immediate hemodynamic effects of aortic regurgitation in man." Am J Cardiol 21(4): 478-486.
- Hart, C. Y., J. C. Burnett, Jr., et al. (2001). "Effects of avertin versus xylazine-ketamine anesthesia on cardiac function in normal mice." Am J Physiol Heart Circ Physiol 281(5): H1938-1945.
- Ikonomidis, J. S., J. A. Jones, et al. (2006). "Expression of matrix metalloproteinases and endogenous inhibitors within ascending aortic aneurysms of patients with Marfan syndrome." Circulation 114(1 Suppl): I365-370.
- Kiotsekoglou, A., A. Bajpai, et al. (2008). "Early impairment of left ventricular long-axis systolic function demonstrated by reduced atrioventricular plane displacement in patients with Marfan syndrome." Eur J Echocardiogr 9(5): 605-613.
- Lansac, d. C., Jondeau (2007). "Distinctive features of thoracic aorta surgery in Marfan Syndrome " MT Cardiology 3(3): 212-225.
- Marsalese, D. L., D. S. Moodie, et al. (1989). "Marfan's syndrome: natural history and long-term follow-up of cardiovascular involvement." J Am Coll Cardiol 14(2): 422-428; discussion 429-431.
- Murdoch, J. L., B. A. Walker, et al. (1972). "Life expectancy and causes of death in the Marfan syndrome." N Engl J Med 286(15): 804-808.
- Scheck, S., Parker, Chang, Fu (1979). "Aortic aneurysm in Marfan's syndrome: changes in the ultrastructure and composition of collagen." Journal of Anatomy 129(3): 645-657.

- Schwinger, R. H., M. Bohm, et al. (1994). "The failing human heart is unable to use the Frank-Starling mechanism." Circ Res 74(5): 959-969.**
- Sheremet'eva, G. F., A. G. Ivanova, et al. (2004). "A comparative study of the aortic wall in patients with Marfan's syndrome and Erdheim's disease." Angiol Sosud Khir 10(4): 22-29.**
- Shores, J., K. R. Berger, et al. (1994). "Progression of aortic dilatation and the benefit of long-term beta-adrenergic blockade in Marfan's syndrome." N Engl J Med 330(19): 1335-1341.**
- Starling, E. H. and M. B. Visscher (1927). "The regulation of the energy output of the heart." J Physiol 62(3): 243-261.**

Chapter 4

A comparison of pharmaceutical treatments for attenuation of aortic root pathology in Marfan syndrome

4.1 Introduction

As advances in cardiac surgery for the aortic root continue to reduce the morbidity and mortality of elective aortic root replacement for patients with aortic root aneurysm, there remains a risk to patients of acute aortic rupture or acute aortic dissection of the aortic root before prophylactic surgery is completed.(Finkbohner, Johnston *et al.* 1995) There is also a risk of dissection in the remaining native aorta after root replacement.(Smith, Fann *et al.* 1994; Pyeritz 2009) If medical management of the disease could be augmented to delay the onset of aneurysmal dilatation, to slow the rate of increase of the size of the aortic aneurysm or to halt pathological changes with the aortic media, this would be of great benefit to the patient. This is especially so for patients with an extreme form of early onset Marfan syndrome(Brooke, Habashi *et al.* 2008) and for women of childbearing years (as aortic aneurysms progress rapidly and are at an increased risk of rupture during pregnancy). Furthermore, if new medical management with pharmaceutical therapy were highly effective, they could potentially reduce the need for surgical management of aortic root dilatation, secondary complications and other cardiovascular manifestations.

Over the last three decades there has been a dramatic increase in the life expectancy of people with Marfan syndrome.(Pyeritz 2009) This could be further improved upon and indeed their quality of life could also be improved as medical management could also attenuate other systemic manifestations.

The central role of TGF- β in Marfan syndrome is now widely acknowledged and is providing a target for possible protective strategies.(Habashi, Judge *et al.* 2006; Matt, Habashi *et al.*

2008) Effective safe therapies are currently being trialled in an attempt to translate the laboratory findings into a highly effective clinical practice.(Lacro, Dietz *et al.* 2007; Detaint, Aegerter *et al.* 2010)

4.1.1 Potential mechanism of action of Losartan

There was a breakthrough in the understanding of Marfan syndrome with the study of lung disease. TGF- β levels were shown to be elevated in the lung parenchyma of emphysematous lung tissue, which is the result of failure of pulmonary septation at an embryonic stage. TGF- β antagonism rescued pulmonary alveolar septation. TGF- β antagonism through systemic administration of TGF-[beta] neutralizing antibody was then shown to have prevented the development of pathological changes in the aortic wall and progressive aortic dilatation.(Pereira, Lee *et al.* 1999; Neptune, Frischmeyer *et al.* 2003) TGF- β antagonism also rescued other manifestations of MFS, including muscle regeneration, architecture, and strength, and mitral valve morphology in the mouse model.(Dietz, Cutting *et al.* 1991; Bunton, Biery *et al.* 2001), Losartan is an angiotensin II type I receptor blocker (ARB) which is used as an anti-hypertensive agent. It was also found to antagonize TGF- β signalling, through inhibition of TGF- β expression and activation, in a study of renal injury in uraemic rats.(Lavoie, Robitaille *et al.* 2005) Administration of Losartan normalized aortic root growth and dimensions in the Marfan mouse and resulted in an aortic wall architecture that was similar to that of normal mice.(Pereira, Lee *et al.* 1999) The therapeutic benefit of Losartan was recently replicated in a small paediatric cohort with a severe form of MFS.(Dallas, Miyazono *et al.* 1995) Losartan, either alone or in addition to beta-blocker therapy, led to a reduction in the rate of change in the aortic root diameter compared with beta-blocker therapy alone.(Dallas, Miyazono *et al.* 1995) Taken together, these data suggest that dysregulation of TGF-beta, which is an autocrine and paracrine growth factor with involvement in a wide

range of biological processes, contributes to the multisystem pathogenesis of Marfan syndrome.(Dietz, Pyeritz *et al.* 1991; Dallas, Miyazono *et al.* 1995; Pereira, Lee *et al.* 1999; Matt, Schoenhoff *et al.* 2009)

4.1.2 Potential mechanism of action of Doxycycline

Experiments have shown that Doxycycline, a tetracycline class antibiotic, at a sub-antimicrobial dose effectively inhibit a broad spectrum of matrix metalloproteinase enzymes and suppresses aneurysm formation coinciding with aortic wall stabilization in animal models and human aortic aneurysm.(Chung, Yang *et al.* 2008) Doxycycline has been investigated in clinical trials for abdominal aortic aneurysmal disease.(Lindeman, Abdul-Hussien *et al.* 2009) MMP 9 production and elastin degradation were reduced by Doxycycline in a study of aortic aneurysms.(Boyle, McDermott *et al.* 1998) MMP-2 and MMP-9mRNA and protein expression were found to be correlated with the size of abdominal aortic aneurysm(Chung, Yang *et al.* 2008) and Doxycycline treatment was associated with a reduction in aortic wall expression of MMP-2 and MMP-9. A recent study has shown delayed aortic rupture and improved survival in a mouse model of Marfan syndrome with down-regulation of MMP-2&-9. However, the beneficial mechanisms of action have not been elucidated.(Xiong, Knispel *et al.* 2008) Doxycycline when given long term was found to be more effective than atenolol in preventing thoracic aortic aneurysms in a murine model of Marfan syndrome.(Chung, Yang *et al.* 2008)

4.1.3 Potential mechanism of action of Pravastatin.

Statins are potent inhibitors of 3-hydroxy-3-methylglutaryl coenzyme A (HMG-CoA) and thereby affect the mevalonate pathway, which is important for the biosynthesis of isoprenoids such as geranylgeranyl pyrophosphate (GGPP) and farnesyl pyrophosphate (FPP), as well as cholesterol.(Goldstein and Brown 1990) GGPP and FPP are important lipid attachments for

the posttranslational modification of several proteins that include the small GTP-binding proteins Ras, Rac, and Rho. Attachment of these lipids, so-called isoprenylation, is essential for activation and intracellular transport of proteins crucial for various cellular functions, such as maintenance of cell shape, motility, factor secretion, differentiation, and proliferation.(Kuipers, Biesta *et al.* 2005) If HMG-CoA reductase is inhibited, there will be less mevalonate, less GGPP and less FPP and consequently less trans-cellular membrane transportation. It seems that statins have an effect on lipid raft-mediated intracellular transport and cell-surface expression of a variety of molecules or on the activation of certain proteins by isoprenylation, thereby affecting many cellular functions.

Previous work in the laboratory in Beaumont Hospital demonstrated a significant reduction in aortic root diameter and aortic root pathology in a murine model of Marfan syndrome with Pravastatin maintenance treatment.

4.2 Aims and objectives

The aim of this study was to determine if this observed attenuation of aortic pathology compared favourably with alternative pharmaceutical therapies which are currently on trial in clinical studies.(Lacro, Dietz *et al.* 2007) The mechanism of action of each of the different therapies could be investigated at an ultra-structural level.

Our specific objectives were:

- To determine if Pravastatin therapy attenuated aortic root pathology measured by histological, echocardiographic and cardiovascular physiology parameters.
- To compare the effects of Pravastatin to both Losartan and Doxycycline.
- To determine if the mechanism of action was similar or different to Losartan and to Doxycycline.

- To provide a basis for a further, more detailed study into the mechanisms of action of Pravastatin in the setting of Marfan syndrome.

4.3 Materials and Methods

A pair of male C1039G Marfan mice were cross bred with C57Bl6 females. Genetic analysis of the offspring was conducted. Male mice identified to have the C1039G mutation were entered into the study, as detailed in the materials and methods chapter. These mice were then entered into different treatment groups. Pharmacological agents were administered as outlined in Section 2.1.3.

The first group was administered Pravastatin from 6 weeks of age. The dose was 0.25g/Litre, equivalent to 50mg/kg/day. This dose was found in previous studies to reduce serum cholesterol levels in C57black6 mice (personal communication from Dr John Byrne).

The second group was administered Losartan from 6 weeks of age. The dose was 0.6g/Litre, which was the dose used in previous studies conducted in Johns Hopkins University. This dose was calculated by titrating the level of Losartan up, so that there was a 20mmHg reduction in the mean systolic blood pressure in the murine model.

The third group was administered Doxycycline from 6 weeks of age. The dose was 0.24g/Litre, which is a sub-antimicrobial dose. This dose was used in previous studies and found to have a broad spectrum inhibitory effect on matrix metalloproteinases.

Each group were born four weeks apart and investigations conducted three and eight months of age. The numbers in each group needed to be large enough to power the study adequately so the results would attain statistical significance. This meant that only one group of mice could be genotyped and tested from each month due to limited resources and capacity to breed and test a limited number of mice per month. Each group were subjected to the exact same conditions, and echocardiography conducted by the same ultra-sonographers at the

same age relative to the other groups. Every effort was made to identify and reduce any variability that could arise between groups.

The drug treatment groups in the Marfan groups had an untreated Marfan group as a control and not all the drug treatment groups had a normal, wild-type, group which received treatment. It would be ideal, to have two type of control groups, one which has the disease without treatment and an internal control which does not have the disease, but received treatment. One control group was use due to limited resources.

These animals were then studied in the following manner;

Aortic root diameter was assessed in-vivo, at 3 months and 8 months for evidence of established and progression of aneurysmal dilatation, by trans-thoracic echocardiography as outlined in the materials and methods section.

Histology of aortic root pathology was assessed. Samples of aortic root were harvested at 8 months. Aortic root thickness was assessed with Haematoxylin and Eosin staining. Architecture of the aortic media at the level of the aortic root was assessed by staining sections with Verhoeff van Gieson stain. The aortic wall architectural score is based on number of islands of damage (n=10 in each group) per full aortic root cross section. An island of damage is defined as an area where there are two or more disrupted elastic lamellae with associated thickening of the aortic media.

Cardiac function was assessed using haemodynamic variables from cardiac catheter recordings of dP/dt maximum and dP/dt minimum as measures of left ventricular systolic and diastolic function at 8 months.

Aortic valve function was assessed using catheter recordings of systolic and diastolic blood pressure. Assessment of the dicrotic notch was made by measuring dP/dt maximum of the

downslope of the aortic trace (immediately after the peak systolic pressure and before the minimum diastolic value reached) at 8 months.

Samples of aortic root were harvested at 8 months for ultra-structural examination with electron microscopy. Measurements of aortic vascular smooth muscle cells were taken. The volume of rough endoplasmic reticulum was measured. The volume of the cisternae of the Golgi-apparatus was measured.

These results were compared to results of both untreated Marfan mice and normal mice from chapter 2, as positive and negative controls, respectively.

Echocardiograms were conducted on a Sequoia ultrasound machine.

This ultrasound machine, when used in M-mode displays a 2-dimensional image as demonstrated in figure 4.1 below.

In this figure we see an M-mode display of ultrasound image of aorta, at the level of the aortic root. This is also the level of the sinuses of Valsalva, which is the site of the origin of the coronary arteries. This image is obtained by first placing the probe over the sternum in long axis and locating the left ventricle and left ventricular outflow tract. The right ventricular outflow tract has a different course to the left as the right one passes into the main pulmonary artery, branches early at right angles to both the left and right pulmonary arteries, they are also deeper than the aorta. Once the left ventricular outflow tract has been localised, the image is switched to M-mode and the probe adjusted to a horizontal/cross-sectional position. In this view, the anterior and posterior aspect of the tract is imaged. As the walls of the ventricle contract and relax, due to systole and diastole as represented on M-mode, their tracing converge and diverge, i.e. the vertical distance between the anterior and posterior surfaces become shorter and longer respectively. The probe is moved very slightly cranially (towards the head). As the probe is moved, the image displays more distal left ventricular

outflow tract, and the aortic valve leaflets may come into view. Once the anterior and posterior aspects of the wall stop converging and diverging, their traces start to move in parallel. This happens at the aortic annulus, where the aortic leaflets attach. Once above the aortic valve leaflets, an image of the tracing is saved, as shown in the figure below. The tracings of the anterior and posterior wall rise and fall. This represents the movement of the aorta due to systole and diastole. The tracing is closer to the probe in systole and further away (lower) in diastole. The tracings may still converge and diverge, but to a much lesser extent. This is due to the aortic pulse pressure. Three areas are agreed upon by the two veterinary radiologists reading the image, to be accurate representations of the aortic root. Three measurements are recorded in diastole.

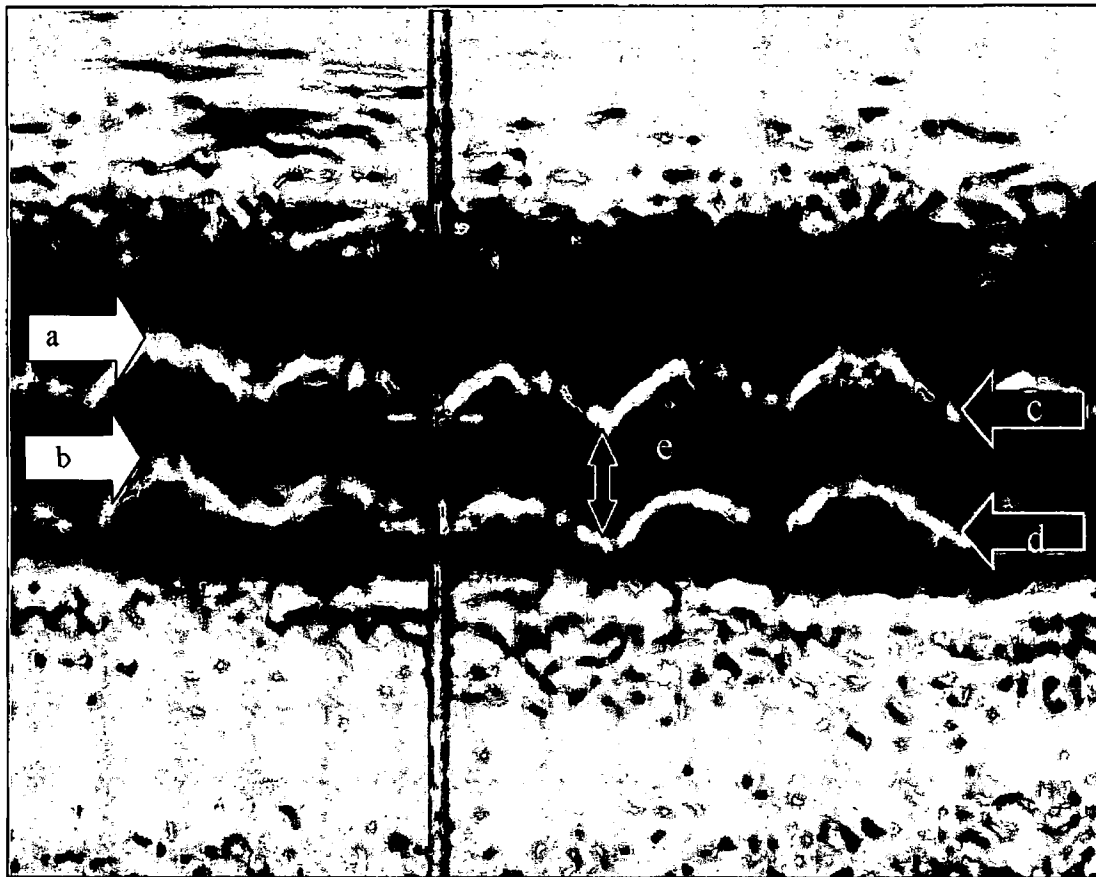


Figure 4.1: M-mode image of aortic root, with anterior and posterior aspects of aorta displayed by arrows in systole and anterior and posterior aspects of the aorta in diastole, labelled a, b, c & d respectively. The measurement of the aortic root diameter in diastole is also displayed, labelled e.

4.4 Results

All results reported will be followed in brackets by +/- estimated standard error of the mean, unless otherwise stated. Statistical analysis was conducted using an Analysis of Variance (ANOVA) with Bonferroni comparisons.

4.4.1 Aortic root diameter results

The aortic root diameter enlarged from 0.16cm (± 0.0019) in the normal group to 0.25cm (± 0.0043) in the Marfan untreated group (results from chapter 3, figure 3.5 and figure 4.3). The aortic root diameter enlargement was attenuated significantly by Pravastatin treatment and reached 0.22cm (± 0.005811) at eight months ($p < 0.0001$), in comparison to the Marfan untreated group (figure 4.2 and 4.3). The aortic root diameter enlargement was also attenuated significantly by Losartan treatment and reached 0.22cm (± 0.005089) at eight months, ($p < 0.0001$) in comparison to the Marfan untreated group (figure 4.2 and 4.3). Doxycycline reduced the aortic root diameter to 0.24cm (± 0.005743) though did not achieve statistical significant difference ($p = 0.09$) in relation to the Marfan untreated group (figure 4.2 and 4.3).

Mean Aortic Root Diameter comparing treatment groups to controls at 8 months

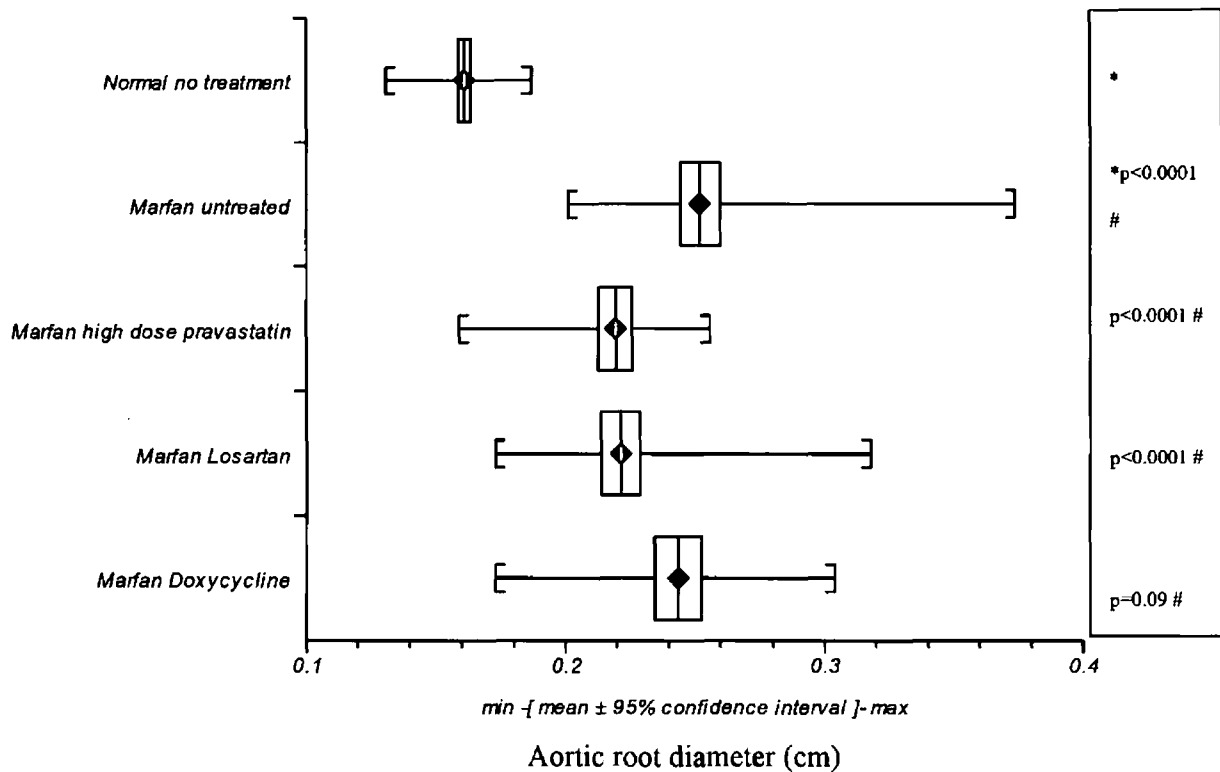


Figure 4.2: Mean aortic root diameter at 8 months comparing Marfan groups treated with pravastatin, losartan or doxycycline to untreated Marfan group and to a normal, untreated group. (P value labelled with * comparing normal, untreated group to Marfan untreated group. P value labelled with # comparing pravastatin or losartan or doxycycline treatment in Marfan groups to untreated Marfan group.)

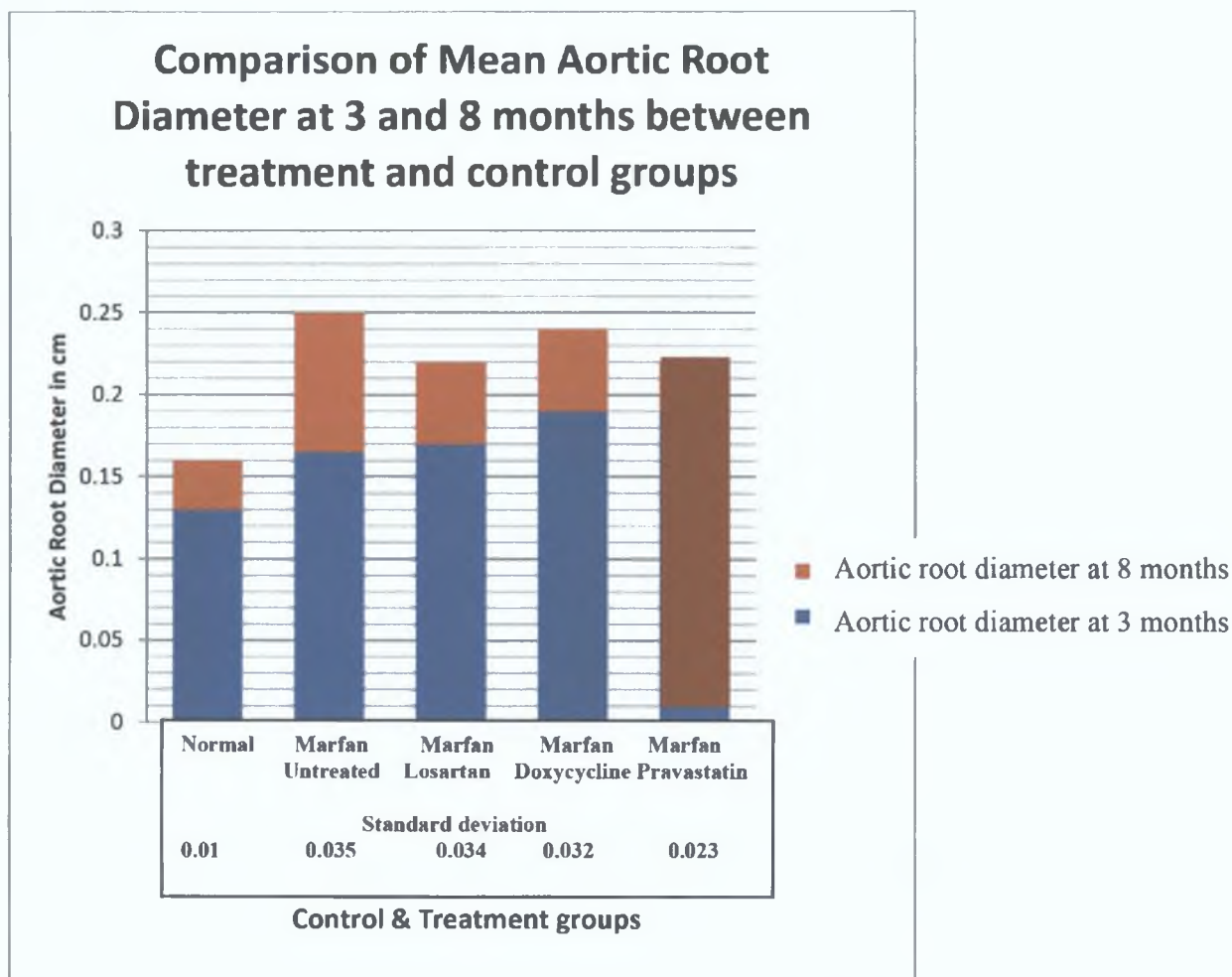


Figure 4.3: Aortic root diameter after 3 months (blue) and after 8 months (red) in centimeters. (Note: no scan conducted at 3 months in Marfan group treated with Pravastatin.) N= 118.

4.4.2 Cardiac Catheterisation Results

In chapter 2 it was found that there was no statistically significant difference in pulse pressure between the normal group, 40.7mmHg and the Marfan untreated group, 39.8mmHg(+/- 1.302217), (figure 4.4). There was no statistical significant difference between the Marfan group treated with high dose Pravastatin, mean = 36.5mmHg (+/-1.448542) and the untreated Marfan group, mean = 39.8mmHg (+/-1.302217), (p = 0.3722) as shown in figure 4.4. The

Losartan treated Marfan group did have a narrower pulse pressure on invasive measuring of the aortic pulse pressure. The pulse pressure reduced to 32.1mmHg (+/-1.397952), ($p < 0.0001$), figure 4.4.

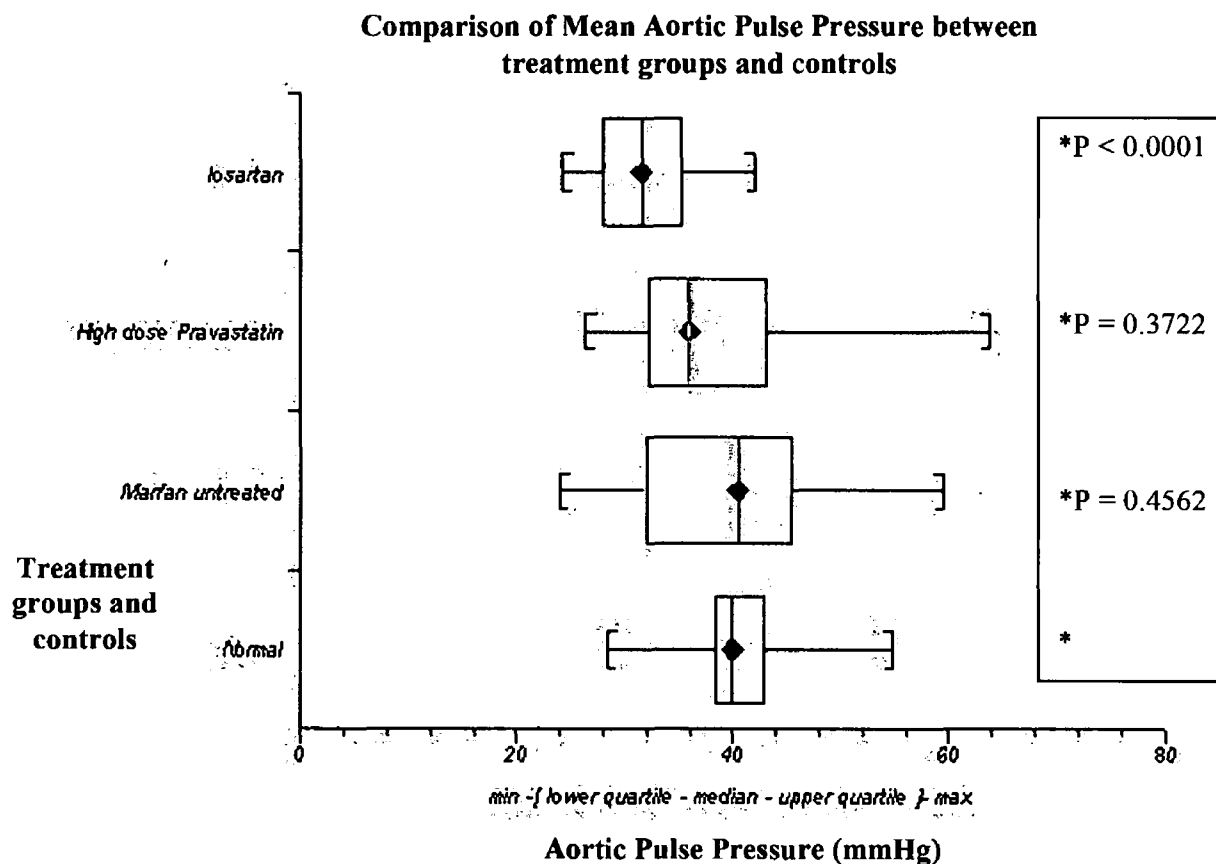


Figure 4.4: Comparison of Mean Aortic Pulse Pressure between Marfan groups treated with losartan or pravastatin versus Marfan untreated group and normal group. N = 100. (p-values refer to comparison with normal untreated group labelled *)

4.4.3 Histology Results

As in chapter 2, three aspects of histology were assessed: aortic wall thickness, architectural score and the amount of elastin within the media of the aortic wall.

Aortic wall thickness (micrometers)

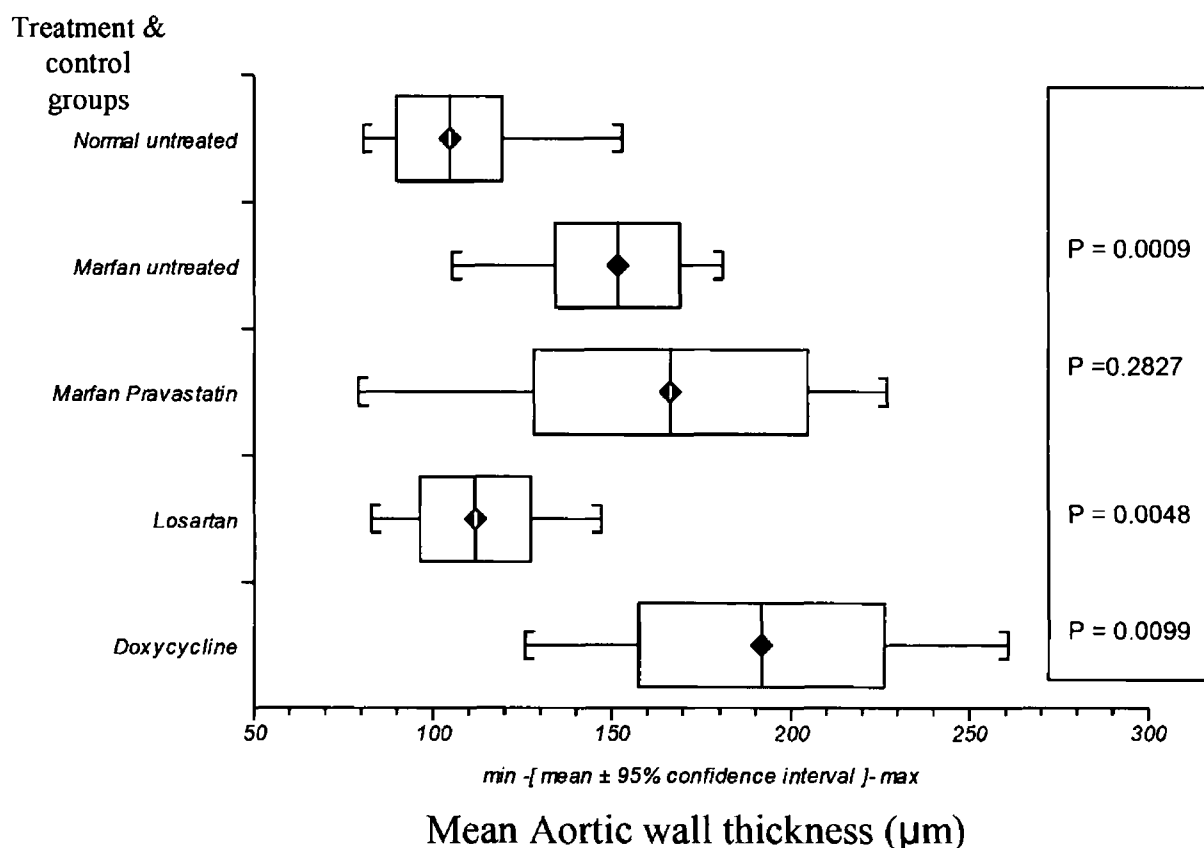


Figure 4.5: Chart of aortic wall thickness (µm), comparing normal, Marfan, and Marfan treated with pravastatin, losartan and doxycycline. N = 50.

The mean aortic wall thickness of the Marfan untreated group was 151.68micrometers (+/- 12.791671), which was significantly different to the mean aortic wall thickness of the normal group which was 104.8 micrometers, (p=0.0009), (figure 4.5). The mean aortic wall thickness of the Pravastatin group was 166.49 micrometers (+/-13.567616), (figure 4.5). There was no statistical difference between the Marfan treated with Pravastatin group and the Marfan untreated group, 151.68 micrometers (+/-12.791671), (p = 0.34), (figure 4.5).

There was a significant reduction in the thickness of the aortic wall in the Losartan group, 111.92 micrometers (± 13.142192), with respect to the untreated Marfan group ($p = 0.0048$), (figure 4.5). Doxycycline showed a significant increase in the aortic wall thickness with respect to the untreated Marfan group ($p = 0.0099$) with the thickness increasing to 191.93 micrometers (± 14.87921), (figure 4.5).

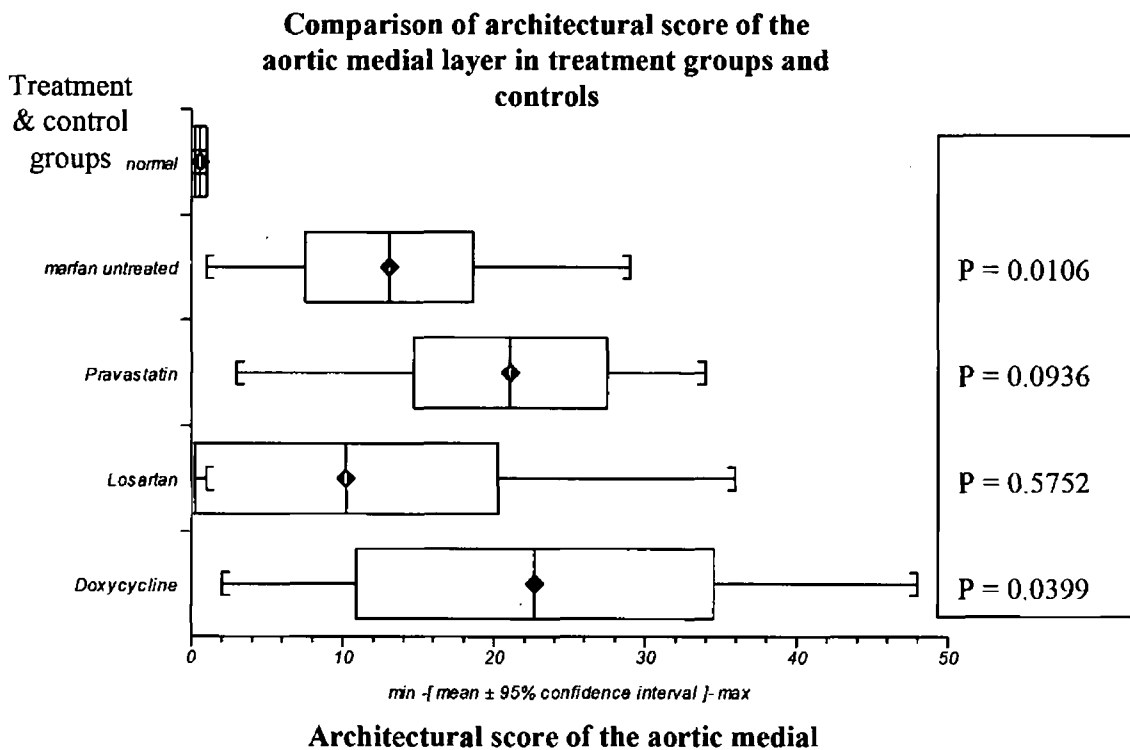
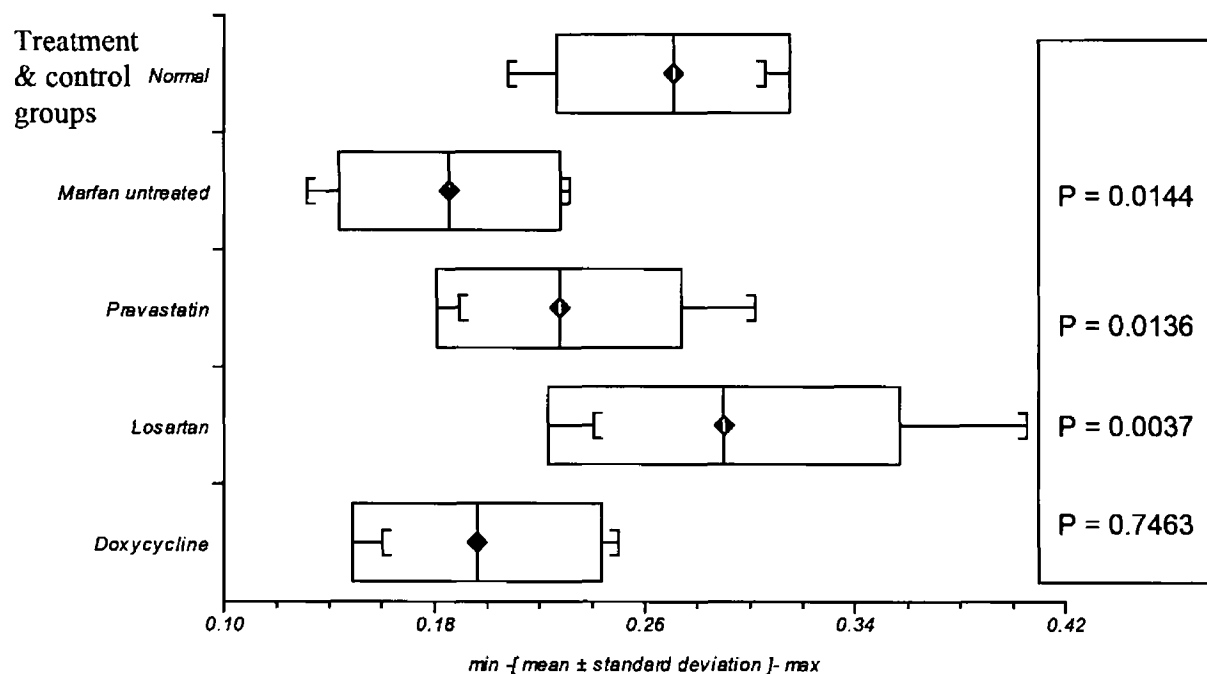


Figure 4.6: Architectural score of the aortic medial layer, a comparison of treatment groups in Marfan syndrome; pravastatin; losartan; doxycycline and normal and Marfan control groups. N = 50.

The architectural score was calculated as describe above in the materials and methods section. In the Marfan untreated group, the architectural score of the aortic media was significantly increased from 0.6 (± 0.163299) in the normal group to 13.076923 (± 2.555691) in the Marfan group ($p = 0.0106$), (figure 4.6). The aortic wall architectural score was not significantly different in the Marfan group treated with Pravastatin, 21.1 (\pm

2.814447) when compared to untreated the Marfan group, ($p = 0.0936$), (figure 4.6). Losartan improved the aortic wall architectural score at 10.25 (± 4.241588), which remained statistically significant in comparison to the Marfan untreated group ($p = 0.5752$), (figure 4.6). Doxycycline had a statistically significant negative effect on the aortic wall architecture, measured at 22.7273 (± 4.566585), with respect to the Marfan untreated group ($p = 0.0399$), (figure 4.6).

Comparison of the mean elastin volume as a proportion of the tunica media of the aortic wall, at the level of the aortic root



Vv Elastin : Media (mean elastin volume as a proportion of the tunica media of the aortic wall, at the level of the aortic root)

Figure 4.7: Elastin volume as a proportion of the tunica media of the aortic wall, at the level of the aortic root, a comparison of treatment groups in Marfan syndrome; pravastatin; losartan; doxycycline and normal and Marfan control groups (n = 25).

In the Marfan untreated group, the volume of elastin within the aortic media of the aortic wall, as a proportion of the volume of the media, was reduced significantly from 0.27(+/-0.019847) in the normal group to 0.18(+/-0.018801) in the Marfan group (p = 0.0144), (figure 4.7). Pravastatin rescued the destruction of elastin within the media significantly, with an increased proportional volume of elastin: media, 0.2275(+/-0.020858) (p = 0.0136), (figure 4.7). Losartan improved the volume of elastin: media further still, and the level rose to above that of normal, 0.29(+/-0.029886), which remained statistically significant in comparison to

the Marfan untreated group ($p = 0.0037$), (figure 4.7). Doxycycline did not improve the volume of elastin significantly, $0.19625(\pm 0.027856)$, with respect to the Marfan untreated group ($p = 0.7463$), (figure 4.7).

4.4.4 Electron Microscopy / Ultra-structural analysis

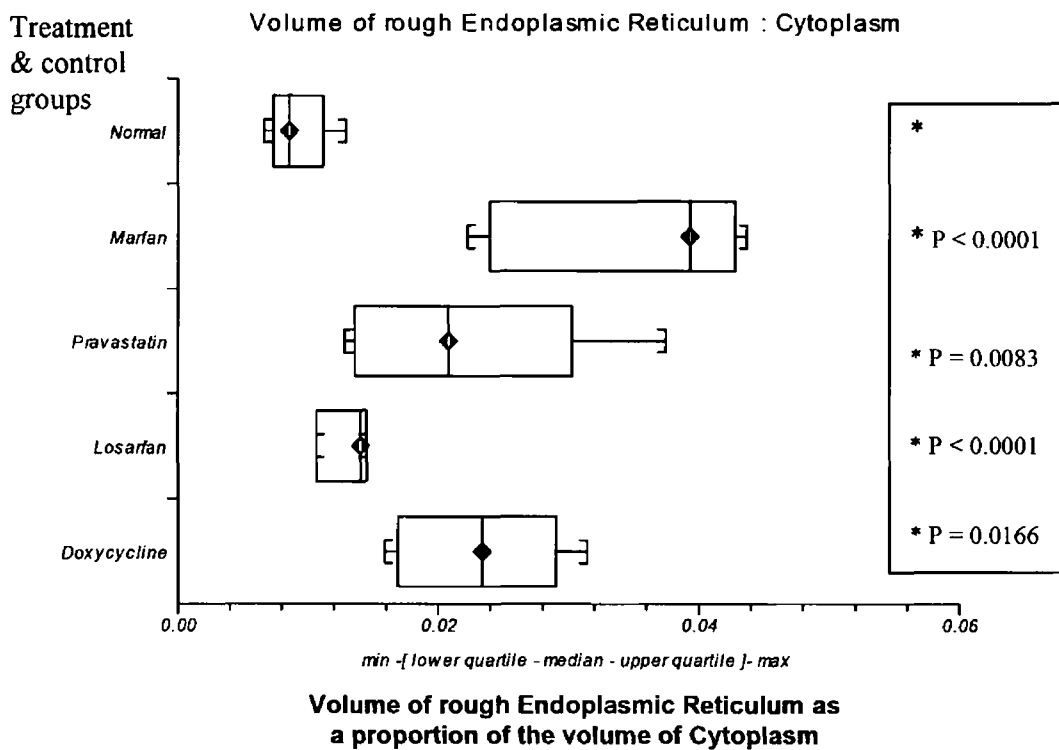


Figure 4.8: Comparison of volume of rough endoplasmic reticulum: Cytoplasm between treatment and control groups.

As observed in chapter one the volume of rough Endoplasmic Reticulum as a proportion of the aortic smooth muscle cell, was increased from $0.00914(\pm 0.001056)$ in normal aortic smooth muscle cells, compared to Marfan aortic smooth muscle cell $0.03461 (\pm 0.004413)$, with $p = 0.0001$, (figure 4.8). Pravastatin reduced the proportion of rough Endoplasmic Reticulum in the Marfan aortic smooth muscle cell to $0.0217(\pm 0.004386)$, with $p = 0.0083$, (figure 4.8). Losartan reduced the proportion of rough Endoplasmic Reticulum to $0.01289(\pm 0.000912)$, with $p < 0.0001$, when compared to the Marfan untreated group (figure 4.8).

Losartan reduced the RER level close to that of normal, so much so that there is no statistical difference between normal and Marfan treated with Losartan ($p = 0.40$) when an analysis of variance with Bonferroni comparisons is conducted. Doxycycline reduced the proportion of rough Endoplasmic Reticulum to $0.023073 (+/-0.002831)$ ($p = 0.0166$) when compared to the Marfan untreated group (figure 4.8).

4.4.5 Electron photomicrographs of aortic tissue from different treatment and control groups.

Note is made of the smooth undulating, wave like pattern of the elastin fibres which provide the strength and compliance of normal aortic tissue (Figure 3.16, in chapter 3). In Figure 3.19 (in chapter 3), the smooth undulating, wave like pattern of the elastin fibres was disrupted and fragmented, as shown by blue arrows. Thus, the strength and compliance of the aortic tissue was compromised. Figures 4.9 – 4.12 represent samples of aortic tissue taken from the Marfan group treated with Pravastatin. There are some breaks in the continuity of the elastic lamellae with a less organised pattern of vascular smooth muscle than compared to normal tissue. In figure 4.12 ultra-structural elements of the aortic vascular smooth muscle are observed, including the structure of the nucleus and the cell's own transportation system, the rough endoplasmic reticulum.

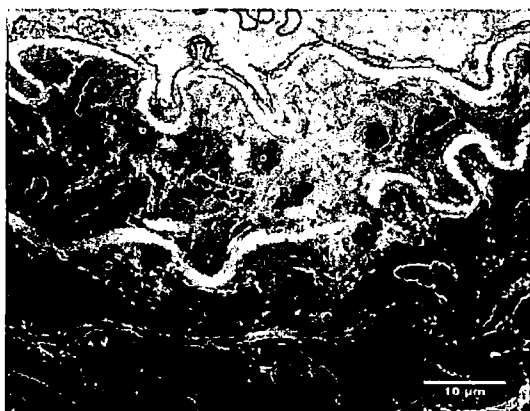


Figure 4.9 Transmission electron micrograph of a uranyl acetate and lead citrate stained resin section of Marfan aortic root tissue, with pravastatin treatment. Scale bar: $10\mu\text{m}$.

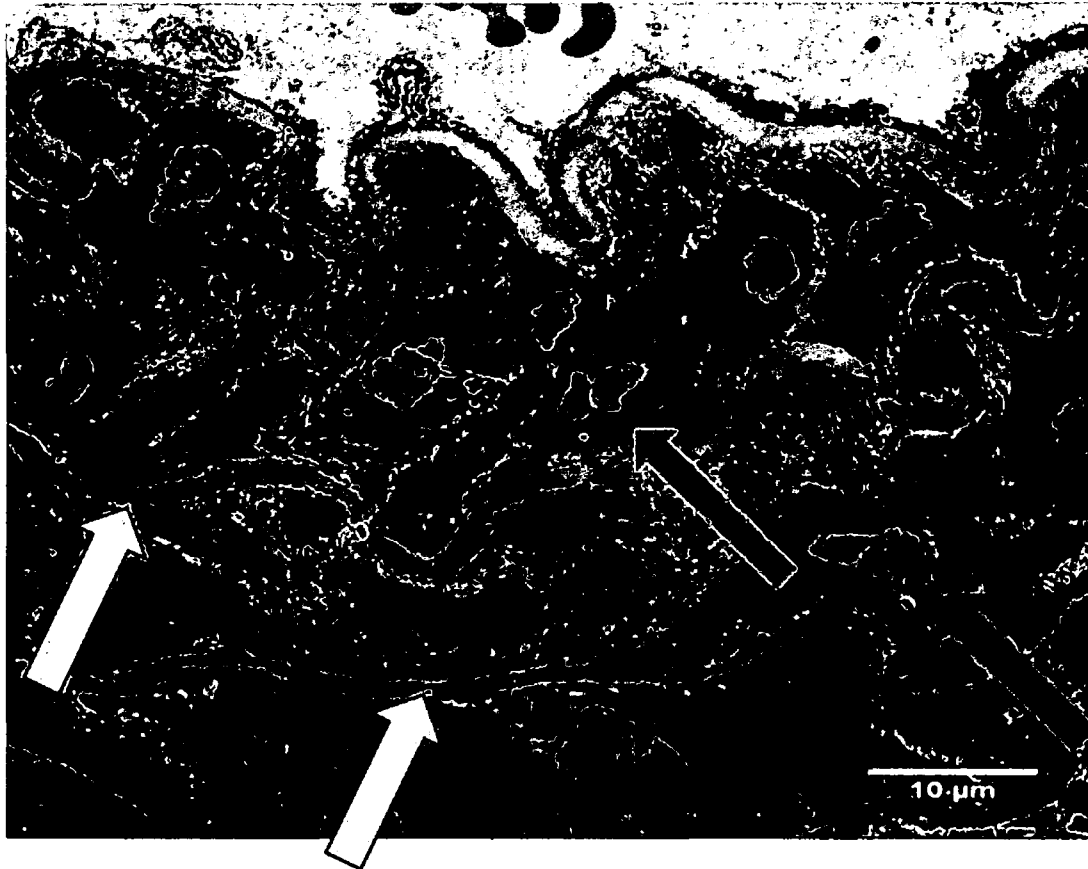


Figure 4.10 Marfan murine aortic root in pravastatin treated group. Scale bar: 10μm. Transmission electron micrograph of a uranyl acetate and lead citrate stained resin section of elastic lamellae (white arrows) and SMCs (black arrows) within the aortic media.

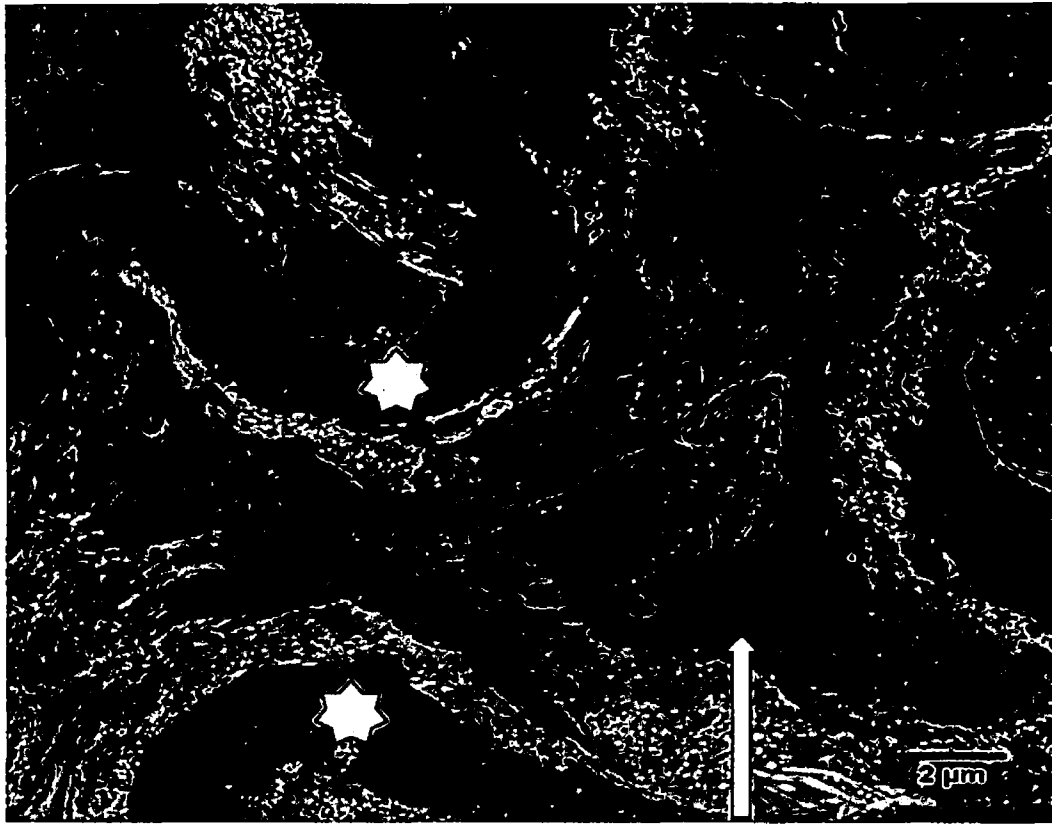


Figure 4.11 Pravastatin treated Marfan murine aortic root. Scale bar: 2 μ m. Transmission electron micrograph of a uranyl acetate and lead citrate stained resin section of a SMC (white arrow) lying between two elastic lamellae (white asterisks).

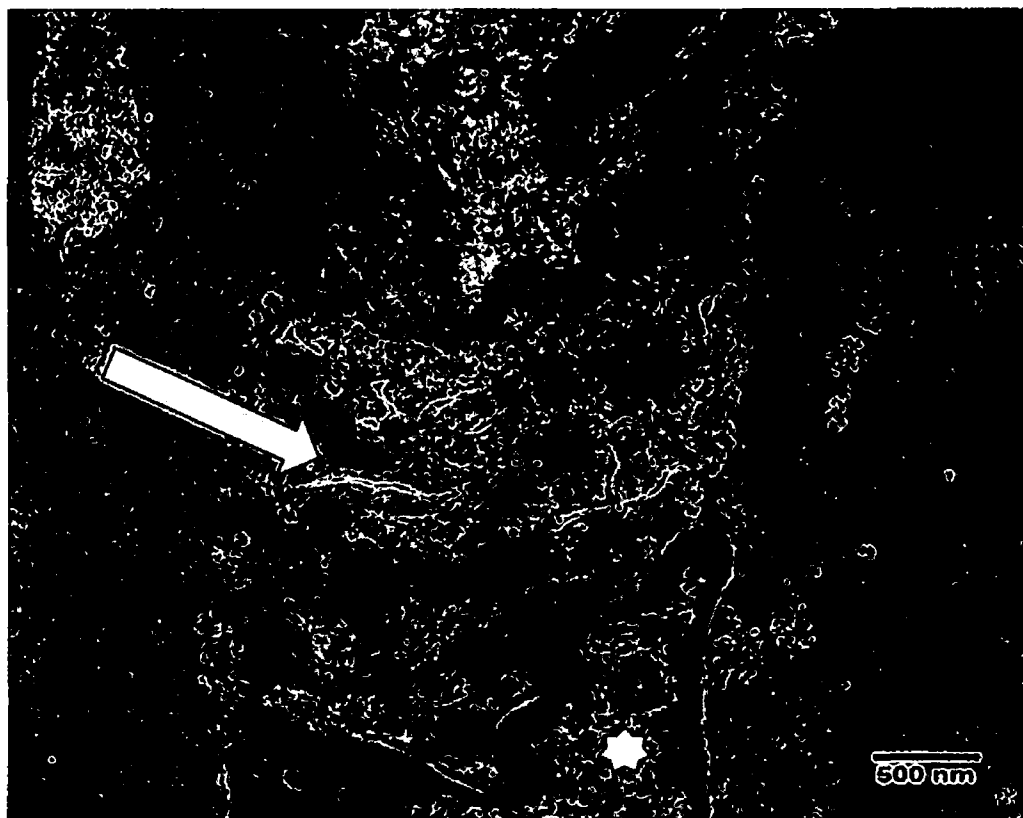


Figure 4.12 Pravastatin treated Marfan murine aortic root. Scale bar: 500nm. Transmission electron micrograph of a uranyl acetate and lead citrate stained resin section of a SMC nucleus (white asterisk) surrounded by RER (white arrow).

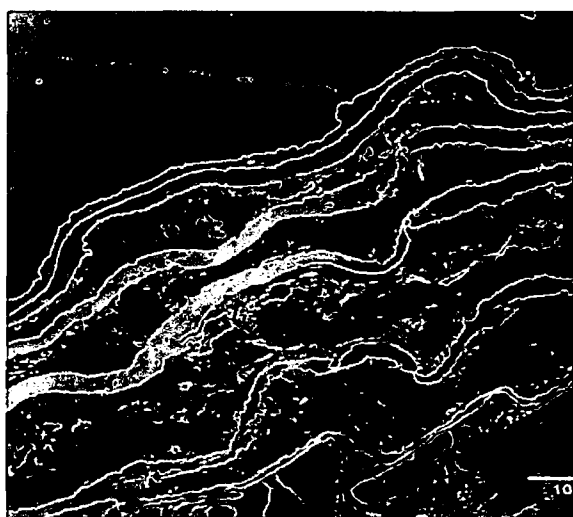


Figure 4.13 Scale bar: 500nm. Transmission electron micrograph of a uranyl acetate and lead citrate stained resin section of Losartan treated Marfan murine aortic root.

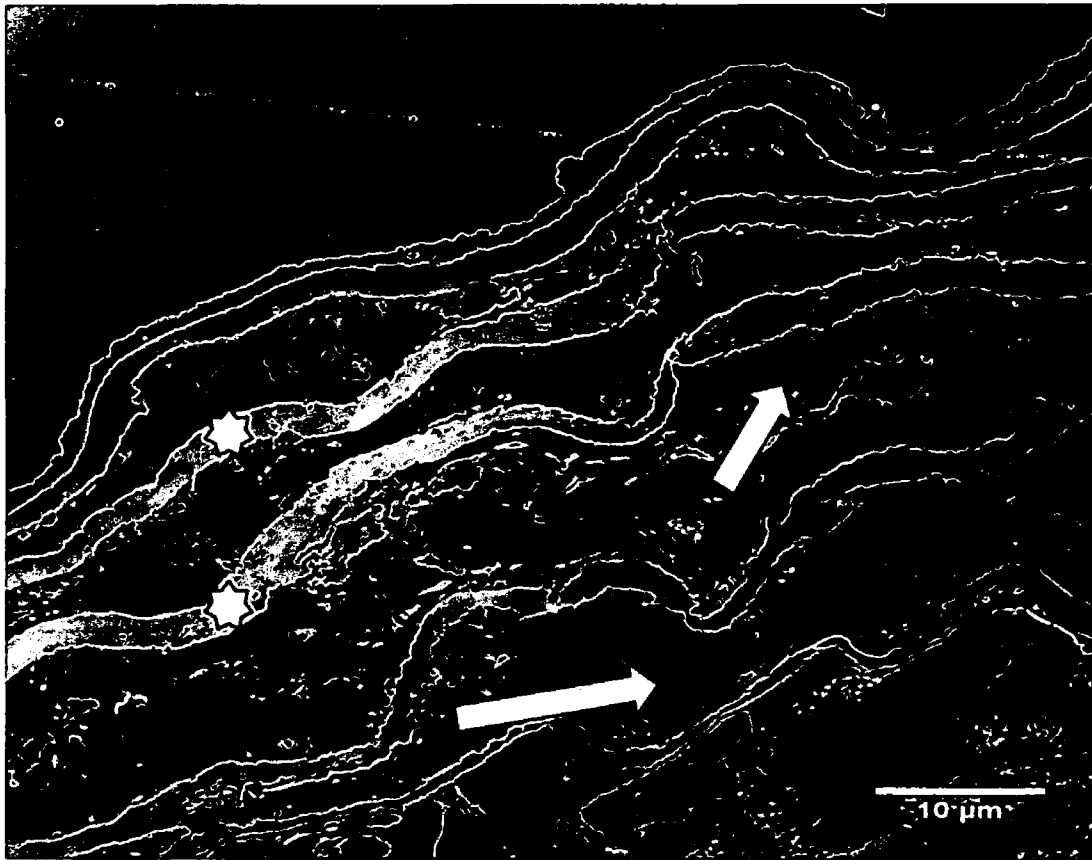


Figure 4.14 Losartan-treated group, Marfan, murine aortic root. Scale bar: 10 μ m
Transmission electron micrograph of a uranyl acetate and lead citrate stained resin section of the concentric bands of elastic lamellae (white asterisks) interspersed with SMCs (white arrows) within the tunica media.

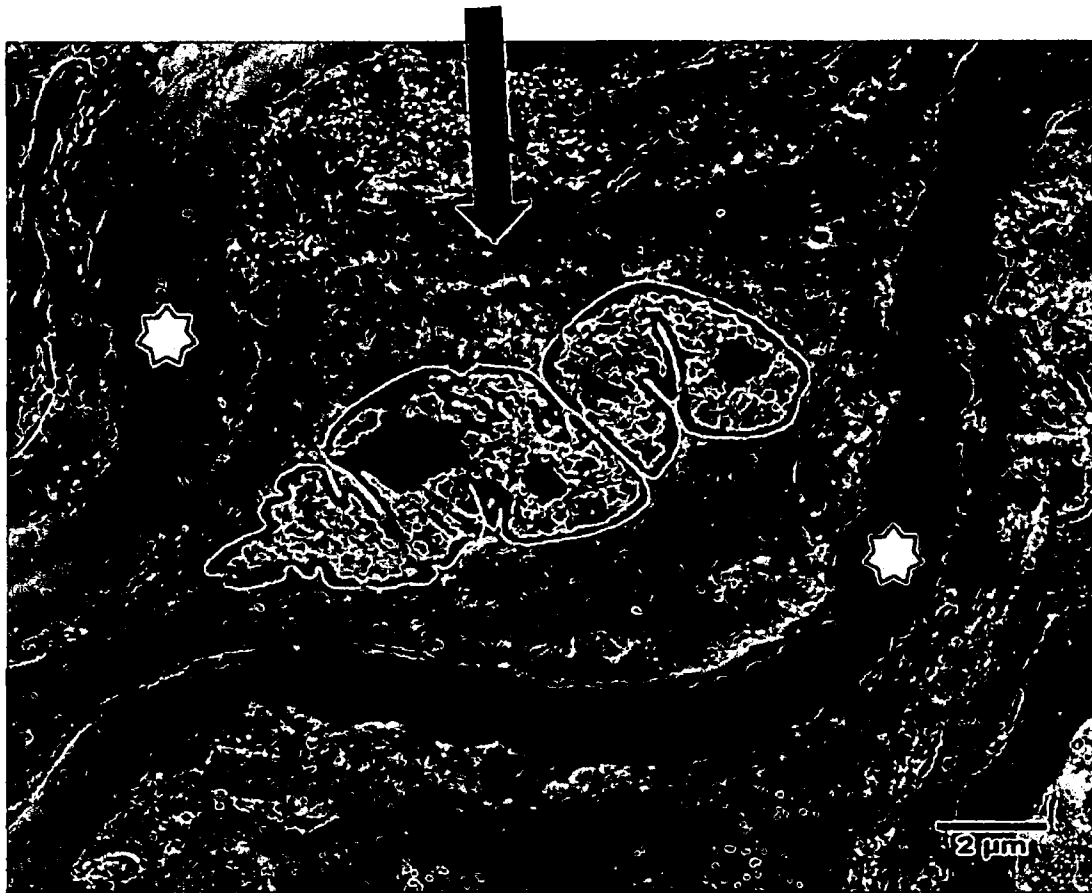


Figure 4.15 Losartan treated Marfan murine aortic root. Scale bar: 2μm. Transmission electron micrograph of a uranyl acetate and lead citrate stained resin section of a SMC (black arrow) lying between two elastic lamellae (white asterisks).

Figures 4.13 – 4.16 show electron photomicrographs of Marfan (murine) aortic root treated with Losartan. Continuity and thickness of the elastic lamellae appear preserved with an arranged pattern of vascular smooth muscle cells in between these layers. Ultra-structural components of the aortic vascular smooth muscle cells, including the nucleus and rough endoplasmic reticulum, are observed (Figure 4.16).

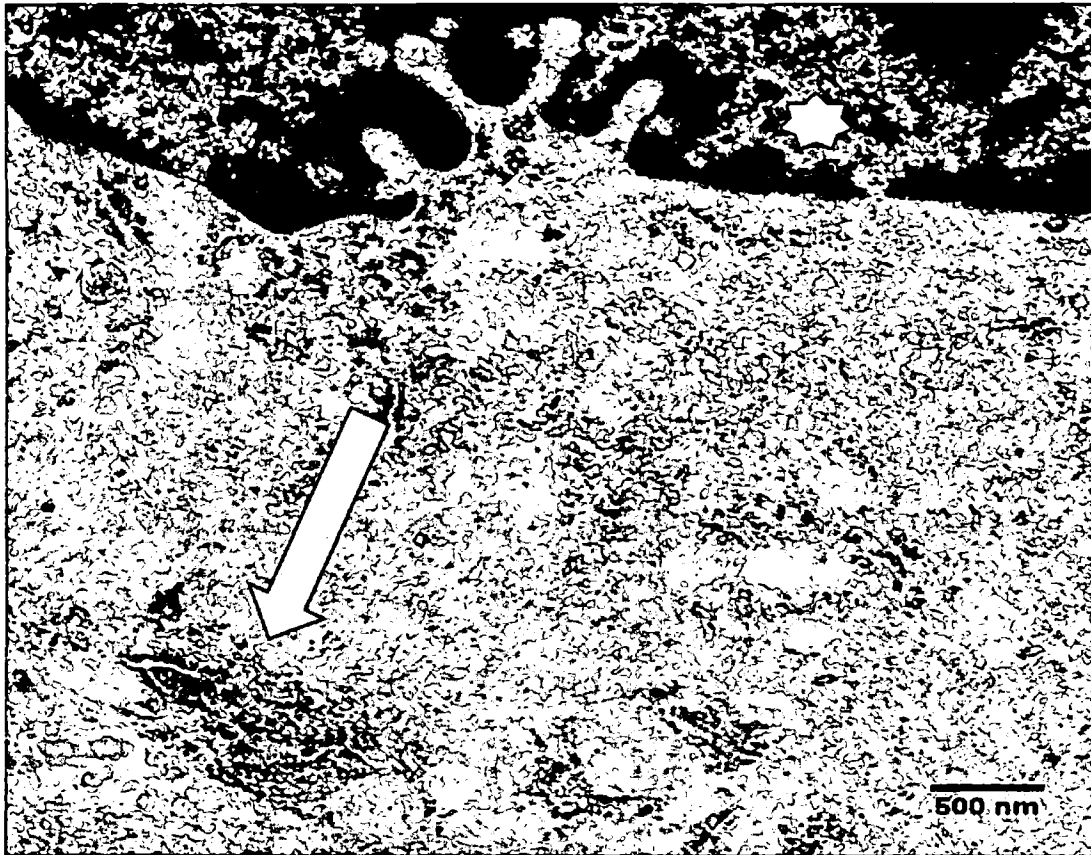


Figure 4.16 Losartan-treated Marfan murine aortic root. Scale bar: 500nm. Transmission electron micrograph of a uranyl acetate and lead citrate stained resin section of a SMC nucleus (white asterisk) surrounded by RER (white arrow).



Figure 4.17 Doxycycline treated Marfan murine aortic root. Scale bar: 10μm. Transmission electron micrograph of a uranyl acetate and lead citrate stained resin section.

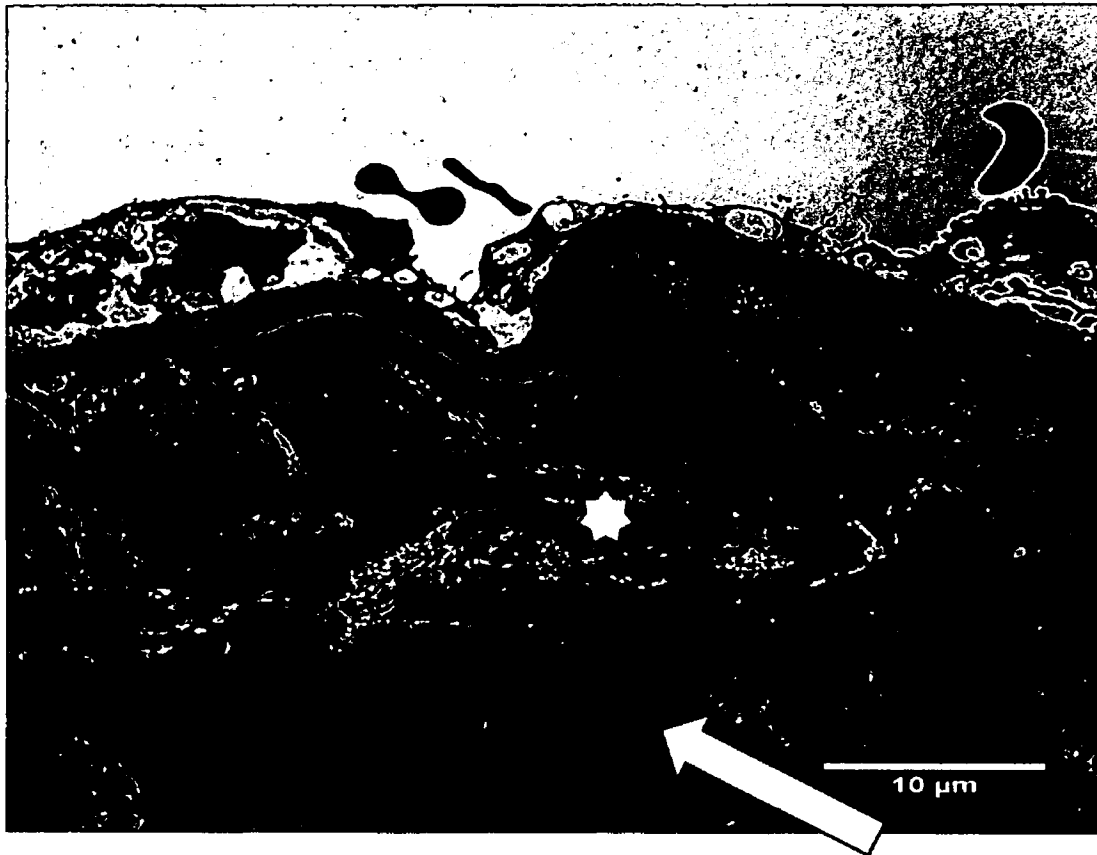


Figure 4.18 Doxycycline treated Marfan murine aortic root. Scale bar: 10 μ m. Transmission electron micrograph of a uranyl acetate and lead citrate stained resin section of a broken elastic lamella (white asterisk) and SMC (white arrow) within the tunica media.

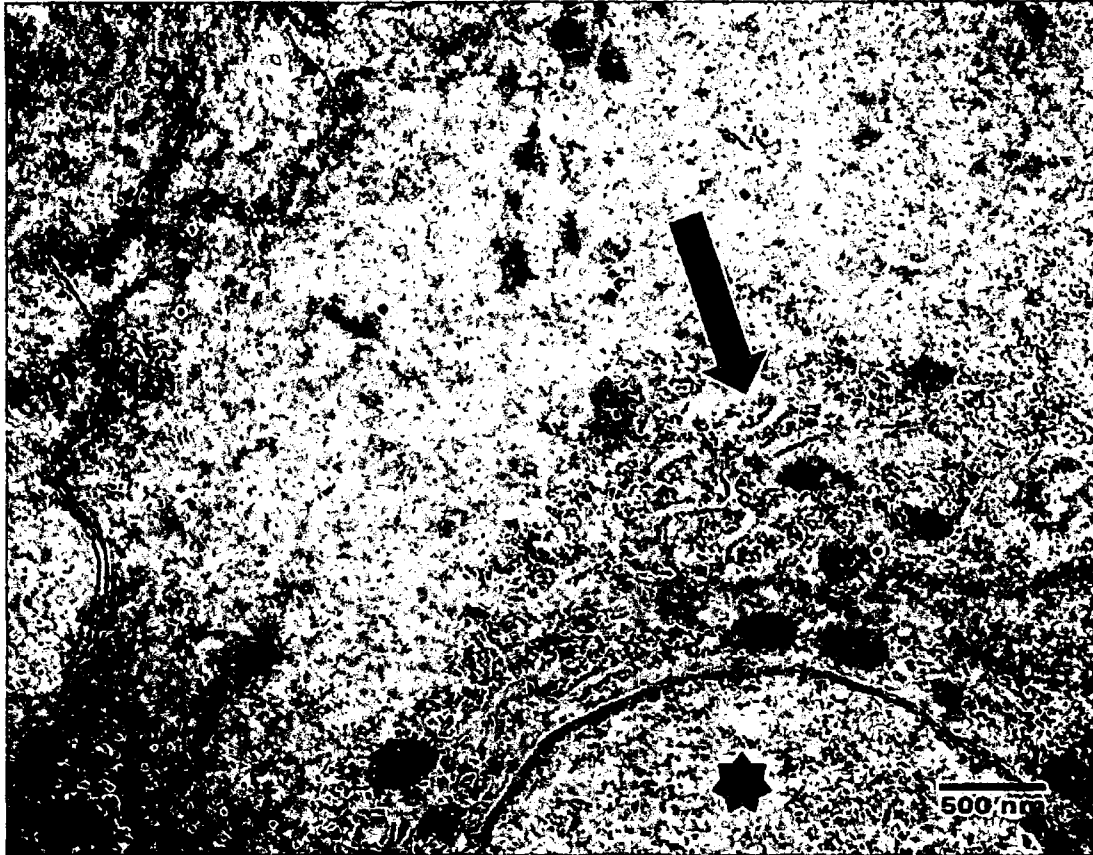


Figure 4.19 Doxycycline treated Marfan murine aortic root. Scale bar: 500nm. Transmission electron micrograph of a uranyl acetate and lead citrate stained resin section of a SMC nucleus (black asterisk) surrounded by RER (black arrow) within the tunica media.

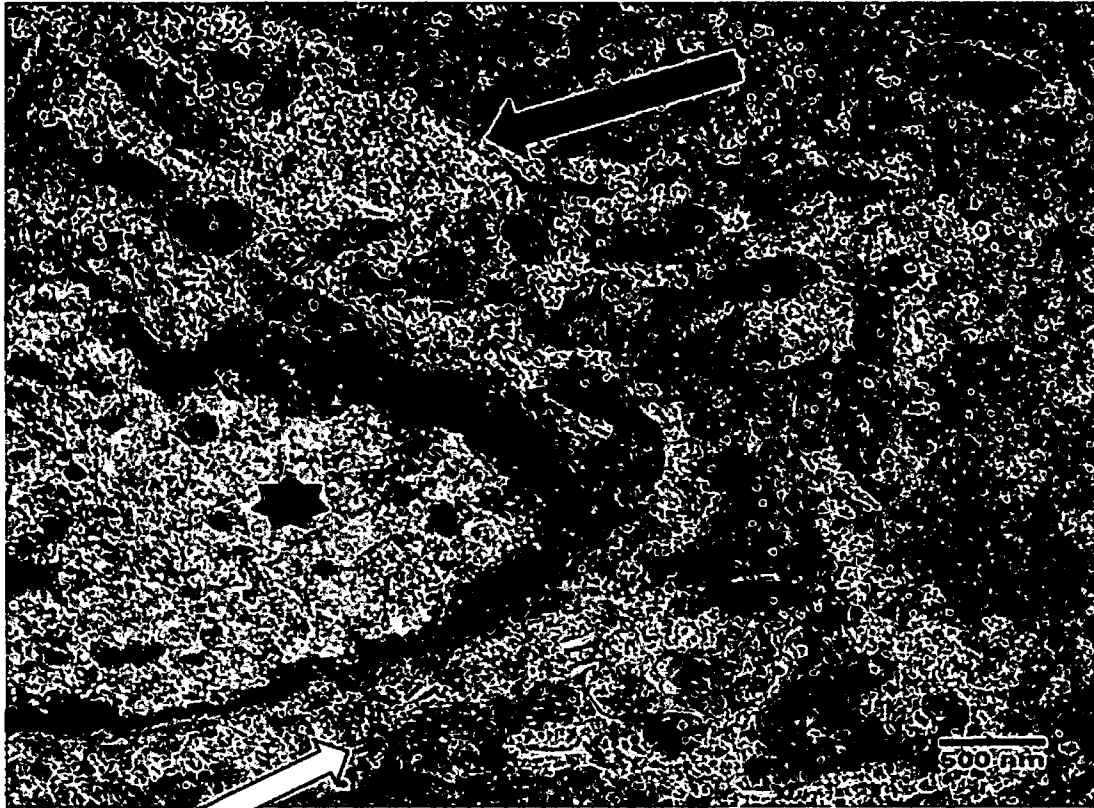


Figure 4.20 Doxycycline treated Marfan murine aortic root. Scale bar: 500nm. Transmission electron micrograph of a uranyl acetate and lead citrate stained resin section of a SMC nucleus (black asterisk) surrounded by RER (black arrow) and a Golgi complex (white arrow).

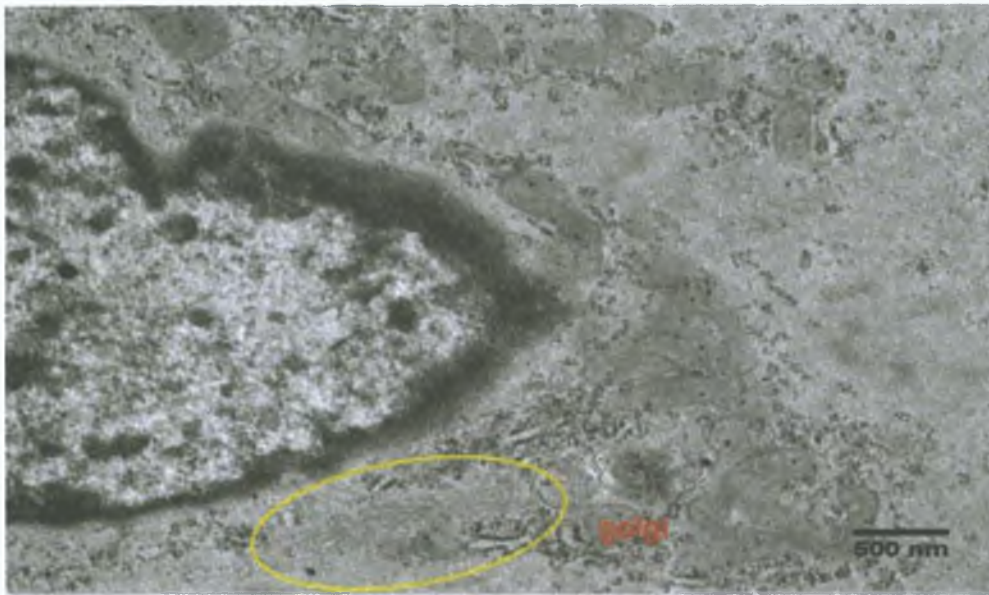


Figure 4.21 Marfan aortic root, doxycycline treatment group, with magnification of aortic vascular smooth muscle. The Golgi apparatus is displayed with a yellow ellipse.

Electron photomicrographs of murine aortic root tissue from the Marfan group with Doxycycline treatment are shown in figures 4.17 - 4.21. Gross disruption and thinning of the elastic lamellae with interposition of the aortic vascular smooth muscle cells are present (Figures 4.17 and 4.18). Ultra-structural differences are observed in the aortic vascular smooth muscle cells with Doxycycline treatment (Figures 4.19 – 4.21), which are similar to that of untreated Marfan aortic vascular smooth muscle cells.

4.5 Discussion

Pravastatin had a beneficial effect by attenuating dilatation of the aortic root diameter by 33.3% in a group of Marfan mice treated with Pravastatin as compared to the group of Marfan mice with no treatment. This was a statistically significant finding. It may also be relevant clinically, as a one third reduction in growth rate is a very significant finding. In the era before open heart surgery, the life expectancy for a person with Marfan syndrome was 45 years of age, due to the risk of aortic dissection, secondary to aortic aneurysmal disease.(Murdoch, Walker *et al.* 1972) In clinical practice growth rates are monitored initially with 6 monthly measurement of the thoracic aorta, then annually once stability is established.(Milewicz, Dietz *et al.* 2005; Hiratzka, Bakris *et al.* 2010) Surgical repair is indicated in Marfan syndrome if the aortic root or ascending thoracic aorta reaches a threshold of 5.0cm or rapid enlargement, 0.5cm per year.(Elefteriades 2002) Studies have shown that beta blockade helps to slow dilatation of the aorta, though in patients with Marfan syndrome, the aorta continues to dilate and dissect despite medical therapy, so beta-blockade does not preclude the need for routine imaging and prophylactic aortic repair when the diameter of the aorta warrants repair.(Shores, Berger *et al.* 1994) These facts mean that a 33.3% reduction in growth rate, found in a murine model, could have a significant clinical impact. Pravastatin also improved elastin volume, though showed no benefit in aberrant aortic wall thickening or architectural disruption. Improvement in elastin volume related to Pravastatin therapy in a murine model of Marfan syndrome is also a novel finding, as elastin content is reduced in Marfan syndrome, (Abraham, Perejda *et al.* 1982) and marked disruption of elastin is evident in untreated groups within this and other studies. (Habashi, Judge *et al.* 2006)

Losartan also had a beneficial effect by attenuating dilatation of the aortic root diameter by 33.3% in a group of Marfan mice treated with Losartan as compared to the group of Marfan mice with no treatment. This is a statistically significant result, which may be clinically relevant due to its magnitude. This result is similar to previous studies with Losartan in murine models of Marfan syndrome.(Habashi, Judge *et al.* 2006) The aberrant aortic wall thickening in the Marfan untreated group was brought to near normal levels with Losartan, which is similar to studies conducted in Johns Hopkins.(Habashi, Judge *et al.* 2006) Elastin volume was preserved in the Losartan treatment group. Unfortunately, Losartan did not improve the amount of architectural disruption within the aortic medial layer. Clinical trials with Losartan treatment for aortic aneurysmal disease have commenced in patients with Marfan syndrome.(Lacro, Dietz *et al.* 2007; Radonic, de Witte *et al.* 2010; Forteza, Evangelista *et al.* 2011)

Pulse pressure was measured and found to be lower in the Marfan group which received Losartan treatment. This would reflect Losartan's blood pressure lowering property rather than an effect on the competency of the aortic valve. This anti-hypertensive effect possibly reduces the strain on the aorta itself, which could be an additional part of Losartan's beneficial effect. The dP/dt max was measured between the groups and the contractility index (dP/dt max divided by the left ventricular end diastolic pressure). Measurements of the contractility index showed no statistical difference between treatment groups.

Doxycycline did not improve aortic root dilatation. It had overall higher 3 month and 8 month aortic root measurements. A significant increase was observed in the aortic wall thickness in the Marfan groups treated with Doxycycline. Architectural disruption was increased with no change in elastin volume when compared to untreated Marfan mice.

The ranges of values for the size of the aortic root diameter, was wider in the treatment and Marfan groups, than that of the normal, no treatment group. This reflects a phenomenon of aneurysmal disease, that once an aortic root becomes aneurysmal, the diameter is enlarging and so becomes more variable in the diseased state. The rate of enlargement of an aortic aneurysm is more rapid in Marfan syndrome and so, more difficult to predict. (Davies, Goldstein *et al.* 2002)

TGF- β signalling appears critical to the pathogenesis in Marfan syndrome. Excessive unsequestered TGF- β is present in the extracellular matrix. This active TGF- β binds to the TGF- β receptor, which is involved with phosphorylation of Smad proteins. Once phosphorylated, they start a cascade which sends a signal to the nucleus to start transcribing messenger RNA which in turn is transported to the rough endoplasmic reticulum, which is located around the nucleus. The rough endoplasmic reticulum synthesizes proteins. Specific messenger RNA transcribed by the nucleus in this situation stimulates production of proteins involved in homeostasis of the extracellular matrix, such as matrix metalloproteinases and proteoglycans. The surface of the rough endoplasmic reticulum has many ribosomes attached. These ribosomes are involved in protein manufacturing. They give the endoplasmic reticulum the “rough” appearance. A ribosome binds to the rough endoplasmic reticulum once it begins to synthesize a protein that is destined for the secretory pathway. These proteins are then shuttled within membrane-bound vesicles to the Golgi apparatus, destined for secretion outside the cell. For this to occur, they first require localisation to the cellular membrane. Localisation is facilitated by a post-translational modification of the protein with a lipophilic group. Isoprenoid pyrophosphates serve as this essential lipophilic group which aids anchoring of the protein to the phospholipid bilayer. Anchoring facilitates interaction with the cell membrane and so transportation across the cell membrane.

Increased levels of unsequestered TGF- β , secondary to fibrillin-1 deficiency in Marfan syndrome, upregulate pSmad signalling, and thus increase the amount of protein production. The excessive level of protein production within the vascular smooth muscle cells is visible at an ultra-structural level as an increased amount of rough endoplasmic reticulum, which is where the proteins are being produced and transported out of the cell. The Marfan group which was treated with Losartan showed similar volumes of rough endoplasmic reticulum to the normal group. This reflected normalisation of the levels of protein production in the Marfan group treated with Losartan. This was previously noted to be related to the TGF- β receptor antagonism effect of Losartan. Excessive protein production is being inhibited “upstream”, blocking TGF- β signalling at the level of the cell membrane receptor and so up-regulation of protein production is halted before it even begins. This causes a marked reduction in the rough endoplasmic reticulum volume within the vascular smooth muscle cell. Statins on the other hand seem to cause a modest but not as marked reduction in RER volume. This suggests that some abnormal protein production is still occurring in the statin (Pravastatin) group, so the statins modest but not complete reduction in RER volume is likely a post-translational protein effect. This post-translational effect could be related to a reduction in the levels of isoprenyl groups available for prenylation of proteins. This would be secondary to inhibition of production of mevalonate by Pravastatin which is a HMG Co-A reductase inhibitor.

In this study Losartan was better than Pravastatin, and Doxycycline has no effect.

Chung *et al.*, found that Doxycycline was more effective than atenolol at preventing thoracic aortic aneurysm in murine model of Marfan syndrome, with preservation of aortic wall elastic fibres and normalisation of aortic wall architecture.(Chung, Yang *et al.* 2008) Aortic root diameter, at 9 months was reduced from 2.31 \pm 0.13mm in the untreated Marfan group versus 1.78 \pm 0.04mm in the Marfan group treated with Doxycycline (0.24g/L) from 6 weeks

of age. They proposed that this protective effect was due to inhibition of matrix metalloproteinase 2 & 9, and a reduction of TGF- β . This was in contrast to the results outlined in this chapter. This study showed an increased level of architectural disruption and a decrease in elastic fibre volume with Doxycycline treatment. A potential cause for a difference between this study and the results from Chung *et al.*, is that $n = 30$ in the treatment group, 10 euthanized at 3, 6 and 9 month. Our results had a larger number, $n = 17$, of aortic specimens assessed at 8 months, and this assessment focused on the aortic root. Chung *et al.* averaged their results from different sections of the aorta, which could have an effect of falsely normalising measurements of the aorta. Our results show a wider variability, despite a higher number of specimens, which might suggest a higher degree of variability of response to Doxycycline treatment. Descending thoracic aortas are relatively spared from disease in this particular murine model of disease. There may have been, an unexpected variability introduced into each of the two conflicting studies.

Habashi *et al.*, found Losartan prevented aortic aneurysm in a murine model of Marfan syndrome (Habashi, Judge *et al.* 2006). The Marfan group treated with Losartan showed improvement in aortic root elastic fibre architecture, aortic wall medial thickness and aortic root diameter (growth rate and absolute diameter) compared to placebo treated Marfan groups and showed full normalisation compared to wild-type mice. Other studies have shown that Losartan reduces the expression of matrix metalloproteinases 2 and 9, (Yang, Kim *et al.* 2009) and are related to TGF- β expression. (Matt, Habashi *et al.* 2008) The initial studies conducted by Habashi *et al.* (Habashi, Judge *et al.* 2006) are similar to our study which shows an improvement in aortic root diameter, aortic wall thickness, though aortic wall architecture was not improved in our study. We also found that the volume of elastic fibres within the aortic root media was preserved with Losartan.

In summary, Losartan is very effective at reducing the aortic root diameter. It also normalises aortic wall thickness and preserved elastic fibre content. It did not preserve aortic wall architecture in our study, although it has been shown in another study to have a positive effect on this parameter.(Habashi, Judge *et al.* 2006) The beneficial effect has previously been noted to be attributed to TGF- β receptor antagonism, with a consequential reduction in excessive protein production.(Habashi, Judge *et al.* 2006; Matt, Habashi *et al.* 2008) Normalisation of protein production was suggested by a reduced amount of cell organelles involved in this function by observations at an ultra-structural level within the vascular smooth muscle cells of the aortic root in Marfan syndrome in the Pravastatin & Losartan treatment groups. Pravastatin treatment compared favourably to Losartan. In fact, Pravastatin is equipotent to Losartan in attenuating absolute aortic root diameter in Marfan syndrome. It also had a beneficial effect on preserving aortic elastic fibre content, though did not reduce aortic wall thickening or aortic wall architecture. The beneficial effect of Pravastatin may be related to reducing the cell's ability to process the excessive amount of protein that arises within the vascular smooth muscle cell in Marfan syndrome. Doxycycline was inferior to both Pravastatin and Losartan. Doxycycline and Losartan have been studied as a combined treatment with beneficial effects on the structure of the aortic wall.(Yang, Kim *et al.* 2010) The results of ultra-structural analysis in this study suggest that Losartan and Pravastatin have different mechanisms of action. This would open up the possibility that if given together for treatment of aortic root pathology in Marfan syndrome, they may have a combined, synergistic effect more potent than if given alone.

4.6 References

- Abraham, P. A., A. J. Perejda, et al. (1982). "Marfan syndrome. Demonstration of abnormal elastin in aorta." J Clin Invest 70(6): 1245-1252.
- Boyle, J. R., E. McDermott, et al. (1998). "Doxycycline inhibits elastin degradation and reduces metalloproteinase activity in a model of aneurysmal disease." J Vase Surg 27(2): 354-361.
- Brooke, B. S., J. P. Habashi, et al. (2008). "Angiotensin II blockade and aortic-root dilation in Marfan's syndrome." N Engl J Med 358(26): 2787-2795.
- Bunton, T. E., N. J. Biery, et al. (2001). "Phenotypic alteration of vascular smooth muscle cells precedes elastolysis in a mouse model of Marfan syndrome." Circ Res 88(1): 37-43.
- Chung, A. W., H. H. Yang, et al. (2008). "Long-term doxycycline is more effective than atenolol to prevent thoracic aortic aneurysm in marfan syndrome through the inhibition of matrix metalloproteinase-2 and -9." Circ Res 102(8): e73-85.
- Dallas, S. L., K. Miyazono, et al. (1995). "Dual role for the latent transforming growth factor-beta binding protein in storage of latent TGF-beta in the extracellular matrix and as a structural matrix protein." J Cell Biol 131(2): 539-549.
- Davies, R. R., L. J. Goldstein, et al. (2002). "Yearly rupture or dissection rates for thoracic aortic aneurysms: simple prediction based on size." Ann Thorac Surg 73(1): 17-27; discussion 27-18.
- Detaint, D., P. Aegerter, et al. (2010). "Rationale and design of a randomized clinical trial (Marfan Sartan) of angiotensin II receptor blocker therapy versus placebo in individuals with Marfan syndrome." Arch Cardiovasc Dis 103(5): 317-325.
- Dietz, H. C., G. R. Cutting, et al. (1991). "Marfan syndrome caused by a recurrent de novo missense mutation in the fibrillin gene." Nature 352(6333): 337-339.
- Dietz, H. C., R. E. Pyeritz, et al. (1991). "The Marfan syndrome locus: confirmation of assignment to chromosome 15 and identification of tightly linked markers at 15q15-q21.3." Genomics 9(2): 355-361.
- Elefteriades, J. A. (2002). "Natural history of thoracic aortic aneurysms: indications for surgery, and surgical versus nonsurgical risks." Ann Thorac Surg 74(5): S1877-1880; discussion S1892-1878.
- Finkbohner, R., D. Johnston, et al. (1995). "Marfan syndrome. Long-term survival and complications after aortic aneurysm repair." Circulation 91(3): 728-733.
- Forteza, A., A. Evangelista, et al. (2011). "[Study of the efficacy and safety of losartan versus atenolol for aortic dilation in patients with Marfan syndrome]." Rev Esp Cardiol 64(6): 492-498.
- Goldstein, J. L. and M. S. Brown (1990). "Regulation of the mevalonate pathway." Nature 343(6257): 425-430.
- Habashi, J. P., D. P. Judge, et al. (2006). "Losartan, an ATI antagonist, prevents aortic aneurysm in a mouse model of Marfan syndrome." Science 312(5770): 117-121.
- Hiratzka, L. F., G. L. Bakris, et al. (2010). "2010 ACCF/AHA/AATS/ACR/ASA/SCA/SCAI/SIR/STS/SVM guidelines for the diagnosis and management of patients with Thoracic Aortic Disease: a report of the American College of Cardiology Foundation/American Heart Association Task Force on Practice Guidelines, American Association for Thoracic Surgery, American College of Radiology, American Stroke Association, Society of Cardiovascular Anesthesiologists, Society for Cardiovascular Angiography and Interventions, Society of Interventional Radiology, Society of Thoracic Surgeons, and Society for Vascular Medicine." Circulation 121(13): e266-369.

- Kuipers, H. F., P. J. Biesta, et al. (2005). "Statins affect cell-surface expression of major histocompatibility complex class II molecules by disrupting cholesterol-containing microdomains." *Hum Immunol* 66(6): 653-665.
- Lacro, R. V., H. C. Dietz, et al. (2007). "Rationale and design of a randomized clinical trial of beta-blocker therapy (atenolol) versus angiotensin II receptor blocker therapy (losartan) in individuals with Marfan syndrome." *Am Heart J* 154(4): 624-631.
- Lavoie, P., G. Robitaille, et al. (2005). "Neutralization of transforming growth factor-beta attenuates hypertension and prevents renal injury in uremic rats." *J Hypertens* 23(10): 1895-1903.
- Lindeman, J. H., H. Abdul-Hussien, et al. (2009). "Clinical trial of doxycycline for matrix metalloproteinase-9 inhibition in patients with an abdominal aneurysm: doxycycline selectively depletes aortic wall neutrophils and cytotoxic T cells." *Circulation* 119(16): 2209-2216.
- Matt, P., J. Habashi, et al. (2008). "Recent advances in understanding Marfan syndrome: should we now treat surgical patients with losartan?" *J Thorac Cardiovasc Surg* 135(2): 389-394.
- Matt, P., F. Schoenhoff, et al. (2009). "Circulating transforming growth factor-beta in Marfan syndrome." *Circulation* 120(6): 526-532.
- Milewicz, D. M., H. C. Dietz, et al. (2005). "Treatment of aortic disease in patients with Marfan syndrome." *Circulation* 111(11): e150-157.
- Murdoch, J. L., B. A. Walker, et al. (1972). "Life expectancy and causes of death in the Marfan syndrome." *N Engl J Med* 286(15): 804-808.
- Neptune, E. R., P. A. Frischmeyer, et al. (2003). "Dysregulation of TGF-beta activation contributes to pathogenesis in Marfan syndrome." *Nat Genet* 33(3): 407-411.
- Pereira, L., S. Y. Lee, et al. (1999). "Pathogenetic sequence for aneurysm revealed in mice underexpressing fibrillin-1." *Proc Natl Acad Sci U S A* 96(7): 3819-3823.
- Pyeritz, R. E. (2009). "Marfan syndrome: 30 years of research equals 30 years of additional life expectancy." *Heart* 95(3): 173-175.
- Radonic, T., P. de Witte, et al. (2010). "Losartan therapy in adults with Marfan syndrome: study protocol of the multi-center randomized controlled COMPARE trial." *Trials* 11: 3.
- Shores, J., K. R. Berger, et al. (1994). "Progression of aortic dilatation and the benefit of long-term beta-adrenergic blockade in Marfan's syndrome." *N Engl J Med* 330(19): 1335-1341.
- Smith, J. A., J. I. Fann, et al. (1994). "Surgical management of aortic dissection in patients with the Marfan syndrome." *Circulation* 90(5 Pt 2): II235-242.
- Xiong, W., R. A. Knispel, et al. (2008). "Doxycycline delays aneurysm rupture in a mouse model of Marfan syndrome." *J Vasc Surg* 47(1): 166-172; discussion 172.
- Yang, H. H., J. M. Kim, et al. (2009). "Long-term effects of losartan on structure and function of the thoracic aorta in a mouse model of Marfan syndrome." *Br J Pharmacol* 158(6): 1503-1512.
- Yang, H. H., J. M. Kim, et al. (2010). "Effectiveness of combination of losartan potassium and doxycycline versus single-drug treatments in the secondary prevention of thoracic aortic aneurysm in Marfan syndrome." *J Thorac Cardiovasc Surg* 140(2): 305-312 e302.

Chapter 5

Pravastatin attenuates aortic root pathology, optimisation of dose and timing of therapy in Marfan syndrome

5.1 Introduction:

Having demonstrated an improvement in aortic root diameter in Marfan syndrome with a novel pharmaceutical therapy, Pravastatin, the hypothesis was that this improvement could be further increased if the dose was increased by a factor of two. This would mean the dose of Pravastatin would increase from 50mg/kg to 100mg/kg. Higher doses of Pravastatin tended towards a more significant beneficial effect on cholesterol lowering.(Byrne 2008) Increasing the dose of Pravastatin has been shown to decrease serum lipid levels.(Hunninghake, Knopp *et al.* 1990) The dose of Pravastatin was titrated up until serum cholesterol levels decreased. Pravastatin has been shown to have dose dependent effects on inflammatory response, independent of lipid lowering effects, in patients suffering from myocardial infarction.(Di Garbo, Bono *et al.* 2000)

The treatment of Marfan syndrome would be a novel indication for this drug which is already established as a treatment for hypercholesterolaemia(Jones, Farmer *et al.* 1991) and secondary prevention for atherosclerotic related disease such as ischemic heart disease(Glasziou, Eckermann *et al.* 2002) and cerebrovascular disease.(Koizumi, Shimizu *et al.* 2002) Pravastatin therapy was shown by Dr. John Byrne & Dr. Jonathan McGuinness to attenuate aortic pathology, when therapy was commenced at 6 weeks of age in a murine model.

There are over 400 sporadic mutations of the fibrillin-1 gene that cause Marfan syndrome. It may be possible to screen offspring of known patients, who have known mutation but, it is not feasible to screen the population for all of the known mutations at birth, or in early

childhood. The diagnosis is essentially clinical. In 1995, a group of the world's leading clinicians and investigators in Marfan syndrome proposed revised diagnostic criteria. Known as the Ghent criteria, they identify major and minor diagnostic findings, which are largely based on clinical observation of various organ systems and on the family history. This has since been updated.(Loeys, Dietz *et al.* 2010) A major criterion is defined as one that carries high diagnostic precision because it is relatively infrequent in other conditions and in the general population. The Ghent criteria were intended to serve as an international standard for clinical and molecular studies and for investigations of genetic heterogeneity and genotype-phenotype correlations. The clinical diagnosis in adults should be made using the revised Ghent criteria, which are unreliable in children. Most clinical features are specific to age, and some features may not manifest until relatively late in life. This feature may make diagnosis in childhood difficult. Aortic root dilatation involving the sinuses of Valsalva in Marfan syndrome occurs in 70-80% of patients.(Hwa, Richards *et al.* 1993) It manifests at an early age and tends to be more common in men than women.

With these facts in mind, the second hypothesis was that the treatment could become more clinically relevant if the treatment benefit was preserved despite commencing therapy at a later stage. This may evaluate the relevance and speed up translation into clinical practice.

Statin therapy may have an effect on the normal aorta.(Steinmetz, Buckley *et al.* 2005) The effect may, be unrelated to its effects in Marfan syndrome. To investigate the extent of effect Pravastatin has on the Marfan disease process specifically, a group of normal, wild-type mice were administered Pravastatin.

The specific objectives of this study therefore were as follows:

- To determine if the observed beneficial effect of Pravastatin therapy was preserved with commencement of treatment at a later stage in the disease process.
- To determine if an increased dose would confer an increased benefit.

- To determine the effect of Pravastatin therapy has on normal aorta.

5.2 Materials and Methods:

A pair of male C1039G Marfan mice was cross bred with C57Bl6 females. Genetic analysis of the offspring was conducted. Male mice identified to have the C1039G mutation were entered into the study, as detailed in the materials and methods section.

These mice were then entered into four different treatment groups.

The first group was administered Pravastatin from 6 weeks of age. The dose was 0.25g/Litre, equivalent to 50mg/kg/day.

The second group was administered Pravastatin from 4 months of age. The dose administered was 50mg/kg/day.

The third group was administered Pravastatin from 5 months of age. The dose administered was 50mg/kg/day.

The fourth group was administered Pravastatin from 6 weeks of age. The dose administered was 100mg/kg/day.

The fifth group contained wild-type mice and was administered Pravastatin from 6 weeks of age. The dose administered was 50mg/kg/day.

The results from untreated Marfan group and untreated wild-type group from the comparison chapter 3 were used as positive and negative controls. Drug administration was conducted as per methods outlined in chapter 2, section 2.1.2.

These animals were then studied in the following manner;

Aortic root diameter was assessed *in-vivo*, at 3 months and 8 months for evidence of progression of aneurysmal dilatation, by trans-thoracic echocardiography as outlined in the materials and methods in chapter 2 section 2.1.4.

Histology of aortic root pathology was assessed as per methods outlined in chapter 2, section 2.6. Samples of aortic root were harvested at 8 months. Aortic root thickness was assessed with Haematoxylin and Eosin staining. Architecture of the aortic media at the level of the aortic root was assessed by staining sections with Verhoeff van Gieson stain. The amount of proteoglycan (within the connective tissue matrix) staining within the aortic media was assessed by histological cross-sections of the aortic root with Alcian blue stain. The intensity of staining was assigned a grade of 1, 2, 3 or 4, with increasing intensity of stain deposition within the aortic media.

5.3 Results

Results when given are immediately followed by +/- standard error of the mean in brackets.

5.3.1 The effect of pravastatin on the normal aorta

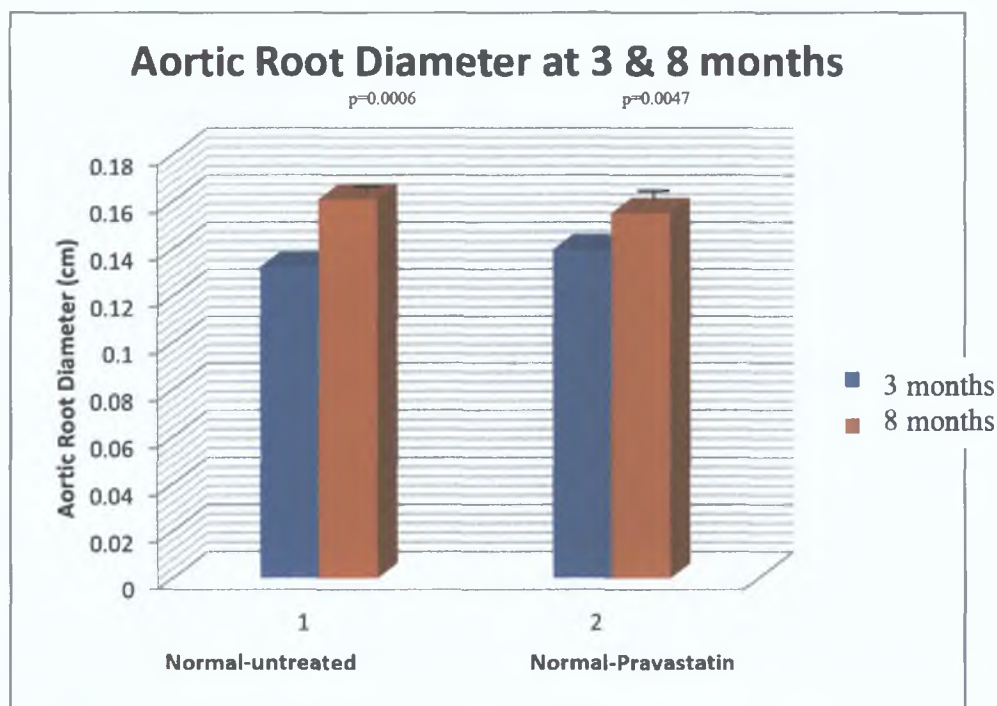


Figure 5.1: Mean aortic root diameter (cm), normal versus normal treated with pravastatin at 3 & 8 months.

The mean aortic root diameter was reduced in the normal group treated with Pravastatin at 8 months compared to normal mice who were not given Pravastatin at 8 months. The mean aortic root diameter was reduced from 0.161cm (+/-0.001) in normal, mice to 0.155cm (+/-0.002) in Pravastatin treated mice, which was statistically significant (p=0.0047).

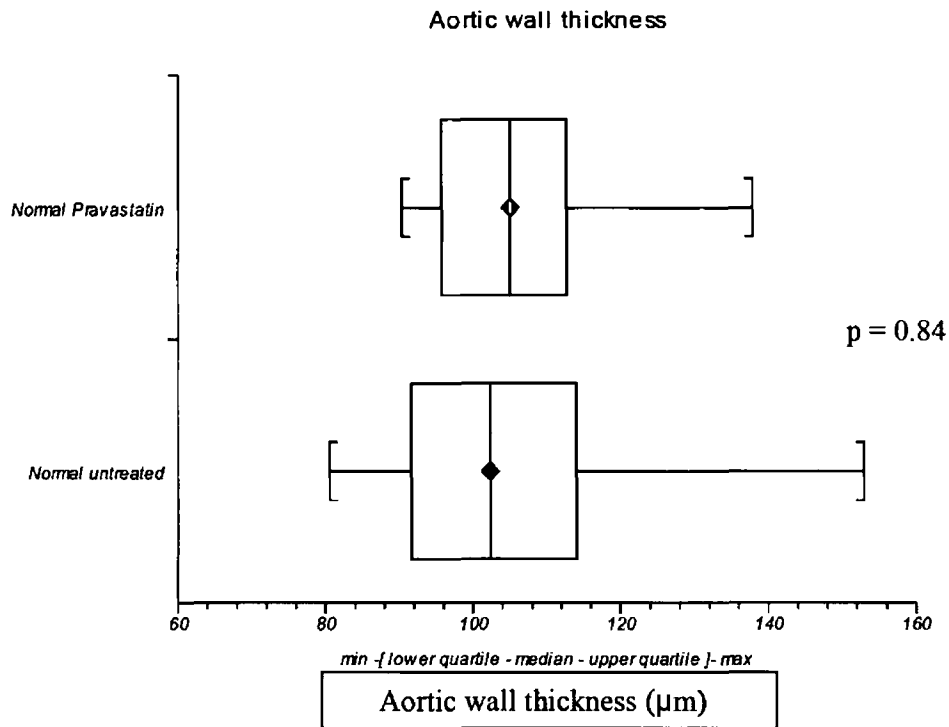


Figure 5.2: Aortic wall thickness (μm) in normal & normal treated with pravastatin groups at 8 months, showing the spread of values & interquartile range. The two groups are similar.

The mean aortic wall thickness was similar in both the normal group, $104.8\mu m(+/-6.5)$ and in the normal treated with Pravastatin group, $106.4\mu m(+/-4.4)$. The aortic specimens were taken from 10 different mice from each group.

The mean aortic wall architectural score was similar in both the normal group, $0.6(+/-0.16)$, and in the normal treated with Pravastatin group, $1.1(+/-0.55)$.

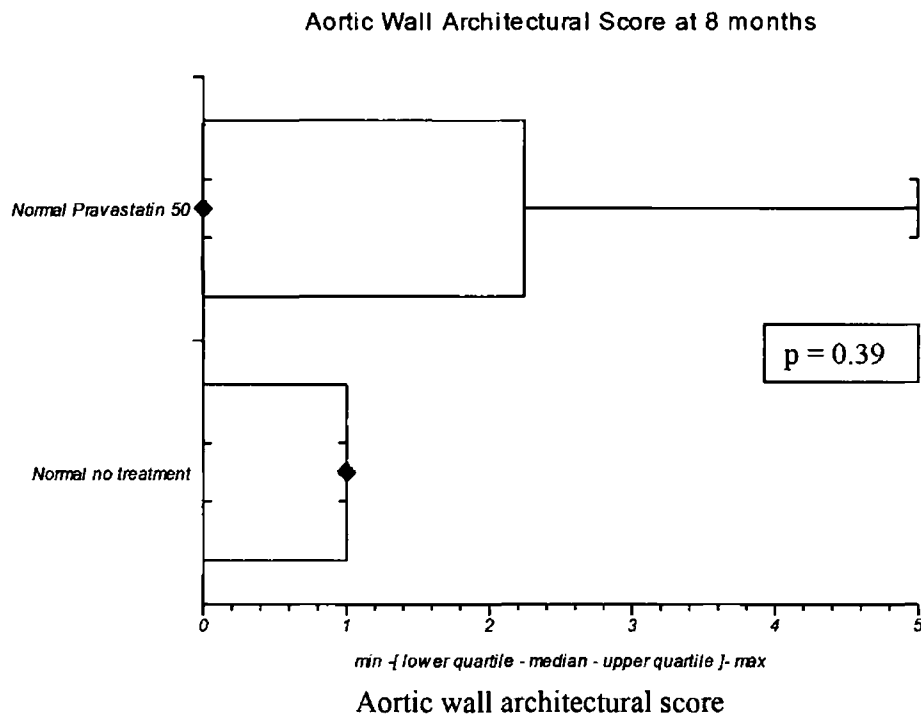


Figure 5.3: The mean aortic wall architectural score in both normal & normal treated with pravastatin.

The range of the mean aortic wall architectural score shows a wider range in the normal Pravastatin treated group, though there is no statistical difference between the groups.

5.3.2 Optimising the dose of pravastatin for aortic pathology in Marfan syndrome

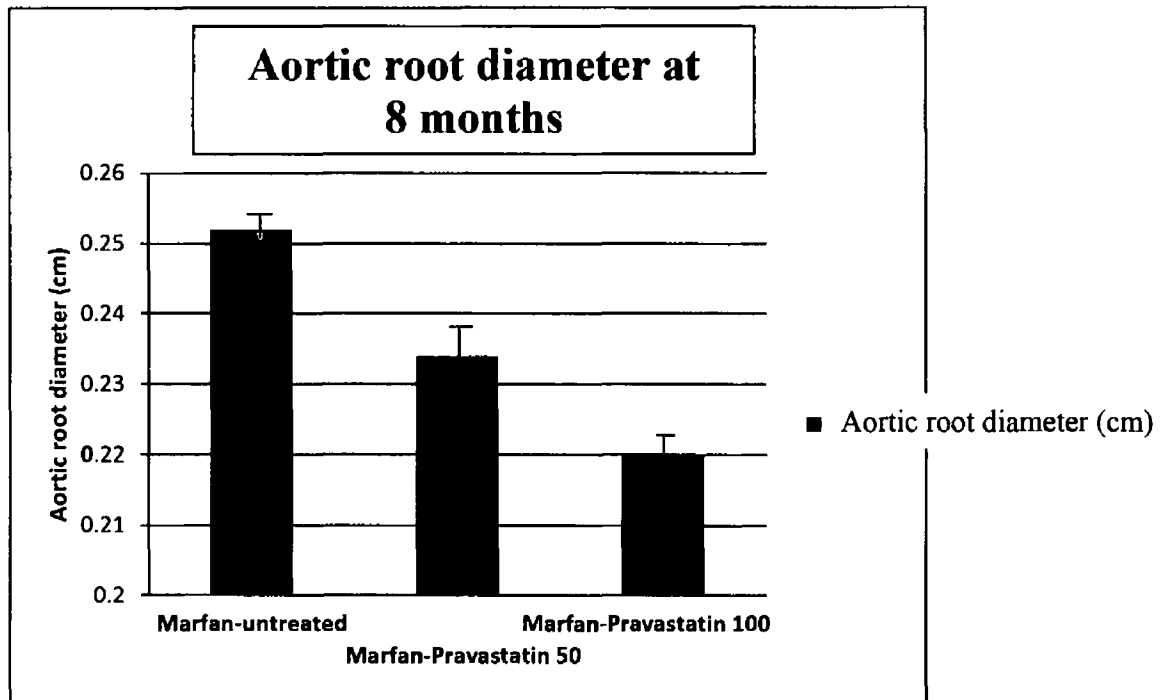


Figure 5.4: Aortic root diameter at 8 months (cm), Pravastatin Dose 50 mg/kg versus 100 mg/kg in Marfan treated versus Marfan untreated. Dosing began at 6 weeks. The figure shows a reduction in aortic root diameter in a dose dependent fashion (n =75). Statistics to accompany figure, in Table 5.1 below.

Marfan Groups	Untreated	Pravastatin 50	Pravastatin 100
Standard deviation	0.035	0.035	0.023
p value		0.0004 [compared to untreated]	<0.0001 [compared to untreated]

Table 5.1: Table to accompany Figure 5.4 Aortic root diameter at 8 months (cm), Pravastatin Dose 50 mg/kg versus 100 mg/kg in Marfan treated versus Marfan

untreated. The table shows a both standard deviations and p-values for the marfan groups derived by analysis of variance with Bonferroni correction.

When Pravastatin therapy was initiated at 6 weeks of age at a dose of 50mg/kg the aortic root diameter at 8 months was reduced from 0.252 cm, to 0.233cm. There was a further reduction in the mean aortic root diameter at 8 months, 0.22cm, when a higher dose of 100mg/kg was administered from 6 weeks of age.

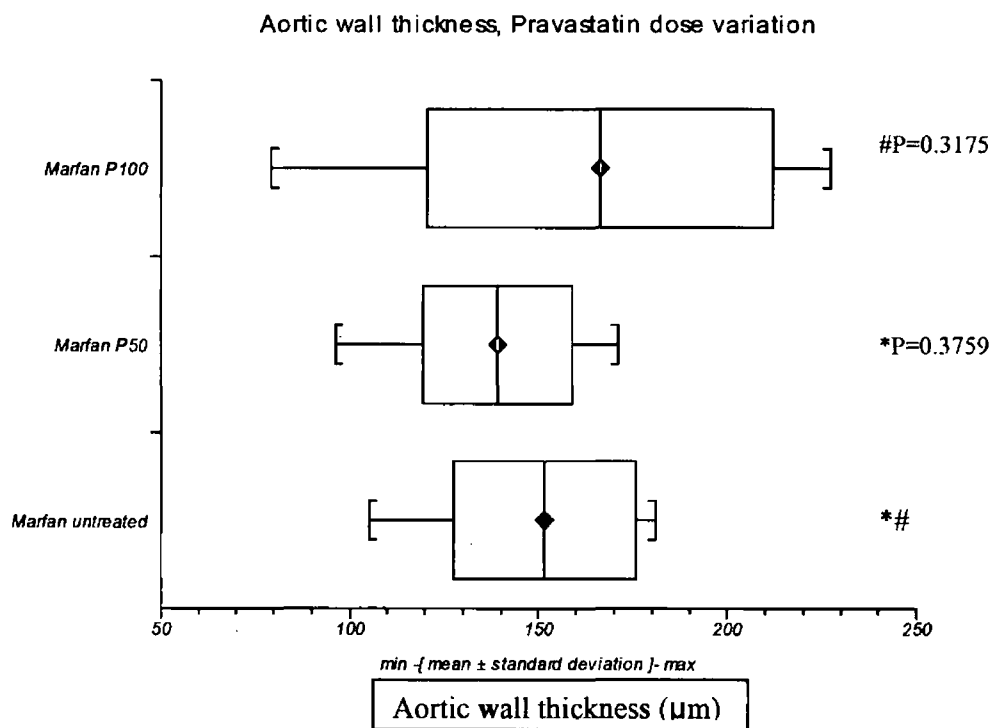


Figure 5.5: Aortic wall thickness (µm), Marfan untreated versus Pravastatin Dose 50 mg/kg versus 100 mg/kg in Marfan groups. Dosing began at 6 weeks. The mean, maximum & minimum values with one standard deviation are displayed. The means are similar, though the range and standard deviation is wider in the Marfan group treated with pravastatin 100mg/kg.

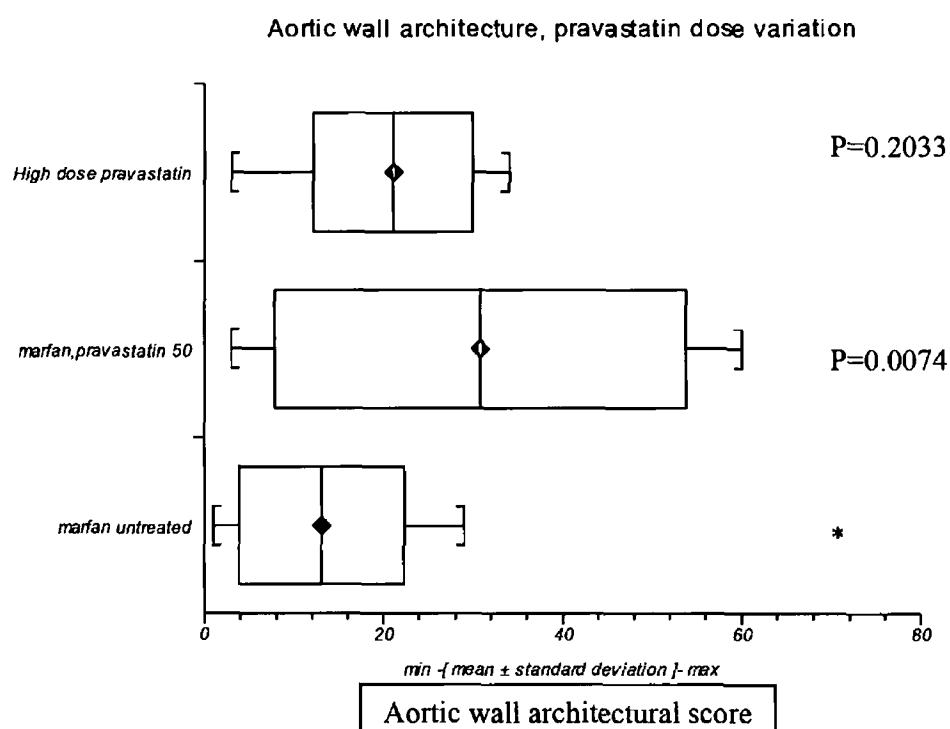


Figure 5.6: Aortic wall architecture, Marfan untreated versus pravastatin dosed Marfan at 50 mg/kg(pravastatin 50) versus 100 mg/kg(High dose pravastatin) . Dosing of these groups began at 6 weeks. The mean, maximum & minimum values with one standard deviation are displayed. The means vary, and both the treatment groups have higher values than the untreated Marfan group, though not in a dose dependent fashion.

Aortic wall architecture was assessed in three Marfan groups. The first group was untreated (n=13), the second and third were administered Pravastatin from 6 weeks of age at a dose of 50mg/kg (n=10) and 100mg/kg (n=10). The mean aortic wall architecture score was 13 for the untreated Marfan group, 30.8 for the 50mg/kg Pravastatin group (p=0.0074) and 21.1 for the 100mg/kg group (p=0.20).

The mean, maximum & minimum values with one standard deviation are displayed. The means vary, and both the treatment groups have higher values than the untreated Marfan group, though not in a dose dependent fashion.

5.3.3 Investigation of the optimum timing of initiation of pravastatin therapy for aortic pathology in Marfan syndrome

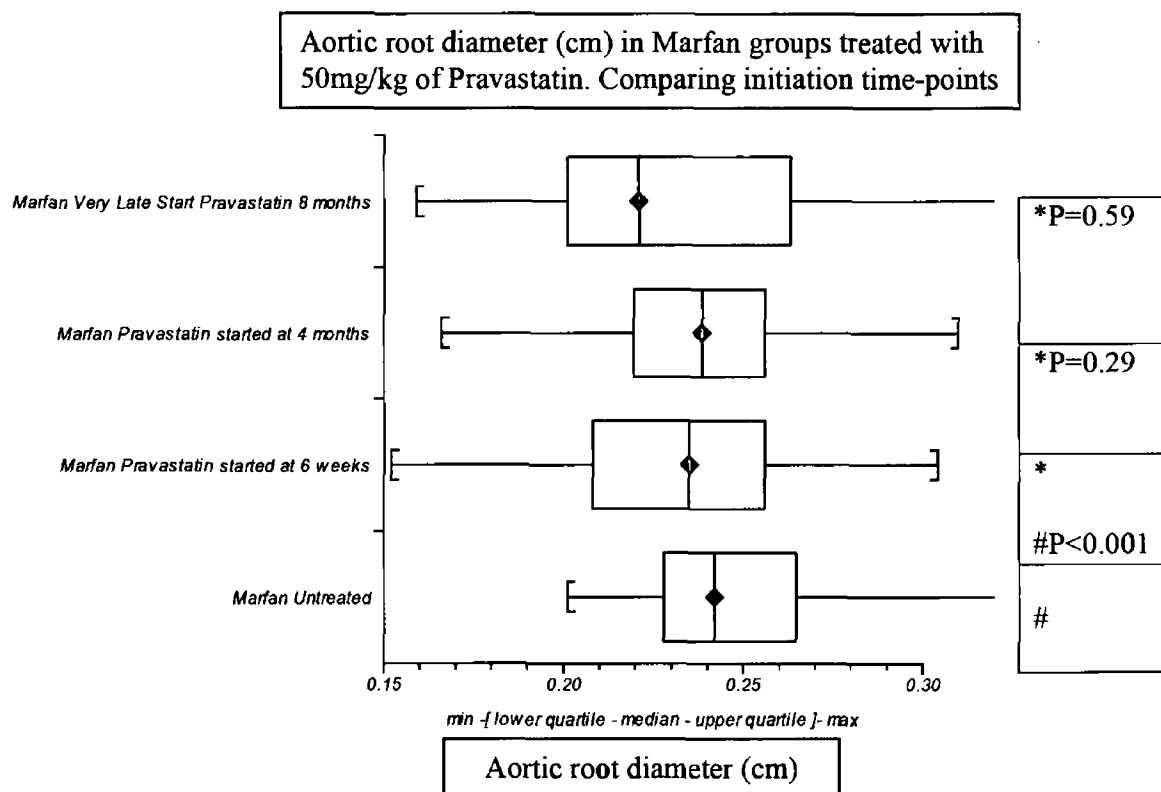


Figure 5.7: Aortic root diameter (cm), at 8 months of age, in Marfan groups treated with 50mg/kg of pravastatin & control untreated Marfan group. Comparing effect of varying age at which treatment was initiated.

Aortic root diameters were observed to be similar in both late start groups to the normal start group at a dose of 50mg/kg.

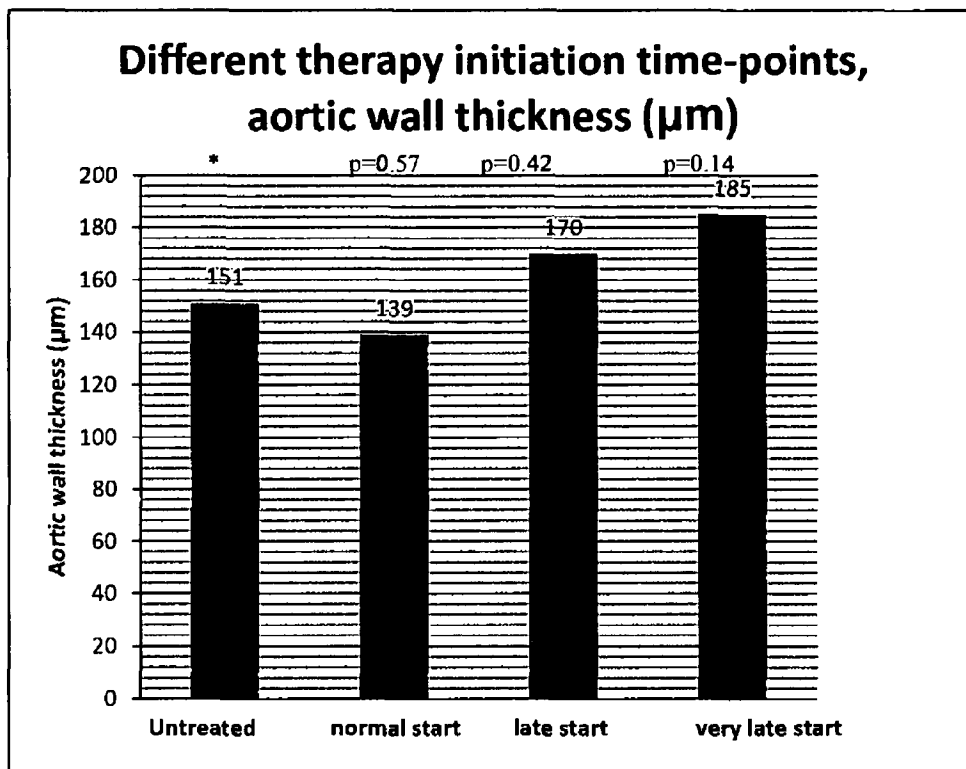


Figure 5.8: Aortic wall thickness (μm), at 8 months of age, in Marfan groups treated with 50mg/kg of pravastatin. Compared effect of varying age at which treatment was initiated, with a control, untreated marfan group. [Normal start refers to treatment initiation at 6 weeks of age. Late start refers to treatment initiation at 4 months of age. Very late start refers to treatment initiation at 5 months of age.]

Mean aberrant aortic wall thickening varied, though the variation did not reach statistical significance.

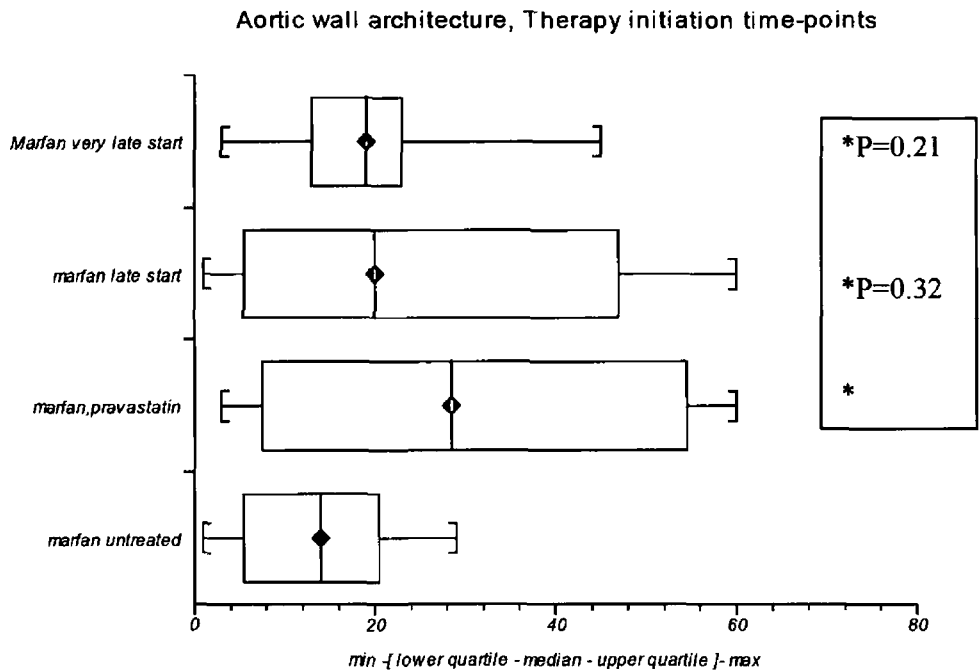


Figure 5.9: Aortic architectural score, at 8 months of age, in Marfan groups treated with 50mg/kg of pravastatin. Compared effect of varying age at which treatment was initiated, with a control, untreated Marfan group. [Normal start refers to treatment initiation at 6 weeks of age. Late start refers to treatment initiation at 4 months of age. Very late start refers to treatment initiation at 5 months of age.]

Aortic architectural disruption showed no statistical-significant difference in the Marfan groups in which Pravastatin was commenced at different time-points.

5.3.4 Effect of pravastatin on proteoglycan deposition within the aortic wall.

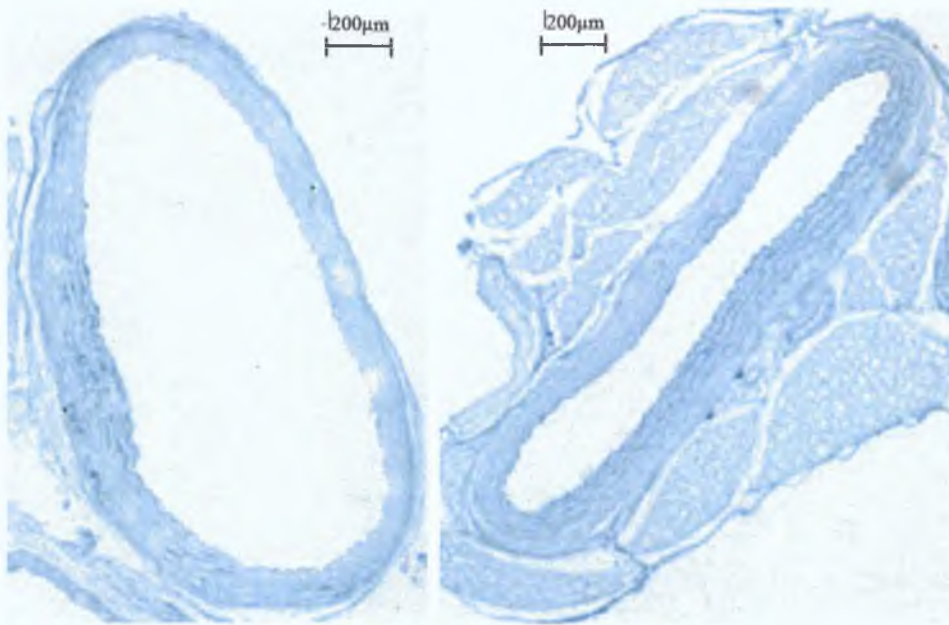


Figure 5.10: Histological images, cross-sections of normal aorta stained with Alcian Blue. This is the normal intensity of staining of the aorta wall, forming a baseline for assessing proteoglycan deposition within the aortic wall.

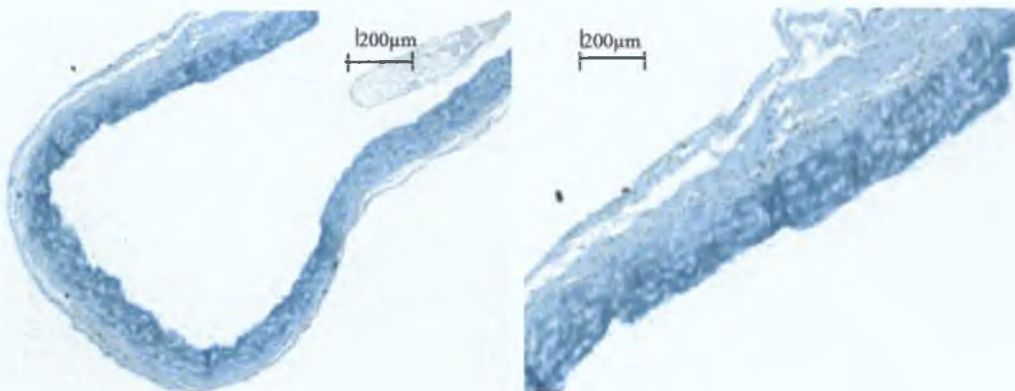


Figure 5.11: Histological images, cross-sections of aorta stained with Alcian Blue from the Marfan group that has received no treatment. There is intense staining of the aorta wall, indicating a significant increase in the amount of proteoglycan deposition within the media.

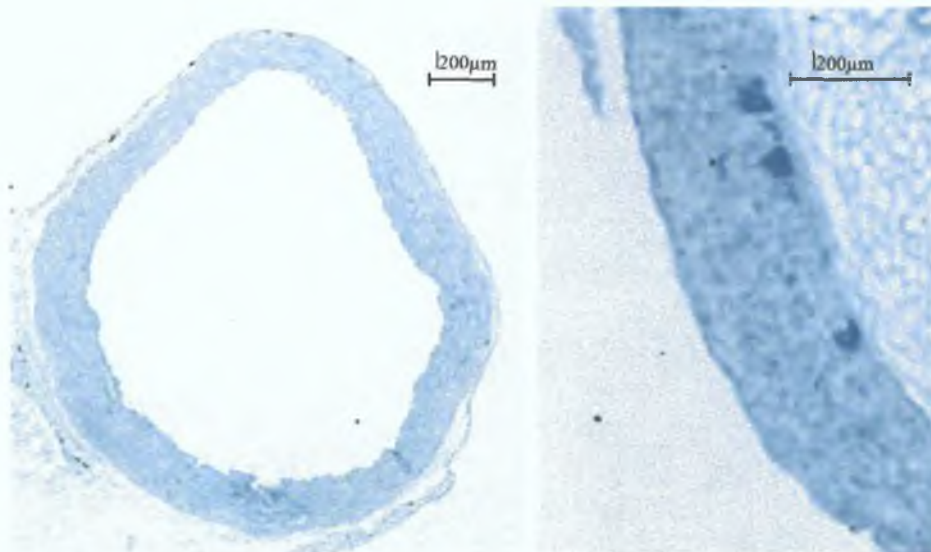


Figure 5.12: Histological images, cross-sections of aorta stained with Alcian Blue from the Marfan group that has received pravastatin (50mg/kg) treatment from six weeks of age. There is less intense staining of the aorta wall, indicating less proteoglycan deposition.

Histological cross-sections of aortic root were stained with Alcian Blue to assess glycogen deposition within the aortic media. Figure 5.10 above displays a baseline staining intensity for normal aorta. Comparing this to the Marfan untreated aortic wall, there is a dramatic increase in the intensity of Alcian Blue staining. This reflects an increase in the amount of glycogen deposition within the aortic media in Marfan syndrome. The intensity of Alcian Blue staining is greatly reduced in the Marfan group treated with Pravastatin (50mg/kg). The reduction in the intensity of staining reflected a reduced level of proteoglycan deposition within the aortic wall in the Pravastatin treatment group. This is qualitative data, following assessment of samples from at least 10 different specimens from each group.

Alcian blue - grade of stainin gbetween normal, marfan & marfan treated with prav

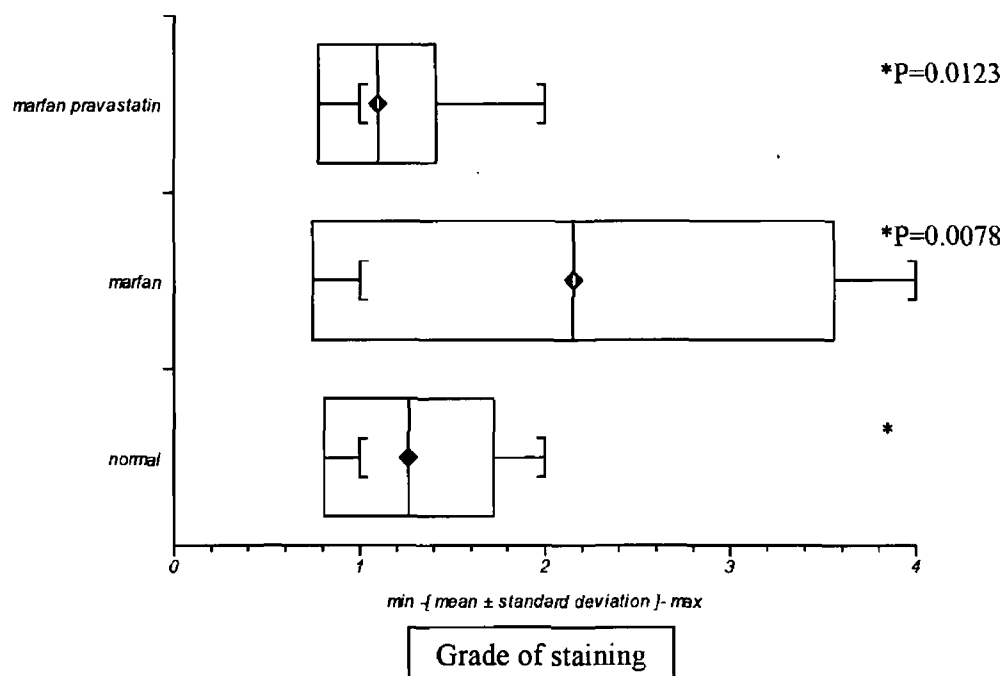


Figure 5.13: Alcian blue grade of staining in Normal, Marfan & Marfan treated with pravastatin groups.

5.4 Discussion

Aortic root growth rate was observed in normal, untreated mice and normal mice treated with Pravastatin. There was a significant difference in growth rate between the two groups. The treatment group had a growth rate 53% that of the untreated group. The overall aortic root diameter at 8 months showed a difference of a 3.7% reduction in the treatment group, which was statistically significant. In human studies the effect of statin treatment on normal aortic wall remains to be elucidated. (Muehling, Oberhuber *et al.* 2008) There was no difference in the thickness of the aortic wall between the groups. Nor was there a significant difference between the aortic architectural score between the two groups. This information would have implications for treating any patient with Pravastatin for aortic aneurysmal disease. It is important to know that Pravastatin reduces dilatation of the aortic root in the normal aorta,

without an increase in thickness, nor disruption of the architecture of the wall. Pravastatin does not have deleterious effects on the structure of the aortic root. Pravastatin treatment has many beneficial effects for patients with cardiovascular disease (Shepherd, Cobbe *et al.* 1995), though rates of statin use in an older female population is only 22%. (Lawlor, Bedford *et al.* 2003) Statins have been shown to reduce the proteolytic activity within the wall of aortic aneurysms of the abdominal aortic wall. (Abisi, Burnand *et al.* 2008) Preoperative statin therapy was associated with improved outcomes in patient who were undergoing abdominal aortic aneurysm repair. (McNally, Agle *et al.* 2010) Recent guidelines recommend that for patients who have thoracic aortic aneurysmal disease, dyslipidaemia should be treated, with statin therapy, for patients with non-coronary atherosclerotic disease, atherosclerotic aortic aneurysm, and co-existing coronary heart disease at high risk for coronary ischaemic events. (Hiratzka, Bakris *et al.* 2010)

As Pravastatin is a novel potential therapy for treating aortic root pathology in Marfan syndrome, the optimal dose is not yet known. The initial dose of 50mg/kg for the murine model was chosen due to its effect on cholesterol metabolism in the wild type. Statin dose was titrated up until the serum cholesterol dropped by >20%. This occurred at 50mg/kg. This was conducted previously by Dr. John Byrne & Dr. Jonathan McGuinness (personal communication). This dose, even though it exceeds a human dose would be considered a bio-equivalent dose in this murine species. It is the dose required to commence inhibition of the HMG Co-A reductase pathway.

Three groups were considered to assess the optimum dose of Pravastatin, an untreated Marfan group, a Marfan group administered 50mg/kg and a Marfan group administered 100mg/kg. These groups were compared to the normal group. The 50mg/kg dose was chosen because of the effect on cholesterol metabolism and the 100mg/kg to ascertain if there is a dose

dependent mechanism involved. The aortic root dilatation in the 50mg/kg (Marfan) group was reduced by 21%. The aortic root dilatation in the 100mg/kg (Marfan) group was reduced by 33%. An increase in the dose, by a factor of two, increased the effect of the treatment by 50%. This showed a dose dependent response to treatment with respect to aortic root diameter attenuation. However there was no significant difference in aortic wall thickness or architecture score with increasing doses. Statins have been shown to reduce the growth rate in infra-renal abdominal aortic aneurysms (Schouten, van Laanen *et al.* 2006) which is suggested to have a different mechanism to that of lipid lowering effect of statin therapy. The dose response that is observed in the 100mg/kg group compared to the 50mg/kg group may be a dose response that involves the pleiotropic effects of statin therapy involving many different mechanisms other than reduction in serum cholesterol. (Wang, Liu *et al.* 2008) In humans the dosage of statins varies between 0.1 – 1 mg/kg and in rodents dosages vary between 1 – 100 mg/kg and even 500 mg/kg. This is because of a known pharmacodynamic resistance to the pharmacological effect in these animals, where higher levels are required.(Bjorkhem-Bergman, Lindh *et al.* 2011)

Due to the variability of phenotypic expression and highly variable genetic mutations responsible for Marfan syndrome, patients with Marfan syndrome often present with established disease. Patients may have aortic aneurysmal disease and are unaware of both their underlying condition and one of the secondary complications of an aneurysmal aorta, with or without aortic incompetence (which can lead to heart failure).(Bakalli, Bekteshi *et al.* 2009) We do not know the effect of treatment of statin therapy or even Losartan therapy in the paediatric population. Doxycycline therapy can cause severe dental staining in developing dentition in the paediatric population and so is less than an ideal therapy. A small trial was conducted with Losartan in a paediatric population and found a reduction in the rate of aortic

root dilatation.(Brooke, Habashi *et al.* 2008) To investigate whether a delayed treatment strategy would be of benefit with established disease, the timing of Pravastatin administration was varied. Normal Pravastatin start time was considered to be 6 weeks of age for the purpose of this study. Late start was considered 4 months and very late start considered 5 months of age. Aortic root diameters were observed to be similar in both late start groups to the normal start group at a dose of 50mg/kg. Aortic architectural disruption showed no statistical difference in the Marfan groups in which Pravastatin was commenced at different time-points. Mean aberrant aortic wall thickening varied, though the variation did not reach statistical significance.

Alcian blue staining showed that glycogen deposition within the aortic media, increases in Marfan syndrome compared to normal. With Pravastatin treatment in Marfan syndrome, the amount of proteoglycan deposition was greatly reduced to normal levels.

Conclusion

In summary, Pravastatin has been shown here to reduce both the growth rate and the overall diameter of a normal aorta, with no significant change in the mean aortic wall thickness and with preservation of aortic wall architecture. An increased dose of Pravastatin, 100mg/kg, had a statistically significant beneficial effect on the aortic root diameter, with further reduction in the aortic root diameter, above that of the 50mg/kg dose. This occurred without a change in the aortic architecture or aortic wall thickness. It was observed that administration of Pravastatin could be commenced later, with a sustained benefit in attenuation of aortic root dilatation.

5.5 References

- Abisi, S., K. G. Burnand, et al. (2008). "Effect of statins on proteolytic activity in the wall of abdominal aortic aneurysms." *Br J Surg* 95(3): 333-337.
- Bakalli, A., T. Bekteshi, et al. (2009). "Late diagnosis of Marfan syndrome with fatal outcome in a young male patient: a case report." *Cases J* 2: 8827.
- Bjorkhem-Bergman, L., J. D. Lindh, et al. (2011). "What is a relevant statin concentration in cell experiments claiming pleiotropic effects?" *Br J Clin Pharmacol* 72(1): 164-165.
- Brooke, B. S., J. P. Habashi, et al. (2008). "Angiotensin II blockade and aortic-root dilation in Marfan's syndrome." *N Engl J Med* 358(26): 2787-2795.
- Byrne, J. S. (2008). "Pravastatin prevents aortic root dilation in Marfan Syndrome." *Circulation* 118(Supplement): 857.
- Di Garbo, V., M. Bono, et al. (2000). "Non lipid, dose-dependent effects of pravastatin treatment on hemostatic system and inflammatory response." *Eur J Clin Pharmacol* 56(4): 277-284.
- Glasziou, P. P., S. D. Eckermann, et al. (2002). "Cholesterol-lowering therapy with pravastatin in patients with average cholesterol levels and established ischaemic heart disease: is it cost-effective?" *Med J Aust* 177(8): 428-434.
- Hiratzka, L. F., G. L. Bakris, et al. (2010). "2010 ACCF/AHA/AATS/ACR/ASA/SCA/SCAI/SIR/STS/SVM guidelines for the diagnosis and management of patients with Thoracic Aortic Disease: a report of the American College of Cardiology Foundation/American Heart Association Task Force on Practice Guidelines, American Association for Thoracic Surgery, American College of Radiology, American Stroke Association, Society of Cardiovascular Anesthesiologists, Society for Cardiovascular Angiography and Interventions, Society of Interventional Radiology, Society of Thoracic Surgeons, and Society for Vascular Medicine." *Circulation* 121(13): e266-369.
- Hunninghake, D. B., R. H. Knopp, et al. (1990). "Efficacy and safety of pravastatin in patients with primary hypercholesterolemia. I. A dose-response study." *Atherosclerosis* 85(1): 81-89.
- Hwa, J., J. G. Richards, et al. (1993). "The natural history of aortic dilatation in Marfan syndrome." *Med J Aust* 158(8): 558-562.
- Jones, P. H., J. A. Farmer, et al. (1991). "Once-daily pravastatin in patients with primary hypercholesterolemia: a dose-response study." *Clin Cardiol* 14(2): 146-151.
- Koizumi, J., M. Shimizu, et al. (2002). "Effect of pravastatin-induced LDL-cholesterol reduction on coronary heart disease and cerebrovascular disease in Japanese: Hokuriku lipid coronary heart disease study-pravastatin atherosclerosis trial (Holicos-PAT)." *J Atheroscler Thromb* 9(5): 251-259.
- Lawlor, D. A., C. Bedford, et al. (2003). "Geographical variation in cardiovascular disease, risk factors, and their control in older women: British Women's Heart and Health Study." *J Epidemiol Community Health* 57(2): 134-140.
- Loeys, B. L., H. C. Dietz, et al. (2010). "The revised Ghent nosology for the Marfan syndrome." *J Med Genet* 47(7): 476-485.
- McNally, M. M., S. C. Agle, et al. (2010). "Preoperative statin therapy is associated with improved outcomes and resource utilization in patients undergoing aortic aneurysm repair." *J Vasc Surg* 51(6): 1390-1396.

- Muehling, B., A. Oberhuber, et al. (2008). "Effect of statin therapy on serum activity of proteinases and cytokines in patients with abdominal aortic aneurysm." Vasc Health Risk Manag 4(6): 1433-1437.
- Schouten, O., J. H. van Laanen, et al. (2006). "Statins are associated with a reduced infrarenal abdominal aortic aneurysm growth." Eur J Vasc Endovasc Surg 32(1): 21-26.
- Shepherd, J., S. M. Cobbe, et al. (1995). "Prevention of coronary heart disease with pravastatin in men with hypercholesterolemia. West of Scotland Coronary Prevention Study Group." N Engl J Med 333(20): 1301-1307.
- Steinmetz, E. F., C. Buckley, et al. (2005). "Treatment with simvastatin suppresses the development of experimental abdominal aortic aneurysms in normal and hypercholesterolemic mice." Ann Surg 241(1): 92-101.
- Wang, C. Y., P. Y. Liu, et al. (2008). "Pleiotropic effects of statin therapy: molecular mechanisms and clinical results." Trends Mol Med 14(1): 37-44.

Chapter 6

Discussion

6.1 Discussion

In 1990, it was known that elastic tissues were fragmented and showed disarray in Marfan syndrome, with associated accumulation of amorphous matrix between elastic fibres. A deficiency of the connective tissue protein fibrillin-1 was noted in the tissue of patients with Marfan syndrome. Abnormalities in fibrillin-1 synthesis, secretion and matrix deposition by cultured cells of patients were also noted.(Hollister, Godfrey *et al.* 1990), (Milewicz, Pyeritz *et al.* 1992). Marfan syndrome was found to be caused by mutations in the fibrillin-1 gene (FBN1) on chromosome 15.(Kainulainen, Pulkkinen *et al.* 1990; Dietz, Cutting *et al.* 1991; Dietz, Pyeritz *et al.* 1991) Early hypotheses of the pathological mechanism in Marfan syndrome focused on a structural weakness of the connective tissue due to fibrillin deficiency and a consequential failure of elastogenesis. This idea purports that a structural failure is bound to occur due to the deficiency of connective tissue. Other features which occur in Marfan syndrome such as long bone overgrowth, myxomatous valves, craniofacial dysmorphism and reduced muscle mass and reduced fat stores cannot be explained by this hypothesis.

It was subsequently discovered that fibrillin-1 was not needed for elastogenesis, though it was needed for maintenance of elastic fibres in post-natal life.(Dietz, Cutting *et al.* 1991; Pereira, Andrikopoulos *et al.* 1997) Elastic fibre breakdown correlated both temporally and spatially with a number of predictable events, including elastic fibre calcification, local recruitment of inflammatory cells, and increased expression of selected matrix-degrading enzymes (MMP 2 & MMP 9) by vascular smooth muscle cells.(Bunton, Biery *et al.* 2001)

While investigating the pathogenesis of Marfan syndrome using a genetically modified murine model of Marfan syndrome, a discovery was made. The lung tissue at birth, in the

diseased models, showed diffuse widening of the distal air space at birth due to failure of septation of the pre-alveolar sacculi, with no associated destructive or inflammatory changes.(Neptune, Frischmeyer *et al.* 2003) A deficiency of fibrillin-1 had impeded a signal for septation and it was found that this was related to excessive TGF- β activity. On foot of this discovery TGF- β inhibition and Losartan became subjects of investigation in Marfan syndrome. Losartan has been found to down-regulate the expression of TGF- β receptors Type I and II in a model of diabetic nephropathy in rats.(Guo and Qiu 2003) Doxycycline at sub-antimicrobial doses was noted to have non-specific/broad spectrum matrix metalloproteinase inhibitory properties. Matrix metalloproteinase levels in carotid plaques, which were removed during carotid endarterectomy, were reduced following Pravastatin therapy.(Crisby, Nordin-Fredriksson *et al.* 2001) This information combined with the fact that matrix metalloproteinase levels were elevated in Marfan aortic root aneurysmal tissue, prompted our team to investigate Pravastatin for the treatment of aortic root pathology in Marfan syndrome.

The first study was conducted using a murine model of Marfan syndrome and compared the natural history of the disease to normal mice. The pattern, timing and extent of the disease in relation to a number of physiological, histological and ultra-structural parameters were observed.(Chapter 3, Section 3.3) This provided important information to understand the pathophysiology of Marfan syndrome. Aortic root diameter and growth rate were found to be elevated in Marfan syndrome with associated histological changes (Section 3.3.1), as in other studies.(Habashi, Judge *et al.* 2006) The aneurysmal dilatation was associated with a decrease in left ventricular contractility and loss of the aortic aortic notch (Section 3.3.2). Aortic pulse pressure was not significantly altered. The progressive aortic root dilatation was associated with histological changes. These histological changes included, progressive aberrant aortic wall thickening and progressive loss of the aortic wall integrity, which was

similar to studies conducted by Habashi *et al.* and Chung *et al.* (Habashi, Judge *et al.* 2006; Chung, Yang *et al.* 2008) This loss of architectural integrity was accompanied by a reduction in the volume of elastin within the aortic media, which was similar to findings by Chung *et al.* (Chung, Yang *et al.* 2008)

Ultra-structural analysis suggested evidence of an increased amount of protein production and transportation within the aortic vascular smooth muscle. This was assessed by the increased volume of rough Endoplasmic Reticulum within the cell. There was also an increased volume of mitochondria located near the rough endoplasmic reticulum. They provide energy for the rough endoplasmic reticulum. This increased level of activity of the cell organelles was associated with the pathological findings of disruption of the aortic medial layer and thickening of this layer, which was similar to a previous study in mice homozygous for a targeted hypomorphic allele of fibrillin-1. (Bunton, Biery *et al.* 2001)

Aortic root growth rate observed in a group of untreated normal mice was compared to a group of normal mice treated with Pravastatin (Section 5.3.1). There was a significant reduction in growth rate, from 3 to 8 months, of the aortic root diameter and a small reduction in the overall aortic root diameter at 8 months. This was achieved without deleterious side effects with regard to aortic wall thickness and architectural integrity (Figures 5.2 and 5.3 in Chapter 5). Long term treatment of patient with a statin can improve the aortic stiffness in human trials (Kontopoulos, Athyros *et al.* 2003), though no other study has proven a beneficial effect of statin therapy on the aortic root diameter in normal mice.

A study was conducted to assess the optimal dose of Pravastatin in the Marfan groups. Two doses, 50mg/kg and 100mg/kg were compared to an untreated Marfan group. A dose dependent benefit was obtained, (Figure 5.4, Chapter 5) with the optimal dose for attenuating the aortic root diameter being 100mg/kg. Unfortunately, aberrant aortic wall thickening &

architectural integrity were not improved by statin therapy (Figures 5.5 and 5.6), with either dose despite a significant reduction in the diameter of the aortic root.

Aortic root pathology is a silent disease and patients with Marfan syndrome often have established aortic root dilatation at the time of diagnosis. It is one of the cardinal features of the disease.(Loeys, Dietz *et al.* 2010) Many studies in relation to potential treatments of Marfan syndrome focus on initiation of treatment prior to onset of aortic dilatation.(Chung, Yang *et al.* 2008; Xiong, Knispel *et al.* 2008) To become more clinically relevant, a study was conducted to assess aortic root pathology when Pravastatin therapy, given to Marfan groups, was delayed. Therapy was initiated with established aortic root dilatation, and so given for a shorter duration in total. Interestingly, there was no statistical significant difference between the groups with regard to aortic root dilatation, thickness nor architectural disruption. This means that despite a later initiation of therapy, and so a shorter duration of therapy, a similar benefit was observed with slowing of aortic root dilatation (Chapter 5, Figure 5.7). A recent study which also investigated delayed initiation of treatment in established aortic aneurysmal disease, needed to use a combination of therapy, both Losartan and Doxycycline to achieve a beneficial result.(Yang, Kim *et al.* 2010)

Pravastatin therapy attenuated dilatation of the aortic root by 33.3% (Chapter 4, Figure 4.3). Therapy had no effect on pulse pressure or myocardial contractility. Pravastatin therapy preserved elastin volume (Chapter 4, Figure 4.8) and reduced glycogen deposition, though showed no benefit in aberrant aortic wall thickening (Chapter 4, Figure 4.6) or architectural disruption(Chapter 4, Figure 4.7).

Losartan attenuated dilatation of the aortic root diameter by 33.3% (Chapter 4, Figure 4.3). Pravastatin is equipotent to Losartan in attenuation of aortic root dilatation in the murine Marfan model. Losartan would be considered by some to be “the gold-standard” for investigative therapies for medical treatment of Marfan pathology due to the recent findings

in Marfan models of disease and its central place in discovery of pathophysiology of Marfan syndrome. Losartan in this study normalised aberrant aortic wall thickening and preserved elastin volume though had little beneficial effect on architectural disruption (Chapter 4, Figure 4.3), which is different to the findings by Habashi *et al.* (Habashi, Judge *et al.* 2006) The reason for the difference between the two studies is unclear.

Doxycycline showed no benefit in attenuating aortic root dilatation in Marfan syndrome (Chapter 4, Figure 4.3). It did not prevent aberrant aortic wall thickness (Chapter 4, Figure 4.6), in fact it exacerbated it (Chapter 4, Figure 4.7). Doxycycline did not preserve architectural structure or elastin volume (Chapter 4, Figure 4.8). Doxycycline's performance was inferior to Losartan and Pravastatin.

Losartan is noted to work by inhibiting TGF- β at the receptor level, before it activates the Smad cascade. (Habashi, Judge *et al.* 2006) This was reflected in the normal volume of rough endoplasmic reticulum measured in the aortic vascular smooth muscle cell (Chapter 4, Figure 4.9). This was associated with many of the beneficial aspects of Losartan. Pravastatin reduced the level of rough endoplasmic reticulum in the aortic vascular smooth muscle (Chapter 4, Figure 4.9) cell but not as completely as Losartan did. This would suggest that Pravastatin is acting by a different mechanism to Losartan. These findings suggest that Pravastatin is acting at a post-translational level. Statins do not affect matrix metalloproteinase mRNA levels. (Luan, Chase *et al.* 2003) Statins reduce the ability of the cell to prenylate proteins such as matrix metalloproteinases. This corresponds to ultra-structural observations (Chapter 4, Figures 4.9). Pravastatin reduces the aortic vascular smooth muscle cells' ability to prenylate proteins. These proteins which are excessively produced in Marfan syndrome (mainly metalloproteinases), are not prenylated and so the disease process is attenuated.

Further investigation into the mechanism of action of statin therapy in Marfan syndrome could include measuring mRNA levels for matrix metalloproteinases. These levels could then

be compared to mRNA levels for matrix metalloproteinases in Marfan syndrome with Losartan therapy and without any intervention. By comparing these measurements, to total metalloproteinase levels in the tissue, one could discover more precisely, the mechanism of action of statin therapy in Marfan syndrome. Ideally one could measure intra-cellular and extra-cellular levels of matrix metalloproteinases. If statins were exerting their beneficial effect by inhibiting prenylation alone, a number of results would be suggestive of this. Messenger RNA levels for matrix metalloproteinase levels would remain elevated. Intra-cellular matrix metalloproteinase levels may remain elevated. Tissue or extra-cellular matrix metalloproteinase levels would be reduced. To conclude that this was unequivocally related to prenylation, if measured, one would expect mevalonate, farnesyl pyrophosphate and geranylgeranyl pyrophosphate levels to be reduced in Marfan treated with Pravastatin and the beneficial effects would be reversed by administration of mevalonate.

The pathogenesis of Marfan syndrome is related to TGF- β activity. This may not be a complete summary of events related to the pathogenesis. Different pathways are currently being investigated. TGF- β can initiate multiple downstream signalling cascades, including both canonical (Smad-dependent) and non-canonical (Smad-independent) pathways.(Derynck and Zhang 2003) It is now known that TGF- β induced activation of p38 mitogen activated protein kinase is mediated independently of Smads.(Yu, Hebert *et al.* 2002) Recently, it was discovered that TRAF6 is specifically required for the Smad-independent activation of JNK and p38 MAP kinase.(Yamashita, Fatyol *et al.* 2008) Statin therapy may have its effect by non-canonical Smad signalling. Statins can decrease JNK phosphorylation and this lead to reduced metalloproteinase activity, via blockade of the Rho-A-JNK-c-Jun-MMP2 (Rho-A; Ras homolog gene family member A, JNK; c-Jun N-terminal kinases) cascade.(Fromigue, Hamidouche *et al.* 2008) These results show that our knowledge of TGF- β signalling is rapidly evolving. So too is our knowledge of potential treatment options and how they

interact with these pathways. The interaction of TGF- β with other pathways is under active investigation. Therefore one cannot relate the pathogenesis of Marfan syndrome purely to TGF- β activity. The fact that potentially highly complex molecular signalling is involved in normal homeostasis of the extracellular matrix of the aortic wall suggests that there may also be highly complex mechanisms involved in dysregulation of homeostasis of the extracellular matrix in Marfan syndrome.

As the pathogenesis is more complex than previously anticipated, this would suggest that challenges and indeed opportunity lie ahead for research into Marfan syndrome. These challenges include understanding both pathogenesis and variable expression of the disease. By understanding these more fully, more targets for therapy may be explored. Discovery of disease specific biomarkers of both disease activity and response to treatment, will improve assessment of prognosis. As discoveries unfold, comprehensive guidelines will need to be drawn up, for optimal management of the condition. This should be conducted following rigorous assessment of treatment options. This too is a challenge for the medical community who are involved in treating Marfan syndrome.

6.2 References

- Bunton, T. E., N. J. Biery, *et al.* (2001). "Phenotypic alteration of vascular smooth muscle cells precedes elastolysis in a mouse model of Marfan syndrome." *Circ Res* **88**(1): 37-43.
- Chung, A. W., H. H. Yang, *et al.* (2008). "Long-term Doxycycline is more effective than atenolol to prevent thoracic aortic aneurysm in marfan syndrome through the inhibition of matrix metalloproteinase-2 and -9." *Circ Res* **102**(8): e73-85.
- Crisby, M., G. Nordin-Fredriksson, *et al.* (2001). "Pravastatin treatment increases collagen content and decreases lipid content, inflammation, metalloproteinases, and cell death in human carotid plaques: implications for plaque stabilization." *Circulation* **103**(7): 926-933.
- Derynck, R. and Y. E. Zhang (2003). "Smad-dependent and Smad-independent pathways in TGF-beta family signalling." *Nature* **425**(6958): 577-584.
- Dietz, H. C., G. R. Cutting, *et al.* (1991). "Marfan syndrome caused by a recurrent de novo missense mutation in the fibrillin gene." *Nature* **352**(6333): 337-339.
- Dietz, H. C., R. E. Pyeritz, *et al.* (1991). "The Marfan syndrome locus: confirmation of assignment to chromosome 15 and identification of tightly linked markers at 15q15-q21.3." *Genomics* **9**(2): 355-361.
- Fromigue, O., Z. Hamidouche, *et al.* (2008). "Blockade of the RhoA-JNK-c-Jun-MMP2 cascade by atorvastatin reduces osteosarcoma cell invasion." *J Biol Chem* **283**(45): 30549-30556.
- Guo, Z. X. and M. C. Qiu (2003). "[Losartan downregulates the expression of transforming growth factor beta type I and type II receptors in kidney of diabetic rat]." *Zhonghua Nei Ke Za Zhi* **42**(6): 403-408.
- Habashi, J. P., D. P. Judge, *et al.* (2006). "Losartan, an AT1 antagonist, prevents aortic aneurysm in a mouse model of Marfan syndrome." *Science* **312**(5770): 117-121.
- Hollister, D. W., M. Godfrey, *et al.* (1990). "Immunohistologic abnormalities of the microfibrillar-fiber system in the Marfan syndrome." *N Engl J Med* **323**(3): 152-159.
- Kainulainen, K., L. Pulkkinen, *et al.* (1990). "Location on chromosome 15 of the gene defect causing Marfan syndrome." *N Engl J Med* **323**(14): 935-939.
- Kontopoulos, A. G., V. G. Athyros, *et al.* (2003). "Long-term treatment effect of atorvastatin on aortic stiffness in hypercholesterolaemic patients." *Curr Med Res Opin* **19**(1): 22-27.
- Loeys, B. L., H. C. Dietz, *et al.* (2010). "The revised Ghent nosology for the Marfan syndrome." *J Med Genet* **47**(7): 476-485.
- Luan, Z., A. J. Chase, *et al.* (2003). "Statins inhibit secretion of metalloproteinases-1, -2, -3, and -9 from vascular smooth muscle cells and macrophages." *Arterioscler Thromb Vasc Biol* **23**(5): 769-775.
- Milewicz, D. M., R. E. Pyeritz, *et al.* (1992). "Marfan syndrome: defective synthesis, secretion, and extracellular matrix formation of fibrillin by cultured dermal fibroblasts." *J Clin Invest* **89**(1): 79-86.
- Neptune, E. R., P. A. Frischmeyer, *et al.* (2003). "Dysregulation of TGF-beta activation contributes to pathogenesis in Marfan syndrome." *Nat Genet* **33**(3): 407-411.
- Pereira, L., K. Andrikopoulos, *et al.* (1997). "Targetting of the gene encoding fibrillin-1 recapitulates the vascular aspect of Marfan syndrome." *Nat Genet* **17**(2): 218-222.
- Xiong, W., R. A. Knispel, *et al.* (2008). "Doxycycline delays aneurysm rupture in a mouse model of Marfan syndrome." *J Vasc Surg* **47**(1): 166-172; discussion 172.

- Yamashita, M., K. Fatyol, *et al.* (2008). "TRAF6 mediates Smad-independent activation of JNK and p38 by TGF-beta." Mol Cell **31**(6): 918-924.
- Yang, H. H., J. M. Kim, *et al.* (2010). "Effectiveness of combination of Losartan potassium and Doxycycline versus single-drug treatments in the secondary prevention of thoracic aortic aneurysm in Marfan syndrome." J Thorac Cardiovasc Surg **140**(2): 305-312 e302.
- Yu, L., M. C. Hebert, *et al.* (2002). "TGF-beta receptor-activated p38 MAP kinase mediates Smad-independent TGF-beta responses." EMBO J **21**(14): 3749-3759.

References

- Abisi, S., K. G. Burnand, *et al.* (2008). "Effect of statins on proteolytic activity in the wall of abdominal aortic aneurysms." *Br J Surg* **95**(3): 333-337.
- Abraham, P. A., A. J. Perejda, *et al.* (1982). "Marfan syndrome. Demonstration of abnormal elastin in aorta." *J Clin Invest* **70**(6): 1245-1252.
- Alpendurada, F., J. Wong, *et al.* (2010). "Evidence for Marfan cardiomyopathy." *Eur J Heart Fail* **12**(10): 1085-1091.
- Arteaga-Solis, E., B. Gayraud, *et al.* (2000). "Elastic and collagenous networks in vascular diseases." *Cell Struct Funct* **25**(2): 69-72.
- Bakalli, A., T. Bekteshi, *et al.* (2009). "Late diagnosis of Marfan syndrome with fatal outcome in a young male patient: a case report." *Cases J* **2**: 8827.
- Baumgartner, D., C. Baumgartner, *et al.* (2006). "Different patterns of aortic wall elasticity in patients with Marfan syndrome: a noninvasive follow-up study." *J Thorac Cardiovasc Surg* **132**(4): 811-819.
- Bellosta, S., D. Via, *et al.* (1998). "HMG-CoA reductase inhibitors reduce MMP-9 secretion by macrophages." *Arterioscler Thromb Vasc Biol* **18**(11): 1671-1678.
- Bjorkhem-Bergman, L., J. D. Lindh, *et al.* (2011). "What is a relevant statin concentration in cell experiments claiming pleiotropic effects?" *Br J Clin Pharmacol* **72**(1): 164-165.
- Boyle, J. R., E. McDermott, *et al.* (1998). "Doxycycline inhibits elastin degradation and reduces metalloproteinase activity in a model of aneurysmal disease." *J Vasc Surg* **27**(2): 354-361.
- Brooke, B. S., J. P. Habashi, *et al.* (2008). "Angiotensin II blockade and aortic-root dilation in Marfan's syndrome." *N Engl J Med* **358**(26): 2787-2795.
- Bunton, T. E., N. J. Biery, *et al.* (2001). "Phenotypic alteration of vascular smooth muscle cells precedes elastolysis in a mouse model of Marfan syndrome." *Circ Res* **88**(1): 37-43.
- Byrne, J. S. (2008). "Pravastatin prevents aortic root dilation in Marfan Syndrome " *Circulation* **118**(Supplement): 857.
- Chatrath, R., L. M. Beauchesne, *et al.* (2003). "Left ventricular function in the Marfan syndrome without significant valvular regurgitation." *Am J Cardiol* **91**(7): 914-916.
- Chung, A. W., H. H. Yang, *et al.* (2008). "Long-term Doxycycline is more effective than atenolol to prevent thoracic aortic aneurysm in marfan syndrome through the inhibition of matrix metalloproteinase-2 and -9." *Circ Res* **102**(8): e73-85.
- Colan, S. D., D. B. McElhinney, *et al.* (2006). "Validation and re-evaluation of a discriminant model predicting anatomic suitability for biventricular repair in neonates with aortic stenosis." *J Am Coll Cardiol* **47**(9): 1858-1865.
- Crisby, M., G. Nordin-Fredriksson, *et al.* (2001). "Pravastatin treatment increases collagen content and decreases lipid content, inflammation, metalloproteinases, and cell death in human carotid plaques: implications for plaque stabilization." *Circulation* **103**(7): 926-933.
- Curci, J. A., D. Mao, *et al.* (2000). "Preoperative treatment with Doxycycline reduces aortic wall expression and activation of matrix metalloproteinases in patients with abdominal aortic aneurysms." *J Vasc Surg* **31**(2): 325-342.
- Dallas, S. L., K. Miyazono, *et al.* (1995). "Dual role for the latent transforming growth factor-beta binding protein in storage of latent TGF-beta in the extracellular matrix and as a structural matrix protein." *J Cell Biol* **131**(2): 539-549.
- David, T. E., C. M. Feindel, *et al.* (1995). "Repair of the aortic valve in patients with aortic insufficiency and aortic root aneurysm." *J Thorac Cardiovasc Surg* **109**(2): 345-351; discussion 351-342.

- Davies, R. R., L. J. Goldstein, *et al.* (2002). "Yearly rupture or dissection rates for thoracic aortic aneurysms: simple prediction based on size." Ann Thorac Surg **73**(1): 17-27; discussion 27-18.
- De Backer, J. F., D. Devos, *et al.* (2006). "Primary impairment of left ventricular function in Marfan syndrome." Int J Cardiol **112**(3): 353-358.
- De Mozzi, P., U. G. Longo, *et al.* (2008). "Bicuspid aortic valve: a literature review and its impact on sport activity." Br Med Bull **85**: 63-85.
- de Oliveira, N. C., T. E. David, *et al.* (2003). "Results of surgery for aortic root aneurysm in patients with Marfan syndrome." J Thorac Cardiovasc Surg **125**(4): 789-796.
- DeBakey, M. E., A. C. Beall, Jr., *et al.* (1966). "Dissecting aneurysms of the aorta." Surg Clin North Am **46**(4): 1045-1055.
- DeBakey, M. E., W. S. Henly, *et al.* (1965). "Surgical Management of Dissecting Aneurysms of the Aorta." J Thorac Cardiovasc Surg **49**: 130-149.
- Derynck, R. and Y. E. Zhang (2003). "Smad-dependent and Smad-independent pathways in TGF-beta family signalling." Nature **425**(6958): 577-584.
- Detaint, D., P. Aegerter, *et al.* (2010). "Rationale and design of a randomized clinical trial (Marfan Sartan) of angiotensin II receptor blocker therapy versus placebo in individuals with Marfan syndrome." Arch Cardiovasc Dis **103**(5): 317-325.
- Di Garbo, V., M. Bono, *et al.* (2000). "Non lipid, dose-dependent effects of Pravastatin treatment on hemostatic system and inflammatory response." Eur J Clin Pharmacol **56**(4): 277-284.
- Dichtl, W., J. Dulak, *et al.* (2003). "HMG-CoA reductase inhibitors regulate inflammatory transcription factors in human endothelial and vascular smooth muscle cells." Arterioscler Thromb Vasc Biol **23**(1): 58-63.
- Dietz, H. C., G. R. Cutting, *et al.* (1991). "Marfan syndrome caused by a recurrent de novo missense mutation in the fibrillin gene." Nature **352**(6333): 337-339.
- Dietz, H. C., R. E. Pyeritz, *et al.* (1991). "The Marfan syndrome locus: confirmation of assignment to chromosome 15 and identification of tightly linked markers at 15q15-q21.3." Genomics **9**(2): 355-361.
- Dockery, P., Y. Tang, *et al.* (1997). "Neuron volume in the ventral horn in Wobbler mouse motoneuron disease: a light microscope stereological study." J Anat **191** (Pt 1): 89-98.
- Dollery, C. M., C. A. Owen, *et al.* (2003). "Neutrophil elastase in human atherosclerotic plaques: production by macrophages." Circulation **107**(22): 2829-2836.
- Elefteriades, J. A. (2002). "Natural history of thoracic aortic aneurysms: indications for surgery, and surgical versus nonsurgical risks." Ann Thorac Surg **74**(5): S1877-1880; discussion S1892-1878.
- Finkbohner, R., D. Johnston, *et al.* (1995). "Marfan syndrome. Long-term survival and complications after aortic aneurysm repair." Circulation **91**(3): 728-733.
- Fishman, A. P. (1989). "Cardiac asthma--a fresh look at an old wheeze." N Engl J Med **320**(20): 1346-1348.
- Forteza, A., A. Evangelista, *et al.* (2011). "[Study of the efficacy and safety of Losartan versus atenolol for aortic dilation in patients with Marfan syndrome]." Rev Esp Cardiol **64**(6): 492-498.
- Fromigue, O., Z. Hamidouche, *et al.* (2008). "Blockade of the RhoA-JNK-c-Jun-MMP2 cascade by atorvastatin reduces osteosarcoma cell invasion." J Biol Chem **283**(45): 30549-30556.
- Gersony, D. R., M. A. McClaughlin, *et al.* (2007). "The effect of beta-blocker therapy on clinical outcome in patients with Marfan's syndrome: a meta-analysis." Int J Cardiol **114**(3): 303-308.

- Glasziou, P. P., S. D. Eckermann, *et al.* (2002). "Cholesterol-lowering therapy with Pravastatin in patients with average cholesterol levels and established ischaemic heart disease: is it cost-effective?" Med J Aust **177**(8): 428-434.
- Goldstein, J. L. and M. S. Brown (1990). "Regulation of the mevalonate pathway." Nature **343**(6257): 425-430.
- Grip, O., S. Janciauskiene, *et al.* (2002). "Atorvastatin activates PPAR-gamma and attenuates the inflammatory response in human monocytes." Inflamm Res **51**(2): 58-62.
- Groenink, M., T. A. Lohuis, *et al.* (1999). "Survival and complication free survival in Marfan's syndrome: implications of current guidelines." Heart **82**(4): 499-504.
- Guo, Z. X. and M. C. Qiu (2003). "[Losartan downregulates the expression of transforming growth factor beta type I and type II receptors in kidney of diabetic rat]." Zhonghua Nei Ke Za Zhi **42**(6): 403-408.
- Habashi, J. P., D. P. Judge, *et al.* (2006). "Losartan, an AT1 antagonist, prevents aortic aneurysm in a mouse model of Marfan syndrome." Science **312**(5770): 117-121.
- Hamby, R. I., S. J. Gulotta, *et al.* (1968). "Immediate hemodynamic effects of aortic regurgitation in man." Am J Cardiol **21**(4): 478-486.
- Hart, C. Y., J. C. Burnett, Jr., *et al.* (2001). "Effects of avertin versus xylazine-ketamine anesthesia on cardiac function in normal mice." Am J Physiol Heart Circ Physiol **281**(5): H1938-1945.
- Hiratzka, L. F., G. L. Bakris, *et al.* (2010). "2010 ACCF/AHA/AATS/ACR/ASA/SCA/SCAI/SIR/STS/SVM guidelines for the diagnosis and management of patients with Thoracic Aortic Disease: a report of the American College of Cardiology Foundation/American Heart Association Task Force on Practice Guidelines, American Association for Thoracic Surgery, American College of Radiology, American Stroke Association, Society of Cardiovascular Anesthesiologists, Society for Cardiovascular Angiography and Interventions, Society of Interventional Radiology, Society of Thoracic Surgeons, and Society for Vascular Medicine." Circulation **121**(13): e266-369.
- Hollister, D. W., M. Godfrey, *et al.* (1990). "Immunohistologic abnormalities of the microfibrillar-fiber system in the Marfan syndrome." N Engl J Med **323**(3): 152-159.
- Hunninghake, D. B., R. H. Knopp, *et al.* (1990). "Efficacy and safety of Pravastatin in patients with primary hypercholesterolemia. I. A dose-response study." Atherosclerosis **85**(1): 81-89.
- Hwa, J., J. G. Richards, *et al.* (1993). "The natural history of aortic dilatation in Marfan syndrome." Med J Aust **158**(8): 558-562.
- Ikonomidis, J. S., J. A. Jones, *et al.* (2006). "Expression of matrix metalloproteinases and endogenous inhibitors within ascending aortic aneurysms of patients with Marfan syndrome." Circulation **114**(1 Suppl): I365-370.
- Jones, P. H., J. A. Farmer, *et al.* (1991). "Once-daily Pravastatin in patients with primary hypercholesterolemia: a dose-response study." Clin Cardiol **14**(2): 146-151.
- Judge, D. P., N. J. Biery, *et al.* (2004). "Evidence for a critical contribution of haploinsufficiency in the complex pathogenesis of Marfan syndrome." J Clin Invest **114**(2): 172-181.
- Kainulainen, K., L. Pulkkinen, *et al.* (1990). "Location on chromosome 15 of the gene defect causing Marfan syndrome." N Engl J Med **323**(14): 935-939.
- Kallenbach, K., M. Karck, *et al.* (2005). "Decade of aortic valve sparing reimplantation: are we pushing the limits too far?" Circulation **112**(9 Suppl): I253-259.
- Kiotseoglou, A., A. Bajpai, *et al.* (2008). "Early impairment of left ventricular long-axis systolic function demonstrated by reduced atrioventricular plane displacement in patients with Marfan syndrome." Eur J Echocardiogr **9**(5): 605-613.

- Koizumi, J., M. Shimizu, *et al.* (2002). "Effect of Pravastatin-induced LDL-cholesterol reduction on coronary heart disease and cerebrovascular disease in Japanese: Hokuriku lipid coronary heart disease study-Pravastatin atherosclerosis trial (Holicos-PAT)." J Atheroscler Thromb 9(5): 251-259.
- Kontopoulos, A. G., V. G. Athyros, *et al.* (2003). "Long-term treatment effect of atorvastatin on aortic stiffness in hypercholesterolaemic patients." Curr Med Res Opin 19(1): 22-27.
- Kuipers, H. F., P. J. Biesta, *et al.* (2005). "Statins affect cell-surface expression of major histocompatibility complex class II molecules by disrupting cholesterol-containing microdomains." Hum Immunol 66(6): 653-665.
- Lacro, R. V., H. C. Dietz, *et al.* (2007). "Rationale and design of a randomized clinical trial of beta-blocker therapy (atenolol) versus angiotensin II receptor blocker therapy (Losartan) in individuals with Marfan syndrome." Am Heart J 154(4): 624-631.
- Lalu, M. M., C. Q. Gao, *et al.* (2003). "Matrix metalloproteinase inhibitors attenuate endotoxemia induced cardiac dysfunction: a potential role for MMP-9." Mol Cell Biochem 251(1-2): 61-66.
- Lansac, d. C., Jondeau (2007). "Distinctive features of thoracic aorta surgery in Marfan Syndrome" MT Cardiology 3(3): 212-225.
- Lansman, S. L., J. N. McCullough, *et al.* (1999). "Subtypes of acute aortic dissection." Ann Thorac Surg 67(6): 1975-1978; discussion 1979-1980.
- Lavoie, P., G. Robitaille, *et al.* (2005). "Neutralization of transforming growth factor-beta attenuates hypertension and prevents renal injury in uremic rats." J Hypertens 23(10): 1895-1903.
- Lawlor, D. A., C. Bedford, *et al.* (2003). "Geographical variation in cardiovascular disease, risk factors, and their control in older women: British Women's Heart and Health Study." J Epidemiol Community Health 57(2): 134-140.
- Lindeman, J. H., H. Abdul-Hussien, *et al.* (2009). "Clinical trial of Doxycycline for matrix metalloproteinase-9 inhibition in patients with an abdominal aneurysm: Doxycycline selectively depletes aortic wall neutrophils and cytotoxic T cells." Circulation 119(16): 2209-2216.
- Liu, J. and D. F. Rigel (2009). "Echocardiographic examination in rats and mice." Methods Mol Biol 573: 139-155.
- Loeys, B. L., H. C. Dietz, *et al.* (2010). "The revised Ghent nosology for the Marfan syndrome." J Med Genet 47(7): 476-485.
- Luan, Z., A. J. Chase, *et al.* (2003). "Statins inhibit secretion of metalloproteinases-1, -2, -3, and -9 from vascular smooth muscle cells and macrophages." Arterioscler Thromb Vasc Biol 23(5): 769-775.
- Marque, V., P. Kieffer, *et al.* (2001). "Aortic wall mechanics and composition in a transgenic mouse model of Marfan syndrome." Arterioscler Thromb Vasc Biol 21(7): 1184-1189.
- Marsalese, D. L., D. S. Moodie, *et al.* (1989). "Marfan's syndrome: natural history and long-term follow-up of cardiovascular involvement." J Am Coll Cardiol 14(2): 422-428; discussion 429-431.
- Matt, P., J. Habashi, *et al.* (2008). "Recent advances in understanding Marfan syndrome: should we now treat surgical patients with Losartan?" J Thorac Cardiovasc Surg 135(2): 389-394.
- Matt, P., F. Schoenhoff, *et al.* (2009). "Circulating transforming growth factor-beta in Marfan syndrome." Circulation 120(6): 526-532.
- Mayhew, T. M. (1991). "The new stereological methods for interpreting functional morphology from slices of cells and organs." Exp Physiol 76(5): 639-665.

- McNally, M. M., S. C. Agle, *et al.* (2010). "Preoperative statin therapy is associated with improved outcomes and resource utilization in patients undergoing aortic aneurysm repair." *J Vasc Surg* **51**(6): 1390-1396.
- Meijboom, L. J., J. Timmermans, *et al.* (2005). "Aortic root growth in men and women with the Marfan's syndrome." *Am J Cardiol* **96**(10): 1441-1444.
- Milewicz, D. M., H. C. Dietz, *et al.* (2005). "Treatment of aortic disease in patients with Marfan syndrome." *Circulation* **111**(11): e150-157.
- Milewicz, D. M., R. E. Pyeritz, *et al.* (1992). "Marfan syndrome: defective synthesis, secretion, and extracellular matrix formation of fibrillin by cultured dermal fibroblasts." *J Clin Invest* **89**(1): 79-86.
- Muehling, B., A. Oberhuber, *et al.* (2008). "Effect of statin therapy on serum activity of proteinases and cytokines in patients with abdominal aortic aneurysm." *Vasc Health Risk Manag* **4**(6): 1433-1437.
- Murdoch, J. L., B. A. Walker, *et al.* (1972). "Life expectancy and causes of death in the Marfan syndrome." *N Engl J Med* **286**(15): 804-808.
- Nagashima, H., Y. Aoka, *et al.* (2002). "A 3-hydroxy-3-methylglutaryl coenzyme A reductase inhibitor, cerivastatin, suppresses production of matrix metalloproteinase-9 in human abdominal aortic aneurysm wall." *J Vasc Surg* **36**(1): 158-163.
- Nataf, P. and E. Lansac (2006). "Dilation of the thoracic aorta: medical and surgical management." *Heart* **92**(9): 1345-1352.
- Neilan, T. G., G. A. Doherty, *et al.* (2006). "Disruption of COX-2 modulates gene expression and the cardiac injury response to doxorubicin." *Am J Physiol Heart Circ Physiol* **291**(2): H532-536.
- Neptune, E. R., P. A. Frischmeyer, *et al.* (2003). "Dysregulation of TGF-beta activation contributes to pathogenesis in Marfan syndrome." *Nat Genet* **33**(3): 407-411.
- Pereira, L., K. Andrikopoulos, *et al.* (1997). "Targetting of the gene encoding fibrillin-1 recapitulates the vascular aspect of Marfan syndrome." *Nat Genet* **17**(2): 218-222.
- Pereira, L., S. Y. Lee, *et al.* (1999). "Pathogenetic sequence for aneurysm revealed in mice underexpressing fibrillin-1." *Proc Natl Acad Sci U S A* **96**(7): 3819-3823.
- Peterson, J. T. (2004). "Matrix metalloproteinase inhibitor development and the remodeling of drug discovery." *Heart Fail Rev* **9**(1): 63-79.
- Porter, K. E., J. Naik, *et al.* (2002). "Simvastatin inhibits human saphenous vein neointima formation via inhibition of smooth muscle cell proliferation and migration." *J Vasc Surg* **36**(1): 150-157.
- Porter, K. E. and N. A. Turner (2002). "Statins for the prevention of vein graft stenosis: a role for inhibition of matrix metalloproteinase-9." *Biochem Soc Trans* **30**(2): 120-126.
- Prokop, E. K., R. F. Palmer, *et al.* (1970). "Hydrodynamic forces in dissecting aneurysms. In-vitro studies in a Tygon model and in dog aortas." *Circ Res* **27**(1): 121-127.
- Pyeritz, R. E. (2009). "Marfan syndrome: 30 years of research equals 30 years of additional life expectancy." *Heart* **95**(3): 173-175.
- Radonic, T., P. de Witte, *et al.* (2010). "Losartan therapy in adults with Marfan syndrome: study protocol of the multi-center randomized controlled COMPARE trial." *Trials* **11**: 3.
- Ramirez, F. and L. Pereira (1999). "Mutations of extracellular matrix components in vascular disease." *Ann Thorac Surg* **67**(6): 1857-1858; discussion 1868-1870.
- Rios, A. S., E. N. Silber, *et al.* (1999). "Effect of long-term beta-blockade on aortic root compliance in patients with Marfan syndrome." *Am Heart J* **137**(6): 1057-1061.
- Scheck, S., Parker, Chang, Fu (1979). "Aortic aneurysm in Marfan's syndrome: changes in the ultrastructure and composition of collagen." *Journal of Anatomy* **129**(3): 645-657.

- Schouten, O., J. H. van Laanen, *et al.* (2006). "Statins are associated with a reduced infrarenal abdominal aortic aneurysm growth." Eur J Vasc Endovasc Surg 32(1): 21-26.
- Schwinger, R. H., M. Bohm, *et al.* (1994). "The failing human heart is unable to use the Frank-Starling mechanism." Circ Res 74(5): 959-969.
- Shepherd, J., S. M. Cobbe, *et al.* (1995). "Prevention of coronary heart disease with Pravastatin in men with hypercholesterolemia. West of Scotland Coronary Prevention Study Group." N Engl J Med 333(20): 1301-1307.
- Sheremet'eva, G. F., A. G. Ivanova, *et al.* (2004). "A comparative study of the aortic wall in patients with Marfan's syndrome and Erdheim's disease." Angiol Sosud Khir 10(4): 22-29.
- Shores, J., K. R. Berger, *et al.* (1994). "Progression of aortic dilatation and the benefit of long-term beta-adrenergic blockade in Marfan's syndrome." N Engl J Med 330(19): 1335-1341.
- Silverman, D. I., K. J. Burton, *et al.* (1995). "Life expectancy in the Marfan syndrome." Am J Cardiol 75(2): 157-160.
- Smith, J. A., J. I. Fann, *et al.* (1994). "Surgical management of aortic dissection in patients with the Marfan syndrome." Circulation 90(5 Pt 2): II235-242.
- Starling, E. H. and M. B. Visscher (1927). "The regulation of the energy output of the heart." J Physiol 62(3): 243-261.
- Steinmetz, E. F., C. Buckley, *et al.* (2005). "Treatment with simvastatin suppresses the development of experimental abdominal aortic aneurysms in normal and hypercholesterolemic mice." Ann Surg 241(1): 92-101.
- Tziakas, D. N., G. K. Chalikias, *et al.* (2004). "Serum profiles of matrix metalloproteinases and their tissue inhibitor in patients with acute coronary syndromes. The effects of short-term atorvastatin administration." Int J Cardiol 94(2-3): 269-277.
- Wang, C. Y., P. Y. Liu, *et al.* (2008). "Pleiotropic effects of statin therapy: molecular mechanisms and clinical results." Trends Mol Med 14(1): 37-44.
- Xiong, W., R. A. Knispel, *et al.* (2008). "Doxycycline delays aneurysm rupture in a mouse model of Marfan syndrome." J Vasc Surg 47(1): 166-172; discussion 172.
- Yamashita, M., K. Fatyol, *et al.* (2008). "TRAF6 mediates Smad-independent activation of JNK and p38 by TGF-beta." Mol Cell 31(6): 918-924.
- Yang, H. H., J. M. Kim, *et al.* (2009). "Long-term effects of Losartan on structure and function of the thoracic aorta in a mouse model of Marfan syndrome." Br J Pharmacol 158(6): 1503-1512.
- Yang, H. H., J. M. Kim, *et al.* (2010). "Effectiveness of combination of Losartan potassium and Doxycycline versus single-drug treatments in the secondary prevention of thoracic aortic aneurysm in Marfan syndrome." J Thorac Cardiovasc Surg 140(2): 305-312 e302.
- Yin, F. C., K. P. Brin, *et al.* (1989). "Arterial hemodynamic indexes in Marfan's syndrome." Circulation 79(4): 854-862.
- Yu, L., M. C. Hebert, *et al.* (2002). "TGF-beta receptor-activated p38 MAP kinase mediates Smad-independent TGF-beta responses." EMBO J 21(14): 3749-3759.
- Zhang, F. L. and P. J. Casey (1996). "Protein prenylation: molecular mechanisms and functional consequences." Annu Rev Biochem 65: 241-269.

Department of Psychology

Mercer Building, Mercer Street Lower, Dublin 2, Ireland.

Tel: +353 1 402 2428 Fax: +353 1 402 2329 email: Psychology@rcsi.ie

Professor Ciarán O'Boyle
B.Sc., PhD, RegPsychol. AFPsSI, AFBPsS
Professor and Chairman

Professor Hannah McGee
BA, PhD, RegPsychol. FPsSI, AFBPsS
Director, Health Services Research Centre

Mrs. Eva Doherty
MA, MPsychSc, RegPsychol. AFPsSI
Senior Lecturer

Dr. Anne Hickey
BA, PhD, RegPsychol. AFPsSI
Lecturer

E-Mail: coboyle@rcsi.ie
hmcgee@rcsi.ie
cdoherty@rcsi.ie
ahickey@rcsi.ie
Website: www.rcsi.ie

RCSI Research Ethics Committee

Chair: Ms B. Nolan

Convenor: Prof. H. McGee

Please quote our reference number in all correspondence: REC 099

11th November 2004.

Dr. J. McGuinness,
Research Registrar,
ILMBACH,
Drynam Road,
Swords,
Co. Dublin.

Dear Dr. McGuinness,

Re: REC 099 Station treatment of the marfan mouse.

We are pleased to advise that ethical approval has been granted by the committee for this study.

This letter provides approval for data collection for the time requested in your application and for an additional 6 months. This is to allow for any unexpected delays in proceeding with data collection. Thus this research ethics approval expires at the end of May 2006.

Where data collection is necessary beyond this point, approval for an extension must be sought from the Research Ethics Committee.

Yours sincerely,

Ms. B. Nolan
(Chair)
Research Ethics Committee